REPORT DOCUMENTATION PAGE

AFRL-SR-BL-TR-98-

6783

1. AGENCY USE ONLY (Leave Blank)	2. REPORT DATE December, 1994	3. REPORT TYPE AND DATES COVERED Final

4. TITLE AND SUBTITLE
USAF Summer Research Program - 1994 High School Apprenticeship Program
Final Reports, Volume 13, Phillips Laboratory

5. FUNDING NUMBERS

6. AUTHORS
Gary Moore

7. PERFORMING ORGANIZATION NAME(S) AND ADDRESS(ES)
Research and Development Labs, Culver City, CA

8. PERFORMING ORGANIZATION REPORT NUMBER

9. SPONSORING/MONITORING AGENCY NAME(S) AND ADDRESS(ES)
AFOSR/NI
4040 Fairfax Dr, Suite 500
Arlington, VA 22203-1613

10. SPONSORING/MONITORING AGENCY REPORT NUMBER

11. SUPPLEMENTARY NOTES
Contract Number: F49620-93-C-0063

12a. DISTRIBUTION AVAILABILITY STATEMENT
Approved for Public Release

12b. DISTRIBUTION CODE

13. ABSTRACT *(Maximum 200 words)*
The United States Air Force High School Apprenticeship Program's (USAF- HSAP) purpose is to place outstanding high school students whose interests are in the areas of mathematics, engineering, and science to work in a laboratory environment. The students selected to participate in the program work in an Air Force Laboratory for a duration of 8 weeks during their summer vacation.

14. SUBJECT TERMS
AIR FORCE HIGH SCHOOL APPRENTICESHIP PROGRAM, APPRENTICEDHIP, AIR FORCE RESEARCH, AIR FORCE, ENGINEERING, LABORATORIES, REPORTS, SCHOOL, STUDENT, SUMMER, UNIVERSITIES

15. NUMBER OF PAGES

16. PRICE CODE

17. SECURITY CLASSIFICATION OF REPORT Unclassified	18. SECURITY CLASSIFICATION OF THIS PAGE Unclassified	19. SECURITY CLASSIFICATION OF ABSTRACT Unclassified	20. LIMITATION OF ABSTRACT UL

UNITED STATES AIR FORCE

SUMMER RESEARCH PROGRAM -- 1994

HIGH SCHOOL APPRENTICESHIP PROGRAM FINAL REPORTS

VOLUME 13

PHILLIPS LABORATORY

RESEARCH & DEVELOPMENT LABORATORIES

5800 Uplander Way

Culver City, CA 90230-6608

Program Director, RDL
Gary Moore

Program Manager, AFOSR
Major David Hart

Program Manager, RDL
Scott Licoscos

Program Administrator, RDL
Gwendolyn Smith

Program Administrator
Johnetta Thompson

Submitted to:

AIR FORCE OFFICE OF SCIENTIFIC RESEARCH

Bolling Air Force Base

Washington, D.C.

December 1994

PREFACE

Reports in this volume are numbered consecutively beginning with number 1. Each report is paginated with the report number followed by consecutive page numbers, e.g., 1-1, 1-2, 1-3; 2-1, 2-2, 2-3.

This document is one of a set of 16 volumes describing the 1994 AFOSR Summer Research Program. The following volumes comprise the set:

VOLUME	TITLE
1	Program Management Report
Summer Faculty Research Program (SFRP) Reports	
2A & 2B	Armstrong Laboratory
3A & 3B	Phillips Laboratory
4	Rome Laboratory
5A & 5B	Wright Laboratory
6	Arnold Engineering Development Center, Frank J. Seiler Research Laboratory, and Wilford Hall Medical Center
Graduate Student Research Program (GSRP) Reports	
7	Armstrong Laboratory
8	Phillips Laboratory
9	Rome Laboratory
10	Wright Laboratory
11	Arnold Engineering Development Center, Frank J. Seiler Research Laboratory, and Wilford Hall Medical Center
High School Apprenticeship Program (HSAP) Reports	
12A & 12B	Armstrong Laboratory
13	Phillips Laboratory
14	Rome Laboratory
15A&15B	Wright Laboratory
16	Arnold Engineering Development Center

HSAP FINAL REPORT TABLE OF CONTENTS   i-xiv

HSAP FINAL REPORTS

SRP Final Report Table of Contents

SRP Final Report Table of Contents

SRP Final Report Table of Contents

SRP Final Report Table of Contents

SRP Final Report Table of Contents

1. INTRODUCTION

The Summer Research Program (SRP), sponsored by the Air Force Office of Scientific Research (AFOSR), offers paid opportunities for university faculty, graduate students, and high school students to conduct research in U.S. Air Force research laboratories nationwide during the summer.

Introduced by AFOSR in 1978, this innovative program is based on the concept of teaming academic researchers with Air Force scientists in the same disciplines using laboratory facilities and equipment not often available at associates' institutions.

AFOSR also offers its research associates an opportunity, under the Summer Research Extension Program (SREP), to continue their AFOSR-sponsored research at their home institutions through the award of research grants. In 1994 the maximum amount of each grant was increased from $20,000 to $25,000, and the number of AFOSR-sponsored grants decreased from 75 to 60. A separate annual report is compiled on the SREP.

The Summer Faculty Research Program (SFRP) is open annually to approximately 150 faculty members with at least two years of teaching and/or research experience in accredited U.S. colleges, universities, or technical institutions. SFRP associates must be either U.S. citizens or permanent residents.

The Graduate Student Research Program (GSRP) is open annually to approximately 100 graduate students holding a bachelor's or a master's degree; GSRP associates must be U.S. citizens enrolled full time at an accredited institution.

The High School Apprentice Program (HSAP) annually selects about 125 high school students located within a twenty mile commuting distance of participating Air Force laboratories.

The numbers of projected summer research participants in each of the three categories are usually increased through direct sponsorship by participating laboratories.

AFOSR's SRP has well served its objectives of building critical links between Air Force research laboratories and the academic community, opening avenues of communications and forging new research relationships between Air Force and academic technical experts in areas of national interest; and strengthening the nation's efforts to sustain careers in science and engineering. The success of the SRP can be gauged from its growth from inception (see Table 1) and from the favorable responses the 1994 participants expressed in end-of-tour SRP evaluations (Appendix B).

AFOSR contracts for administration of the SRP by civilian contractors. The contract was first awarded to Research & Development Laboratories (RDL) in September 1990. After completion of the 1990 contract, RDL won the recompetition for the basic year and four 1-year options.

1

2. PARTICIPATION IN THE SUMMER RESEARCH PROGRAM

The SRP began with faculty associates in 1979; graduate students were added in 1982 and high school students in 1986. The following table shows the number of associates in the program each year.

Table 1: SRP Participation, by Year

YEAR	Number of Participants			TOTAL
	SFRP	GSRP	HSAP	
1979	70			70
1980	87			87
1981	87			87
1982	91	17		108
1983	101	53		154
1984	152	84		236
1985	154	92		246
1986	158	100	42	300
1987	159	101	73	333
1988	153	107	101	361
1989	168	102	103	373
1990	165	121	132	418
1991	170	142	132	444
1992	185	121	159	464
1993	187	117	136	440
1994	192	117	133	442

Beginning in 1993, due to budget cuts, some of the laboratories weren't able to afford to fund as many associates as in previous years; in one case a laboratory did not fund any additional associates. However, the table shows that, overall, the number of participating associates increased this year because two laboratories funded more associates than they had in previous years.

3. RECRUITING AND SELECTION

The SRP is conducted on a nationally advertised and competitive-selection basis. The advertising for faculty and graduate students consisted primarily of the mailing of 8,000 44-page SRP brochures to chairpersons of departments relevant to AFOSR research and to administrators of grants in accredited universities, colleges, and technical institutions. Historically Black Colleges and Universities (HBCUs) and Minority Institutions (MIs) were included. Brochures also went to all participating USAF laboratories, the previous year's participants, and numerous (over 600 annually) individual requesters.

Due to a delay in awarding the new contract, RDL was not able to place advertisements in any of the following publications in which the SRP is normally advertised: *Black Issues in Higher Education*, *Chemical & Engineering News*, *IEEE Spectrum* and *Physics Today*.

High school applicants can participate only in laboratories located no more than 20 miles from their residence. Tailored brochures on the HSAP were sent to the head counselors of 180 high schools in the vicinity of participating laboratories, with instructions for publicizing the program in their schools. High school students selected to serve at Wright Laboratory's Armament Directorate (Eglin Air Force Base, Florida) serve eleven weeks as opposed to the eight weeks normally worked by high school students at all other participating laboratories.

Each SFRP or GSRP applicant is given a first, second, and third choice of laboratory. High school students who have more than one laboratory or directorate near their homes are also given first, second, and third choices.

Laboratories make their selections and prioritize their nominees. AFOSR then determines the number to be funded at each laboratory and approves laboratories' selections.

Subsequently, laboratories use their own funds to sponsor additional candidates. Some selectees do not accept the appointment, so alternate candidates are chosen. This multi-step selection procedure results in some candidates being notified of their acceptance after scheduled deadlines. The total applicants and participants for 1994 are shown in this table.

Table 2: 1994 Applicants and Participants

PARTICIPANT CATEGORY	TOTAL APPLICANTS	SELECTEES	DECLINING SELECTEES
SFRP	600	192	30
(HBCU/MI)	(90)	(16)	(7)
GSRP	322	117	11
(HBCU/MI)	(11)	(6)	(0)
HSAP	562	133	14
TOTAL	1484	442	55

3

4. SITE VISITS

During June and July of 1994, representatives of both AFOSR/NI and RDL visited each participating laboratory to provide briefings, answer questions, and resolve problems for both laboratory personnel and participants. The objective was to ensure that the SRP would be as constructive as possible for all participants. Both SRP participants and RDL representatives found these visits beneficial. At many of the laboratories, this was the only opportunity for all participants to meet at one time to share their experiences and exchange ideas.

5. HISTORICALLY BLACK COLLEGES AND UNIVERSITIES AND MINORITY INSTITUTIONS (HBCU/MIs)

In previous years, an RDL program representative visited from seven to ten different HBCU/MIs to promote interest in the SRP among the faculty and graduate students. Due to the late contract award date (January 1994) no time was available to visit HBCU/MIs this past year.

In addition to RDL's special recruiting efforts, AFOSR attempts each year to obtain additional funding or use leftover funding from cancellations the past year to fund HBCU/MI associates. This year, seven HBCU/MI SFRPs declined after they were selected. The following table records HBCU/MI participation in this program.

Table 3: SRP HBCU/MI Participation, by Year

YEAR	SFRP		GSRP	
	Applicants	Participants	Applicants	Participants
1985	76	23	15	11
1986	70	18	20	10
1987	82	32	32	10
1988	53	17	23	14
1989	39	15	13	4
1990	43	14	17	3
1991	42	13	8	5
1992	70	13	9	5
1993	60	13	6	2
1994	90	16	11	6

6. SRP FUNDING SOURCES

Funding sources for the 1994 SRP were the AFOSR-provided slots for the basic contract and laboratory funds. Funding sources by category for the 1994 SRP selected participants are shown here.

Table 4: 1994 SRP Associate Funding

FUNDING CATEGORY	SFRP	GSRP	HSAP
AFOSR Basic Allocation Funds	150	98[*1]	121[*2]
USAF Laboratory Funds	37	19	12
HBCU/MI By AFOSR (Using Procured Addn'l Funds)	5	0	0
TOTAL	192	117	133

*1 - 100 were selected, but two canceled too late to be replaced.
*2 - 125 were selected, but four canceled too late to be replaced.

7. COMPENSATION FOR PARTICIPANTS

Compensation for SRP participants, per five-day work week, is shown in this table.

Table 5: 1994 SRP Associate Compensation

PARTICIPANT CATEGORY	1991	1992	1993	1994
Faculty Members	$690	$718	$740	$740
Graduate Student (Master's Degree)	$425	$442	$455	$455
Graduate Student (Bachelor's Degree)	$365	$380	$391	$391
High School Student (First Year)	$200	$200	$200	$200
High School Student (Subsequent Years)	$240	$240	$240	$240

The program also offered associates whose homes were more than 50 miles from the laboratory an expense allowance (seven days per week) of $50/day for faculty and $37/day for graduate students.

Transportation to the laboratory at the beginning of their tour and back to their home destinations at the end was also reimbursed for these participants. Of the combined SFRP and GSRP associates, 58% (178 out of 309) claimed travel reimbursements at an average round-trip cost of $860.

Faculty members were encouraged to visit their laboratories before their summer tour began. All costs of these orientation visits were reimbursed. Forty-one percent (78 out of 192) of faculty associates took orientation trips at an average cost of $498. Many faculty associates noted on their evaluation forms that due to the late notice of acceptance into the 1994 SRP (caused by the late award in January 1994 of the contract) there wasn't enough time to attend an orientation visit prior to their tour start date. In 1993, 58 % of SFRP associates took orientation visits at an average cost of $685.

Program participants submitted biweekly vouchers countersigned by their laboratory research focal point, and RDL issued paychecks so as to arrive in associates' hands two weeks later.

HSAP program participants were considered actual RDL employees, and their respective state and federal income tax and Social Security were withheld from their paychecks. By the nature of their independent research, SFRP and GSRP program participants were considered to be consultants or independent contractors. As such, SFRP and GSRP associates were responsible for their own income taxes, Social Security, and insurance.

8. CONTENTS OF THE 1994 REPORT

The complete set of reports for the 1994 SRP includes this program management report augmented by fifteen volumes of final research reports by the 1994 associates as indicated below:

Table 6: 1994 SRP Final Report Volume Assignments

LABORATORY	VOLUME		
	SFRP	GSRP	HSAP
Armstrong	2	7	12
Phillips	3	8	13
Rome	4	9	14
Wright	5A, 5B	10	15
AEDC, FJSRL, WHMC	6	11	16

AEDC   =   Arnold Engineering Development Center
FJSRL   =   Frank J. Seiler Research Laboratory
WHMC   =   Wilford Hall Medical Center

APPENDIX A -- PROGRAM STATISTICAL SUMMARY

A. Colleges/Universities Represented

Selected SFRP and GSRP associates represent 158 different colleges, universities, and institutions.

B. States Represented

SFRP -Applicants came from 46 states plus Washington D.C. and Puerto Rico. Selectees represent 40 states.

GSRP - Applicants came from 46 states and Puerto Rico. Selectees represent 34 states.

HSAP - Applicants came from fifteen states. Selectees represent ten states.

C. Academic Disciplines Represented

The academic disciplines of the combined 192 SFRP associates are as follows:

Electrical Engineering	22.4%
Mechanical Engineering	14.0%
Physics: General, Nuclear & Plasma	12.2%
Chemistry & Chemical Engineering	11.2%
Mathematics & Statistics	8.1%
Psychology	7.0%
Computer Science	6.4%
Aerospace & Aeronautical Engineering	4.8%
Engineering Science	2.7%
Biology & Inorganic Chemistry	2.2%
Physics: Electro-Optics & Photonics	2.2%
Communication	1.6%
Industrial & Civil Engineering	1.6%
Physiology	1.1%
Polymer Science	1.1%
Education	0.5%
Pharmaceutics	0.5%
Veterinary Medicine	0.5%
TOTAL	**100%**

Table A-1. Total Participants

Number of Participants	
SFRP	192
GSRP	117
HSAP	133
TOTAL	442

Table A-2. Degrees Represented

Degrees Represented			
	SFRP	GSRP	TOTAL
Doctoral	189	0	189
Master's	3	47	50
Bachelor's	0	70	70
TOTAL	192	117	309

Table A-3. SFRP Academic Titles

Academic Titles	
Assistant Professor	74
Associate Professor	63
Professor	44
Instructor	5
Chairman	1
Visiting Professor	1.
Visiting Assoc. Prof.	1
Research Associate	3
TOTAL	192

Table A-4. Source of Learning About SRP

SOURCE	SFRP		GSRP	
	Applicants	Selectees	Applicants	Selectees
Applied/participated in prior years	26%	37%	10%	13%
Colleague familiar with SRP	19%	17%	12%	12%
Brochure mailed to institution	32%	18%	19%	12%
Contact with Air Force laboratory	15%	24%	9%	12%
Faculty Advisor (GSRPs Only)	--	--	39%	43%
Other source	8%	4%	11%	8%
TOTAL	100%	100%	100%	100%

Table A-5. Ethnic Background of Applicants and Selectees

	SFRP		GSRP		HSAP	
	Applicants	Selectees	Applicants	Selectees	Applicants	Selectees
American Indian or Native Alaskan	0.2%	0%	1%	0%	0.4%	0%
Asian/Pacific Islander	30%	20%	6%	8%	7%	10%
Black	4%	1.5%	3%	3%	7%	2%
Hispanic	3%	1.9%	4%	4.5%	11%	8%
Caucasian	51%	63%	77%	77%	70%	75%
Preferred not to answer	12%	14%	9%	7%	4%	5%
TOTAL	100%	100%	100%	100%	99%	100%

Table A-6. Percentages of Selectees receiving their 1st, 2nd, or 3rd Choices of Directorate

	1st Choice	2nd Choice	3rd Choice	Other Than Their Choice
SFRP	70%	7%	3%	20%
GSRP	76%	2%	2%	20%

APPENDIX B -- SRP EVALUATION RESPONSES

1. OVERVIEW

Evaluations were completed and returned to RDL by four groups at the completion of the SRP. The number of respondents in each group is shown below.

Table B-1. Total SRP Evaluations Received

Evaluation Group	Responses
SFRP & GSRPs	275
HSAPs	116
USAF Laboratory Focal Points	109
USAF Laboratory HSAP Mentors	54

All groups indicate near-unanimous enthusiasm for the SRP experience.

Typical comments from 1994 SRP associates are:

"[The SRP was an] excellent opportunity to work in state-of-the-art facility with top-notch people."

"[The SRP experience] enabled exposure to interesting scientific application problems; enhancement of knowledge and insight into 'real-world' problems."

"[The SRP] was a great opportunity for resourceful and independent faculty [members] from small colleges to obtain research credentials."

"The laboratory personnel I worked with are tremendous, both personally and scientifically. I cannot emphasize how wonderful they are."

"The one-on-one relationship with my mentor and the hands on research experience improved [my] understanding of physics in addition to improving my library research skills. Very valuable for [both] college and career!"

Typical comments from laboratory focal points and mentors are:

"This program [AFOSR - SFRP] has been a 'God Send' for us. Ties established with summer faculty have proven invaluable."

"Program was excellent from our perspective. So much was accomplished that new options became viable "

"This program managed to get around most of the red tape and 'BS' associated with most Air Force programs. Good Job!"

"Great program for high school students to be introduced to the research environment. Highly educational for others [at laboratory]."

"This is an excellent program to introduce students to technology and give them a feel for [science/engineering] career fields. I view any return benefit to the government to be 'icing on the cake' and have usually benefitted."

The summarized recommendations for program improvement from both associates and laboratory personnel are listed below (Note: basically the same as in previous years.)

A.   Better preparation on the labs' part prior to associates' arrival (i.e., office space, computer assets, clearly defined scope of work).

B.   Laboratory sponsor seminar presentations of work conducted by associates, and/or organized social functions for associates to collectively meet and share SRP experiences.

C.   Laboratory focal points collectively suggest more AFOSR allocated associate positions, so that more people may share in the experience.

D.   Associates collectively suggest higher stipends for SRP associates.

E.   Both HSAP Air Force laboratory mentors and associates would like the summer tour extended from the current 8 weeks to either 10 or 11 weeks; the groups state it takes 4-6 weeks just to get high school students up-to-speed on what's going on at laboratory. (Note: this same arguement was used to raise the faculty and graduate student participation time a few years ago.)

2. 1994 USAF LABORATORY FOCAL POINT (LFP) EVALUATION RESPONSES

The summarized results listed below are from the 109 LFP evaluations received.

1. LFP evaluations received and associate preferences:

Table B-2. Air Force LFP Evaluation Responses (By Type)

| Lab | Evals Recv'd | How Many Associates Would You Prefer To Get ? | | | | | | | | (% Response) | | | |
| | | SFRP | | | | GSRP (w/Univ Professor) | | | | GSRP (w/o Univ Professor) | | | |
		0	1	2	3+	0	1	2	3+	0	1	2	3+
AEDC	10	30	50	0	20	50	40	0	10	40	60	0	0
AL	44	34	50	6	9	54	34	12	0	56	31	12	0
FJSRL	3	33	33	33	0	67	33	0	0	33	67	0	0
PL	14	28	43	28	0	57	21	21	0	71	28	0	0
RL	3	33	67	0	0	67	0	33	0	100	0	0	0
WHMC	1	0	0	100	0	0	100	0	0	0	100	0	0
WL	46	15	61	24	0	56	30	13	0	76	17	6	0
Total	121	25%	43%	27%	4%	50%	37%	11%	1%	54%	43%	3%	0%

LFP Evaluation Summary. The summarized repsonses, by laboratory, are listed on the following page. LFPs were asked to rate the following questions on a scale from 1 (below average) to 5 (above average).

2. LFPs involved in SRP associate application evaluation process:
    a. Time available for evaluation of applications:
    b. Adequacy of applications for selection process:
3. Value of orientation trips:
4. Length of research tour:
5   a. Benefits of associate's work to laboratory:
    b. Benefits of associate's work to Air Force:
6.   a. Enhancement of research qualifications for LFP and staff:
    b. Enhancement of research qualifications for SFRP associate:
    c. Enhancement of research qualifications for GSRP associate:
7.   a. Enhancement of knowledge for LFP and staff:
    b. Enhancement of knowledge for SFRP associate:
    c. Enhancement of knowledge for GSRP associate:
8. Value of Air Force and university links:
9. Potential for future collaboration:
10.   a. Your working relationship with SFRP:
    b. Your working relationship with GSRP:
11. Expenditure of your time worthwhile:

12. Quality of program literature for associate:

13.   a. Quality of RDL's communications with you:

      b. Quality of RDL's communications with associates:

14. Overall assessment of SRP:

Laboratory Focal Point Reponses to above questions

	AEDC	AL	FJSRL	PL	RL	WHMC	WL
# Evals Recv'd	10	32	3	14	3	1	46
Question #							
2	90 %	62 %	100 %	64 %	100 %	100 %	83 %
2a	**3.5**	**3.5**	4.7	4.4	4.0	4.0	**3.7**
2b	4.0	3.8	4.0	4.3	4.3	4.0	3.9
3	4.2	3.6	4.3	3.8	4.7	4.0	4.0
4	3.8	3.9	4.0	4.2	4.3	NO ENTRY	4.0
5a	4.1	4.4	4.7	4.9	4.3	3.0	4.6
5b	4.0	4.2	4.7	4.7	4.3	3.0	4.5
6a	**3.6**	4.1	**3.7**	4.5	4.3	**3.0**	4.1
6b	3.6	4.0	4.0	4.4	4.7	3.0	4.2
6c	3.3	4.2	4.0	4.5	4.5	3.0	4.2
7a	3.9	4.3	4.0	4.6	4.0	3.0	4.2
7b	4.1	4.3	4.3	4.6	4.7	3.0	4.3
7c	3.3	4.1	4.5	4.5	4.5	5.0	4.3
8	4.2	4.3	5.0	4.9	4.3	5.0	4.7
9	3.8	4.1	4.7	5.0	4.7	5.0	4.6
10a	4.6	4.5	5.0	4.9	4.7	5.0	4.7
10b	4.3	4.2	5.0	4.3	5.0	5.0	4.5
11	4.1	4.5	4.3	4.9	4.7	4.0	4.4
12	4.1	3.9	4.0	4.4	4.7	3.0	4.1
13a	**3.8**	**2.9**	4.0	4.0	4.7	**3.0**	**3.6**
13b	**3.8**	**2.9**	4.0	4.3	4.7	**3.0**	**3.8**
14	4.5	4.4	5.0	4.9	4.7	4.0	4.5

3. 1994 SFRP & GSRP EVALUATION RESPONSES

The summarized results listed below are from the 275 SFRP/GSRP evaluations received.

Associates were asked to rate the following questions on a scale from
1 (below average) to 5 (above average)

1. The match between the laboratories research and your field:		4.6
2. Your working relationship with your LFP:		4.8
3. Enhancement of your academic qualifications:		4.4
4. Enhancement of your research qualifications:		4.5
5. Lab readiness for you: LFP, task, plan:		4.3
6. Lab readiness for you: equipment, supplies, facilities:		4.1
7. Lab resources:		4.3
8. Lab research and administrative support:		4.5
9. Adequacy of brochure and associate handbook:		4.3
10. RDL communications with you:		4.3
11. Overall payment procedures:		**3.8**
12. Overall assessment of the SRP:		4.7
13. a. Would you apply again?	Yes:	85%
b. Will you continue this or related research?	Yes:	95%
14. Was length of your tour satisfactory?	Yes:	86%

15. Percentage of associates who engaged in:

a. Seminar presentation:		52%
b. Technical meetings:		32%
c. Social functions:		03%
d. Other		01%

16. Percentage of associates who experienced difficulties in:

    a. Finding housing: 12%
    b. Check Cashing: 03%

17. Where did you stay during your SRP tour?

    a. At Home: 20%
    b. With Friend: 06%
    c. On Local Economy: 47%
    d. Base Quarters: 10%

THIS SECTION FACULTY ONLY:

18. Were graduate students working with you?   Yes: 23%

19. Would you bring graduate students next year?   Yes: 56%

20. Value of orientation visit:

    Essential: 29%
    Convenient: 20%
    Not Worth Cost: 01%
    Not Used: 34%

THIS SECTION GRADUATE STUDENTS ONLY:

21. Who did you work with:

    University Professor: 18%
    Laboratory Scientist: 54%

4. 1994 USAF LABORATORY HSAP MENTOR EVALUATION RESPONSES

The summarized results listed below are from the 54 mentor evaluations received.

1. Mentor apprentice preferences:

Table B-3. Air Force Mentor Responses

Laboratory	# Evals Recv'd	How Many Apprentices Would You Prefer To Get ?			
		HSAP Apprentices Preferred			
		0	1	2	3+
AEDC	6	0	100	0	0
AL	17	29	47	6	18
PL	9	22	78	0	0
RL	4	25	75	0	0
WL	18	22	55	17	6
Total	54	20%	71%	5%	5%

Mentors were asked to rate the following questions on a scale from
1 (below average) to 5 (above average)

2. Mentors involved in SRP apprentice application evaluation process:
   a. Time available for evaluation of applications:
   b. Adequacy of applications for selection process:
3. Laboratory's preparation for apprentice:
4. Mentor's preparation for apprentice:
5. Length of research tour:
6. Benefits of apprentice's work to U.S. Air force:
7. Enhancement of academic qualifications for apprentice:
8. Enhancement of research skills for apprentice:
9. Value of U.S. Air Force/high school links:
10. Mentor's working relationship with apprentice:
11. Expenditure of mentor's time worthwhile:
12. Quality of program literature for apprentice:
13.   a. Quality of RDL's communications with mentors:
       b. Quality of RDL's communication with apprentices:
14. Overall assessment of SRP:

	AEDC	AL	PL	RL	WL
# Evals Recv'd	6	17	9	4	18
Question #					
2	100 %	76 %	56 %	75 %	61 %
2a	4.2	4.0	**3.1**	**3.7**	**3.5**
2b	4.0	4.5	4.0	4.0	3.8
3	4.3	**3.8**	**3.9**	**3.8**	**3.8**
4	4.5	**3.7**	**3.4**	4.2	**3.9**
5	**3.5**	4.1	**3.1**	**3.7**	**3.6**
6	4.3	3.9	4.0	4.0	4.2
7	4.0	4.4	4.3	4.2	3.9
8	4.7	4.4	4.4	4.2	4.0
9	4.7	4.2	3.7	4.5	4.0
10	4.7	4.5	4.4	4.5	4.2
11	4.8	4.3	4.0	4.5	4.1
12	4.2	4.1	4.1	4.8	3.4
13a	**3.5**	**3.9**	**3.7**	4.0	**3.1**
13b	4.0	4.1	3.4	4.0	3.5
14	4.3	4.5	3.8	4.5	4.1

5. 1994 HSAP EVALUATION RESPONSES

The summarized results listed below are from the 116 HSAP evaluations received.

HSAP apprentices were asked to rate the following questions on a scale from
1 (below average) to 5 (above average)

1. Match of lab research to you interest: 3.9

2. Apprentices working relationship with their mentor and other lab scientists: 4.6

3. Enhancement of your academic qualifications: 4.4

4. Enhancement of your research qualifications: 4.1

5. Lab readiness for you: mentor, task, work plan   **3.7**

6. Lab readiness for you: equipment supplies facilities   4.3

7. Lab resources: availability   4.3

8. Lab research and administrative support: 4.4

9. Adequacy of RDL's apprentice handbook and administrative materials: 4.0

10. Responsiveness of RDL's communications: **3.5**

11. Overall payment procedures: **3.3**

12. Overall assessment of SRP value to you: 4.5

13. Would you apply again next year?   Yes: 88%

14. Was length of SRP tour satisfactory?   Yes: 78%

15. Percentages of apprentices who engaged in:

    a. Seminar presentation: 48%
    b. Technical meetings: 23%
    c. Social functions: 18%

THERMAL ANALYSIS OF
HADN AND S-HAN5

Christopher D. Amos

Desert High School
1575 Payne Avenue
Edwards, CA 93523

THERMAL ANALYSIS OF
HADN AND S-HAN5

Christopher D. Amos
Desert High School

Abstract

The thermal properties of HADN and S-HAN5 and their mixtures were studied. Using the method of differential scanning calorimetry, several mixtures were tested for stability and compatibility. None of the mixtures at a 99% oxidizer, 1% additive level differed significantly from the pure oxidizers except for 2,2'-dipyridylamine in S-HAN5. This seems to indicate that the additives are compatible with the oxidizers but they do not make the oxidizers any more stable.

THERMAL ANALYSIS OF
HADN AND S-HAN5

Christopher D. Amos

Introduction

Everyone is concerned about the environment. This even includes the rocket propellant industry. Their most commonly used oxidizer, ammonium perchlorate, forms hydrochloric acid when it reacts with the fuel. That acid is sprayed out with the exhaust gases and into the atmosphere where it could cause extensive damage to the environment. Now, other oxidizers are being considered. New oxidizers must be environmentally acceptable without giving up high performance. Aero Jet has done some work with hydroxylammonium nitrate (HAN5), and it seems to be a promising oxidizer. Another consideration is ammonium dinitramide (ADN) which was recently introduced to the United States. However, to use with solution propellants, a liquid oxidizer is needed; ADN is a solid. Hydroxylammonium dinitramide (HADN) has been synthesized through an ion exchange process, and it is a liquid at room temperature. Since it is sensitive to both light and heat, work is being done to stabilize HADN for future use.

Methodology

HADN and stabilized HAN5 (S-HAN5) were both tested with various additives for compatibility and stability. These were checked

for through differential scanning calorimetry. Differential scanning calorimetry measures heat flow in substances as their temperatures are increased at a constant rate. In the differential scanning calorimeter (DSC), this is accomplished through the use of a reference pan and a sample pan. The heat flow of the substance tested equals the heat flow of the sample pan minus the heat flow of the reference pan. For the most part, as the temperature increases, the heat flow stays the same. On a plot of heat flow versus temperature, this gives a relatively flat baseline. The DSC also finds glass transitions, melting and boiling points, and decomposition temperatures, which show up as changes in the baseline or peaks on a plot.

All tests were conducted with a Du Pont Instruments 912 Dual Sample Differential Scanning Calorimeter using hermetic aluminum pans. Small samples of each mixture are place in the pans, sealed, and placed in the calorimeter. Testing was conducted in a nitrogen atmosphere with a flow rate of 50 mL/min. The DSC was set to read the data every 1.4 seconds. All samples began heating at room temperature (approximately 25°C). ADN samples were heated up to 300°C. Unstabilized HAN5 samples were heated up to 250°C. All other samples were heated to 200°C. The heating rate was 10°C/min.

The following compounds were used for testing: ammonium dinitramide; hydroxylammonium dinitramide; stabilized hydroxylammonium nitrate; hydroxylammonium nitrate with 5%

ammonium nitrate; 3-hexyne-2,5-diol; 3-methylsulfolane; 2,2'-dipyridylamine; ammonium nitrate; diammonium hydrogen phosphate; ammonium dihydrogen phosphate.

Results

Mixture	Weight(mg)	Onset(^{O}C)	Area(J/g)	Peak(^{O}C)
S-HAN5	1.14	153.31	186.6	158.12
	1.25	166.74	774.2	169.23
	1.05	159.99	1703	163.41
	1.12	172.47	2057	176.43
Mean Temp.	163.13	Standard deviation		7.19
S-HAN5 w/	2.16	174.42	215.7	176.30
hexyne,diol	1.38	174.34	832.3	177.26
	1.33	158.77	1935	163.04
Mean Temp.	169.18	Std. deviation		7.36
S-HAN5 w/	1.59	169.26	2052	173.63
methylsulfolane	1.27	179.59	857.4	182.58
	1.44	177.78	1897	182.06
Mean Temp.	175.54	Std. deviation		4.50
S-HAN5 w/	1.12	131.45	3606	136.57
dipyridylamine	1.21	183.24	1006	186.36
Mean Temp.	157.35	Std. deviation		25.90
HADN	1.89	157.44	530.1	160.01
	0.79	142.47	3935	146.06
	0.75	158.11	1900	161.23
	1.50	144.69	1548	149.41

Mixture	Weight(mg)	Onset($^{\circ}$C)	Area(J/g)	Peak($^{\circ}$C)
	0.96	146.77	2200	150.53
	0.89	157.78	1760	161.40
Mean Temp.	151.73	Std. deviation		6.32
HADN w/	0.79	154.03	1491	156.75
hexyne,diol	0.50	149.12	4297	152.19
	1.49	145.84	1487	149.81
	0.57	154.30	2110	156.86
Mean Temp.	150.82	Std. deviation		3.54
HADN w/ S-HAN5	1.30	112.86	1774	115.54
	1.53	151.14	1409	155.43
	0.46	157.83	3660	160.56
	0.91	156.51	1665	160.05
Mean Temp.	144.59	Std. deviation		18.49
HADN w/	1.12	158.22	1136	160.80
methylsulfolane	1.26	155.97	330.2	157.78
	0.76	158.80	1517	161.48
	0.57	157.75	2474	160.84
Mean Temp.	157.69	Std. deviation		1.06
HADN	1.43	151.15	1128	154.68
	1.63	154.36	1258	157.13
	1.27	155.54	1307	158.50
	0.89	155.32	1241	159.63
	1.34	155.26	853.1	158.23
	1.10	154.54	1353	158.06

Mixture	Weight(mg)	Onset($^{\circ}$C)	Area(J/g)	Peak($^{\circ}$C)
	1.04	154.00	1236	158.46
	1.36	154.98	1338	157.99
Mean Temp.	154.39	Std. deviation		1.322
HADN w/	1.20	150.44	1235	153.44
hexyne,diol	0.97	146.23	1328	153.66
	0.66	154.36	825.5	180.23
	0.91	147.55	1241	152.71
	0.57	148.95	1124	172.30
	1.09	143.43	1412	148.97
Mean Temp.	148.49	Std. deviation		3.41
HADN w/ S-HAN5	1.87	150.52	1301	153.33
	0.79	154020	1142	159.65
	0.73	153.68	1043	159.81
	1.10	148.05	1158	152.24
	1.73	133.56	1275	136.96
	1.25	152.16	1246	155.64
Mean Temp.	148.70	Std. deviation		7.07
S-HAN5	1.80	190.54	569.0	194.12
	0.54	185.11	10.42	186.62
	1.66	180.81	469.1	183.78
	1.55	155.24	950.8	161.16
	1.82	159.39	888.2	164.09
Mean Temp.	174.22	Std. deviation		14.20
HADN w/	1.53	154.31	1180	157.59
methylsulfolane	1.04	154.56	1244	159.20

1-7

Mixture	Weight(mg)	Onset(^{o}C)	Area(J/g)	Peak(^{o}C)	
	1.93	149.08	1225	152.67	
	1.46	153.48	1352	156.61	
	0.80	152.18	1279	158.01	
	0.70	151.64	1251	161.66	
Mean Temp.	152.54	Std. deviation		1.87	
HADN	1.19	137.08	889.2	144.11	
	1.40	138.17	455.6	142.99	
	0.95	145.60	1151	163.49	
	0.85	147.99	1126	180.45	
	0.86	137.57	1205	145.30	
	0.75	131.81	1247	165.59	
Mean Temp.	139.71	Std. deviation		5.46	
HADN	0.35	156.35	672.5	182.63	
	0.36	158.48	743.0	183.32	
	0.86	139.47	652.6	148.63	
	0.92	151.67	1158	162.66	
	0.47	155.08	1090	182.78	
	0.71	151.46	992.5	179.74	
	0.44	156.00	1366	164.12	
	0.19	159.86	1142	182.68	
Mean Temp.	153.55	Std. deviation		5.98	
HADN w/ ammonium		1.06	140.90	680.3	142.52
nitrate	0.71	166.04	1184	169.45	
	0.51	157.51	971.6	182.17	
	0.43	149.02	1120	166.55	

Mixture	Weight(mg)	Onset($^{\circ}$C)	Area(J/g)	Peak($^{\circ}$C)
	1.14	151.06	1230	154.55
	0.49	157.18	963.3	182.95
Mean Temp.	155.29	Std. deviation		7.78
HADN w/	0.74	145.07	1277	159.97
dipyridylamine	1.53	147.82	1253	152.71
	0.90	145.95	1283	159.17
	1.12	143.38	1322	150.76
	0.53	161.98	1171	172.00
	0.77	163.06	449.0	188.31
Mean Temp.	151.21	Std. deviation		8.11
HADN w/ diammonium	0.49	151.22	1551	169.09
hydrogen phosphate	1.44	143.42	1388	149.03
	1.85	149.86	1270	153.58
	0.79	152.54	761.5	184.54
	0.77	152.30	1148	163.92
	1.69	142.08	1147	149.83
Mean Temp.	148.57	Std. deviation		4.22
HADN w/ ammonium	0.99	150.96	1230	153.98
dihydrogen	0.92	151.34	1122	160.99
phosphate	0.32	157.28	1016	184.35
	0.69	154.26	985.4	182.93
	1.53	149.16	1373	152.83
	1.48	171.42	1304	177.55
Mean Temp.	155.74	Std. deviation		7.48

Mixture	Weight(mg)	Onset($^{\circ}$C)	Area(J/g)	Peak($^{\circ}$C)
HADN w/ diammonium	1.48	152.47	1249	156.49
& ammonium	1.46	150.17	1446	152.27
phosphate	2.05	128.79	1236	135.08
(0.5% each)	1.44	147.84	1108	162.28
	0.36	158.75	737.6	183.93
	1.11	152.29	1211	159.38
Mean Temp.	148.39	Std. deviation	9.37	
ADN (endothermic)	0.42	90.12	122.1	92.79
	1.22	91.66	127.1	94.10
	2.87	92.67	145.1	95.42
	1.59	91.88	134.0	94.79
Mean Temp.	91.58	Std. deviation	0.92	
ADN (exothermic)	0.42	161.97	1552	190.86
	1.22	157.05	1417	190.46
	1.76	157.36	1695	189.81
	0.82	162.40	1518	191.32
	2.87	157.91	2027	169.23
	1.59	156.82	1509	191.71
Mean Temp.	158.92	Std. deviation	2.34	
HAN5 w/ pin hole	1.35	189.02	451.9	189.78
	1.14	190.89	163.7	192.74
	0.71	207.60	542.2	217.21
	1.03	209.90	773.5	216.29

Mixture	Weight(mg)	Onset($^{\circ}$C)	Area(J/g)	Peak($^{\circ}$C)	
	0.71	200.57	878.5	210.21	
	1.51	200.12	715.6	202.09	
Mean Temp.	199.68	Std. deviation		7.74	
HAN w/o pin hole		1.43	172.12	993.8	174.81
	0.47	174.31	458.1	179.55	
	1.00	174.60	864.4	176.83	
	1.03	132.92	4155	136.57	
Mean Temp.	163.49	Std. deviation		17.67	

Conclusion

As a result of the differential scanning calorimetry testing, several things were learned. First, ADN, HADN, and S-HAN5 had similar temperatures of decomposition. Before selecting an oxidizer for future use from the previous choices, other factors such as stability in a propellant and ease of production will affect which one is chosen, if any. Second, the additives mixed in with HADN seemed to have no significant effects on DSC testing. This seems to indicate HADN is compatible with those additives. This knowledge will help if HADN is ever used in a propellant. In the S-HAN5 testing, only the 2,2'-dipyridylamine seemed to have much of an effect on the decomposition temperature; however, since the 2,2'-dipyridylamine test had such a large standard deviation, further testing is recommended. Since the standard deviation was large for several of the

additives, other tests can be use to get better results. Such
tests might include gas evolution analysis and thermogravimetric
analysis. Lastly, the DSC method might be changed to produce
better results. Higher concentrations of additives (4-5%) would
make changes in the onset temperature a little more noticeable.
Sealed glass capillaries, instead of the potentially reactive
aluminum pans, might provide more consistency in results.
Finally perhaps a slower heating rate (5°C/min or even less)
would reduce the variation in results.

References

Speyer, Robert F. 1994. <u>Thermal Analysis of Materials</u>. New
    York: Marcel Dekker.

Wendlandt, Wesley. 1986. <u>Thermal Analysis</u>. New York: John
    Wiley & Sons.

REFLECTED LASER COMMUNICATION SYSTEMS

Rhianna DaSalla
Space Experiments Directorate

West Mesa High School
6701 Fortuna Road, NW
Albuquerque, New Mexico 87121-1399

Final Report for:
High School Apprenticeship Program

REFLECTED LASER COMMUNICATION SYSTEMS

Rhianna DaSalla
Space Experiments Directorate
Phillips Laboratory

Abstract

The study was done on a concept for a reflected laser communication system. The proposed communication system is achieved by directing a laser towards a retroreflector located at the remote point of the link. The remote site encodes telemetry on the reflected laser with an optical modulator. The primary advantage of this approach is that equipment at the remote sight can be extremely low in power and weight. Other benefits include less weight and volume required aboard the satellite, the complex parts are on the ground for easy access, and potential for very high data rates.

REFLECTED LASER COMMUNICATION SYSTEMS

Rhianna DaSalla

In the past communicational methods through long distances have been hard to achieve. During the 1920s the Pony Express was the most highly advanced system used for communications. Since then we have seen various radio transmitting devices: walkie talkies, CBs, phone lines and satellite communication. Todays most advanced method of communication are satellites, which we are currently working to improve.

Satellites currently use on-board transmitters to send information from the spacecraft to the ground. At times this information may be sent from one satellite to another and then to the ground. The information sent includes both data from the scientific instruments and experiments aboard as well as on-board conditions and current mechanical status. This data provides information regarding the status of the satellite and its systems. An alternate approach to current systems is laser communications, which does not require extensive hardware on the satellite. The problem of most concern is communications from the satellite to Earth.

As the amount of data to be sent to the ground station increases the size, weight, complexity of the transmitter also increases. Size and weight increases lead to less volume and weight available for scientific instruments in the payload. Also, ground stations can only receive on certain frequencies at certain times so even having an appropriate transmitter does not guarantee that all the available data can be sent down.

The desirable motive would be to eliminate the need for an on board

transmitter entirely or devise a system that is reduced in size, weight, and volume. One proposed solution is to use a system based on reflected laser light. A beam of light can carry enormous amounts of information as is done in fiber-optic communication. However, to avoid using a cable from the satellite to the ground, the light would have to be a coherent, tightly focused, laser beam. The problem is that a laser beam generator is big and heavy so replacing an on-board transmitter with a laser device isn't really and improvement. The proposed suggestion is that perhaps a neutral beam could be generated on the ground, sent to the spacecraft, modulated to carry the data, and sent back down thus requiring only a reflector and modulator on the satellite. It has been presented that and earth-satellite-earth laser downlink system which is compact, simple, and low-power enough could be considered for use on very small satellites. This approach offer the potential advantage of significantly reducing the size, power and weight of hardware required aboard the satellite for laser communications while maintaining the advantages of laser communications in general (high data rate, low probability-of-intercept, etc.).

New advances in military and global-environmental monitoring sensors or space science experiments will require data obtained simultaneously from constellations of satellites. The expense of such constellations of satellites is prohibitive if one uses the current mode of large, expensive, low-risk satellites produced by the DOD and NASA in programs which take decades to complete. If constellations of current technology satellites are to be produced they must be small, light-weight, effective, inexpensive, and rapidly deployed.

A motivating feature of reflected laser communication over other types

of satellite communication systems is the minimal impact such a system will have on spacecraft resources, primarily power. Another benefit is the significant reduction in the over all complexity and cost of a spacecraft that can be achieved by reducing the power demands of a key subsystem such as communications. From a satellite-to-Earth communications link for spacecraft in low Earth orbit, it is expected that valuable information will result from this research for many other potential applications (for balloon payloads as well as spacecraft).

Laser communications from ground to low earth orbit is relatively simple because most of the hardware is on the ground and the satellite need only be provided with a relatively simple sensor. The project includes a laser site on the ground which illuminates the s a satellite with either a continuous beam or a uniform train of pulses. On board the satellite is a corner cube, which reflects the incident laser light directly back to the transmitter on the ground (retro-reflection). Associated with the corner cube is a modulation mechanism which reacts rapidly to change the intensity or the polarization of individual reflected pulses. By appropriately controlling this retromodulator the laser light pulses reflected back to the ground station are encoded with the communications signal.

It would be desirable for many small satellite applications to have a downlink system which is extremely low-power and compact. For this reason this system is designed to keep the vast majority of the space, weight and power required for a satellite communications system off the spacecraft by using a ground laser and a spacecraft mounted retroreflector/optical modulator. The assembly consists of four independently controlled

INTEGRATION INFORMATION

I. Instrument Parameters
   A. Volumetric Envelope: The experiment will consist of two boxes, and electronics box and a retromodulator/receiver box.
      1. The electronics box is roughly 5 x 5 x 2 1/2 inches.
      2. The retromodulator box is roughly 5 x 5 x 2 1/4 inches.
   B. Weight: The total weight of the experiment is expected to be 4 to 5 lbs.
      1. The weight of the electronics box is about 2 lbs.
      2. The weight of the retromodulator housing is about 2 lbs.
   C. Power requirements: The total power consumed by the experiment is expected to be about 6 watts when on.
      1. There will be a standby mode for this experiment consuming about 3 watts. During this mode the retromodulator would be held at operating temperature.
   D. Thermal Requirements (for satellite use): The experiment will temperature control the retromodulator in the range of 20 to 30 degrees C for operation.
      1. The retromodulators most be kept below 50 degrees C at all times for survival requirements. Minimal survival temperature is approximately -20°C.
   E. Telemetry Requirements: The experiment will require about 2 to 4 bytes/minute whenever the experiment is operating or in standby mode.
   F. Pointing Requirements: The top of the retromodulator box must be mounted nadir pointing.
      1. The retromodulator must have an unobstructed 45 degree half angle view of the Earth
         a. Pointing accuracy is about 5 to 10 degrees.
      2. The retromodulator can be pointed at the sun without damage.
   G. Sensitivity and Contamination: The retromodulator optics must be kept clean.
   H. Potential Hazards And Safety Constraints: There are no safety constraints associated with the instrument.

retromodulators with the necessary temperature controllers and a receiver (see figure 1-1). There will have to be a constant temperature because of the fact that in space and in the upper atmosphere (see graph 1-2) the temperature drops exceptionally low (-77oC). The different retromodulators will be used to test amplitude and polarization modulation schemes. Filters will be built into the retromodulators for testing selected wavelengths and simultaneous downlinks by using different frequency lasers. The retromodulators will be constructed from hollow corner cubes and ferroelectric liquid crystal (FLC) device which acts as a controllable light valve. The instrument must be placed in a stand by mode for at least 30 minutes before being turned on the bring the retromodulator to operating temperature.

The retromodulator assembly will be mounted on the spacecraft such that it has a clear view of the Earth. Most of the complexity of a reflected-laser communication system for satellites in low earth orbit is on the ground in the transmitter/receiver tracking station. Power requirements are not a constraint for ground stations in the same way they are for satellites. Complexity is also not as great of concerns for the Earth stations since modifications or repairs can be made without loss of mission. In case something fails or breaks down it is much easier to fix it on the ground than in space. For example the Hordell telescope repair exceeded a half billion dollars if you include the STS costs. The receiver portion of the experiment will consist of a simple photo detector and field of view expanding optics. Receivers exist at the ground stations for detecting both amplitude modulated signals and polarizations modulated signals at various laser

Figure 1-1
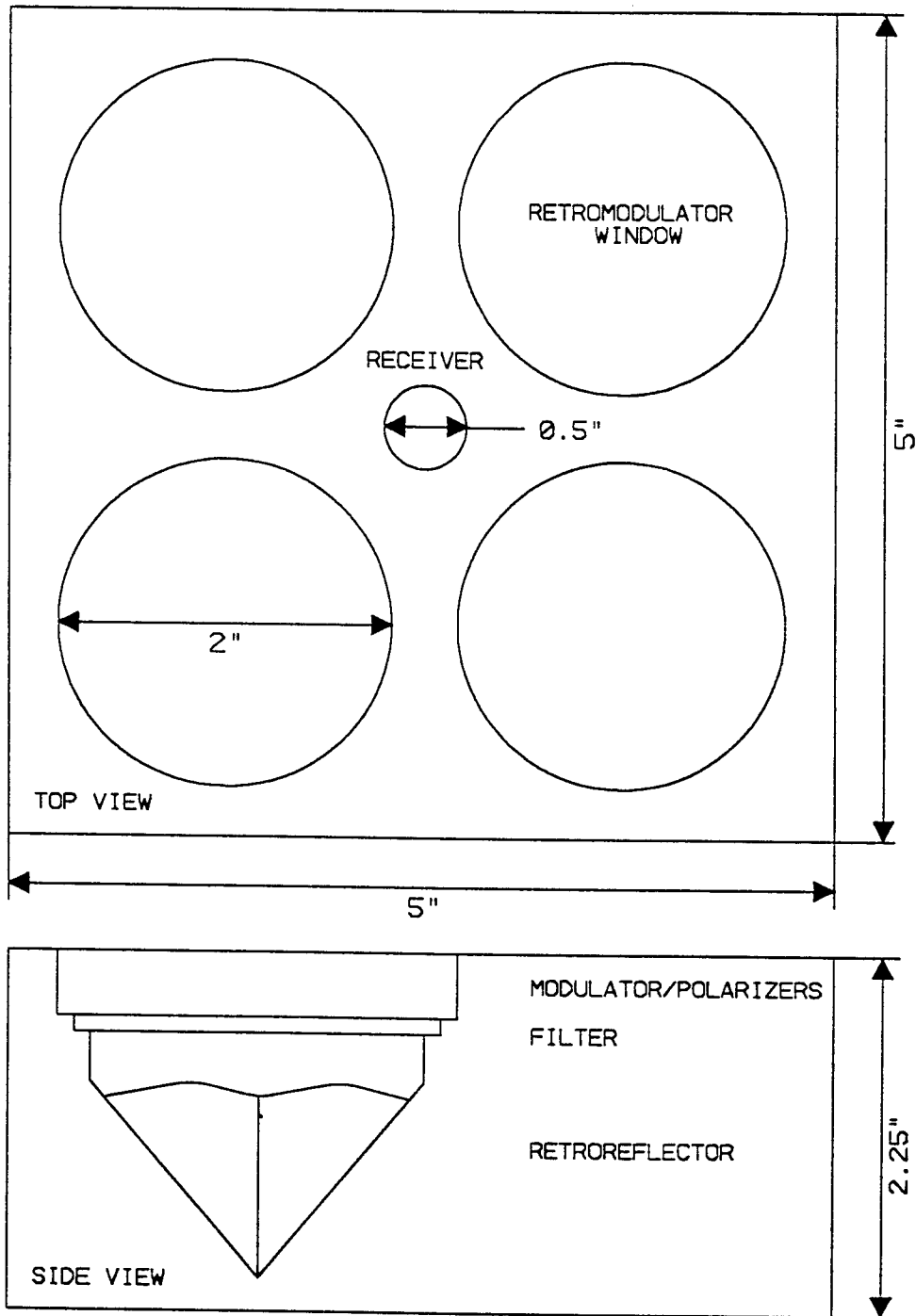
A diagram of the retromodulator housing. Four retromodulators are mounted in this housing along with a receiver. Each of the four retromodulators are different and comprise a separate experimental investigation into retromodulator design.

Graph 1-2

UPPER AIR TEMPERATURES FOR HOLLOMAN SITE, OCTOBER
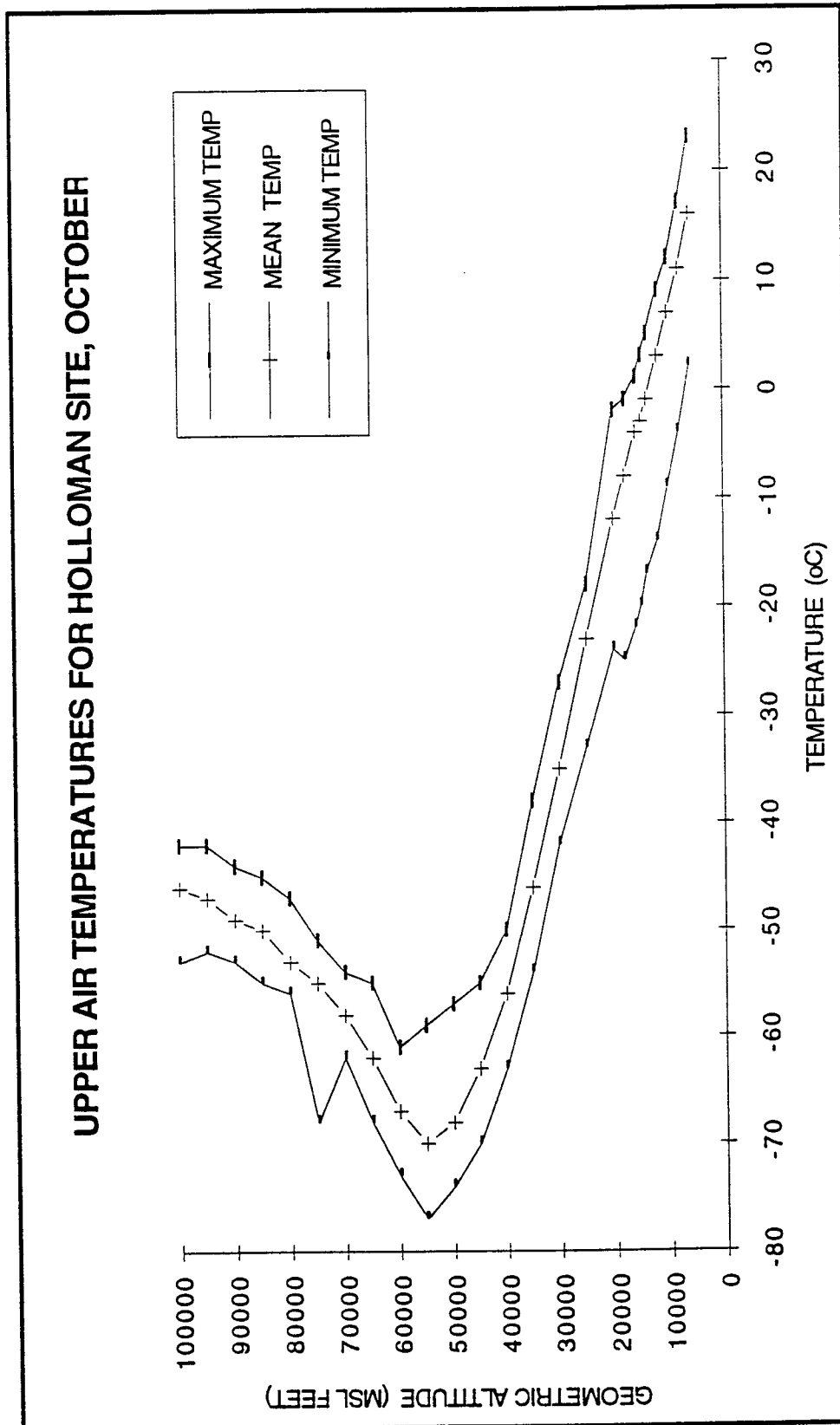
wavelengths. The ground receiver system will be a large aperture (1-meter class) telescope co-aligned with the laser transmitter, and a direct detection detector system (see figure 1-3).

The light-weight, efficient nature of the spacecraft system has its drawbacks, however, in the increased size and complexity of the ground station. This probably indicates that the system is best suited for data communications to a group of satellites.

Balloon systems are currently being used to perform low cost validation of spacecraft technology. In late September, early October 1994 there is a proposed balloon flight in conjunction with the Department of Energy in order to validate the technology being proposed. This is the second step in technology validation. The first being an on ground testing, the third being the actual satellite testing. The balloon mission will last anywhere from six to eight hours, and will be launched from the southern portion of Kirtland Airforce Base, Albuquerque, NM. The Starfire Optical Range will provide the use of a laser and telescope to support both the balloon and satellite experiments. At the times the balloon is visible the Starfire Optical Range will illuminate the retromodulator portion of the payload. In addition, Phillips Laboratory Laser/Optical facilities at Maui, HI and Malabar, FL will be used to support the proposed satellite experiment. Laser communication experiments were also included in a recent Phillips Laboratory/University of New Mexico satellite proposal to NASA. Reflected laser communications have come farther than known.

Figure 1-3

SPACECRAFT MOUNTED RETROREFLECTOR/
OPTICAL MODULATOR

UNMODULATED LASER BEAM

MODULATED REFLECTED
BEAM

LASER

TELESCOPE

STARFIRE OPTICAL RANGE
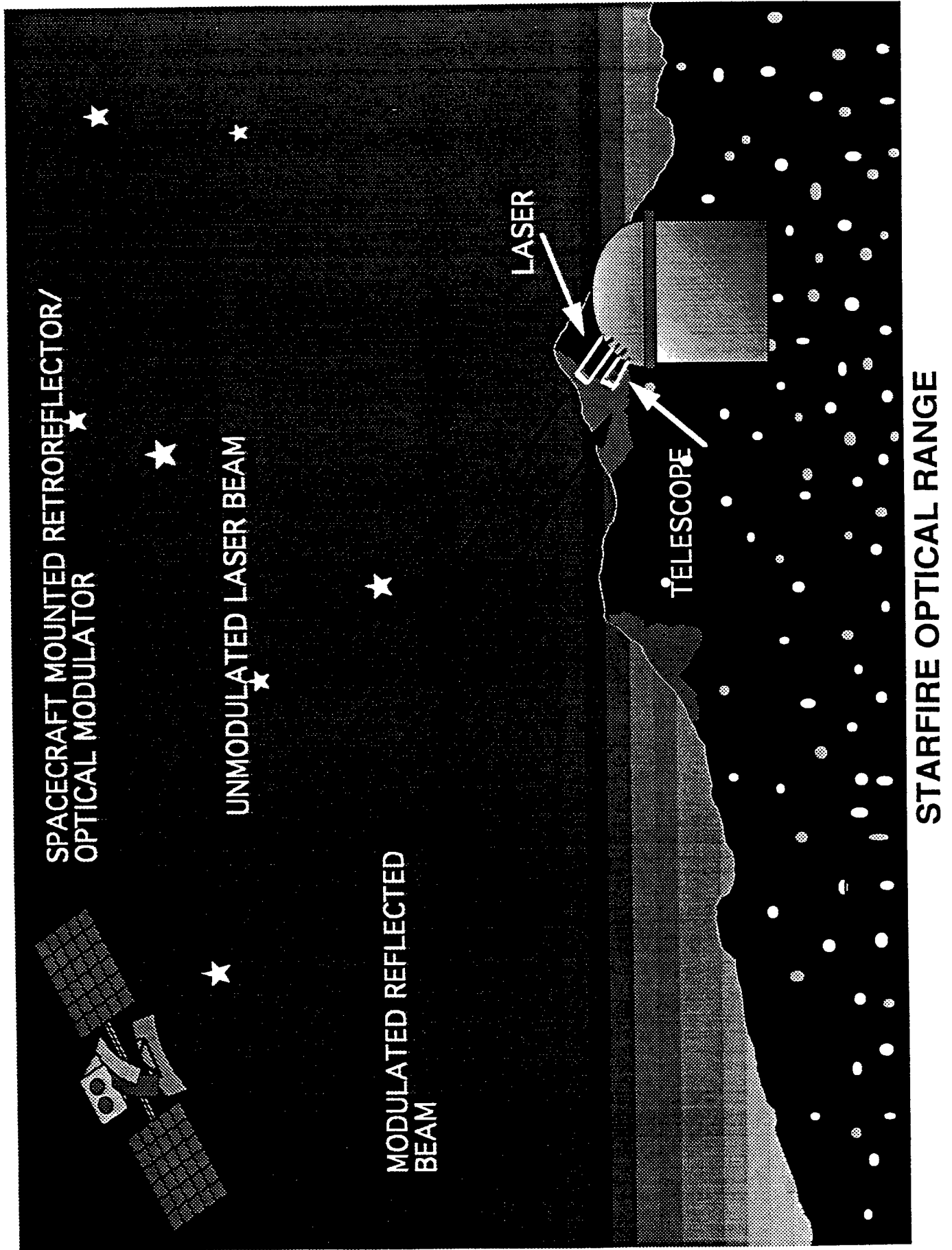
Bibliography

Swenson, Dr. Charles M. <u>Reflected Laser Communication Systems AFOSR Summer Research Program</u>, unpublished proposal. August, 1994.

Swenson, Dr. Charles M. <u>Reflected Laser Communication Systems STEDI Small Satellite Proposal</u>, unpublished proposal. August, 1994.

Swenson, Dr. Charles M., Gary Jensen. <u>A Laser Downlink For Small Satellites Using An Optically Modulating Retroreflector</u>, unpublished manuscript. August, 1994.

CONSTRUCTION AND TESTING
OF A DUAL PHOTODIODE RECEIVER UNIT

Alexander E. Duff

La Cueva High School
8001 Wilshire Blvd. NE
Albuquerque, NM 87109

Final Report for:
High School Apprenticeship Program
Phillips Laboratory

July 1994

CONSTRUCTION AND TESTING
OF A DUAL PHOTODIODE RECEIVER UNIT

Alexander E. Duff
La Cueva High School

Abstract

The speed of a laser being swept by a scanning mirror was important to measure. The speed of the beam could be measured if it was known how long it took to travel across a known distance. An electronics box was constructed for this purpose. The box included photodiodes that responded to light when it passed over them. The speed of the laser could then be measured using an oscilloscope that measured the time interval between the beam hitting the photodiodes. After the box had been constructed, testing was done, and the box performed its purpose flawlessly.

CONSTRUCTION AND TESTING
OF A DUAL PHOTODIODE RECEIVER UNIT

Alexander E. Duff
La Cueva High School

Introduction

In some applications involving imaging and lasers, it is useful to know how fast a beam of light is moving, or the rate the light is changing across an aperture. A potential application of this knowledge is the imaging of satellites by reflecting a laser off a satellite onto a row of receivers that take images at fixed time intervals. In this way, a complete image of a satellite can be taken with only one row of receivers.

Discussion of Problem

One way to measure the velocity of a laser is to build a photodiode receiver unit that can sense when light is directed at the photodiodes and output that information to an oscilloscope. If there are two photodides in the receiver and the distance between them is known, the oscilloscope can measure the time difference, and the speed can be determined using the equation:

$$R = \frac{D}{T}$$

Where R is the rate, D is the distance, and T is the time. Therefore a dual photodiode receiver unit, known as DAPUT, was constructed to measure the scan rate of the laser. The box consisted of an external power source, an on/off switch, internal power supply, two photodiodes, and two outputs to coaxial type cable.

Methodology

The first step in building DAPUT, or dual photodiode receiver unit, was to design the circuit for the photodiodes to the outputs. With the help of Dave Holmes, an electric technician, a circuit was developed around two Burr-Brown OPA111 operational amplifiers, and two Siemens BPX 66 pin photodiodes. See circuit configuration (Fig. 1). The circuit would receive a signal, a light source, and the current generated would run through the amplifier to an output. Two pins of the amplifier were for the power source, four pins were unused and grounded, one pin was connected to the photodiode, and one pin was used for the output.

After designing the circuit, the parts were bought that would be necessary for the construction. Machining tools such as the drill press, band saw, and the mill were used in the construction. After thoroughly planning the location of parts and construction of the box, building actually began by cutting the circuit board to fit inside the box using the bandsaw. Next, holes were drilled in the front panel for the photodiodes and screws to fasten the board to the panel. Then, the mill was used to grind away mounting cones on the base of the box so the power supply would fit. The final step in preparing the box was to cut holes in the rear panel for the power cable, switch, LED light to indicate when the box is on, and output terminals. After all this was completed, the parts were mounted on the box.

The next step was to wire the parts together, such as connecting the power switch to the power supply, and the power cable to a fuse. Finally, the components were soldered to the circuit board as well as the power and output cables, to complete the box. Figure 2 shows the front panel of the completed DAPUT with screws holding the circuit board in the four corners, and the photodiodes centered vertically, and figure 3 shows a view of the inside construction from over the right rear corner shows the power supply (A), circuit board (B), and output cables (C).

When all these steps had been completed, testing began on the outputs to see if voltage was being generated. The box seemed to be functioning well, so the box was connected from its outputs to an oscilloscope to confirm that changes in light intensity were reflected by the output. This test was also successful. Figure 4 shows the initial uncompensated test results of light input. Channel 1 is seen on top (A), channel 2 in the middle (B), and the voltage in the LED providing light is the bottom (C). The circuits had to be compensated with capacitors to prevent the current in the feedback loop from causing a ringing effect on the test results. Figure 5 shows the channel 2 output both uncompensated (D) and compensated with a 2pF capacitor (E). Figure 6 shows the channel 1 output both uncompensated (F) and compensated with a 1pF capacitor (G). Channel 2 required a larger capacitor because there was more length to the wiring, and consequenly, more electronic "noise" was picked up.

The final procedure was to setup the actual experiment with the scanning mirror, laser, and photodide box. The laser did sweep across the photodiodes, and the output was clear. DAPUT was successful in its purpose.

Results

Measurements taken were the time interval between voltage outputs from the photodiodes, period of the mirrors scan, and the distance between the DAPUT and the scanning mirror. In the first instance, the time between the beam hitting each of the photodiodes was 10.8 mS. Since the distance between photodiodes was known to be 4 in, or 10 cm the rate was calculated to be 9.26 M/S.

Following these equations:

$$SIN\ \theta = \theta \qquad\qquad TAN\ \theta = \theta$$

For small θs

The angle formed by the two photodiodes and the laser could be found simply by dividing the distance beteween the photodiodes and the length from the laser to DAPUT, 6.9 meters. Therefore, the angle divided by the time, or angle rate, was calculated to be 1.34 RAD/S. In the second instance, the time interval was 4.7 mS and the rate was calculated to be 21.27 M/S and the angle rate was 3.08 RAD/S.

Conclusions

After the careful planning and construction, DAPUT was a total success. The mission it was designed to accomplish, to measure the rate at which a laser beam was changing, was completed. Also, the areas of electronics, construction of circuits, lasers, and optics were introduced. This project was successful for many reasons. DAPUT will be used in the future experiments of this branch, and the author was introduced to the fields of optics, electronics, and machining.
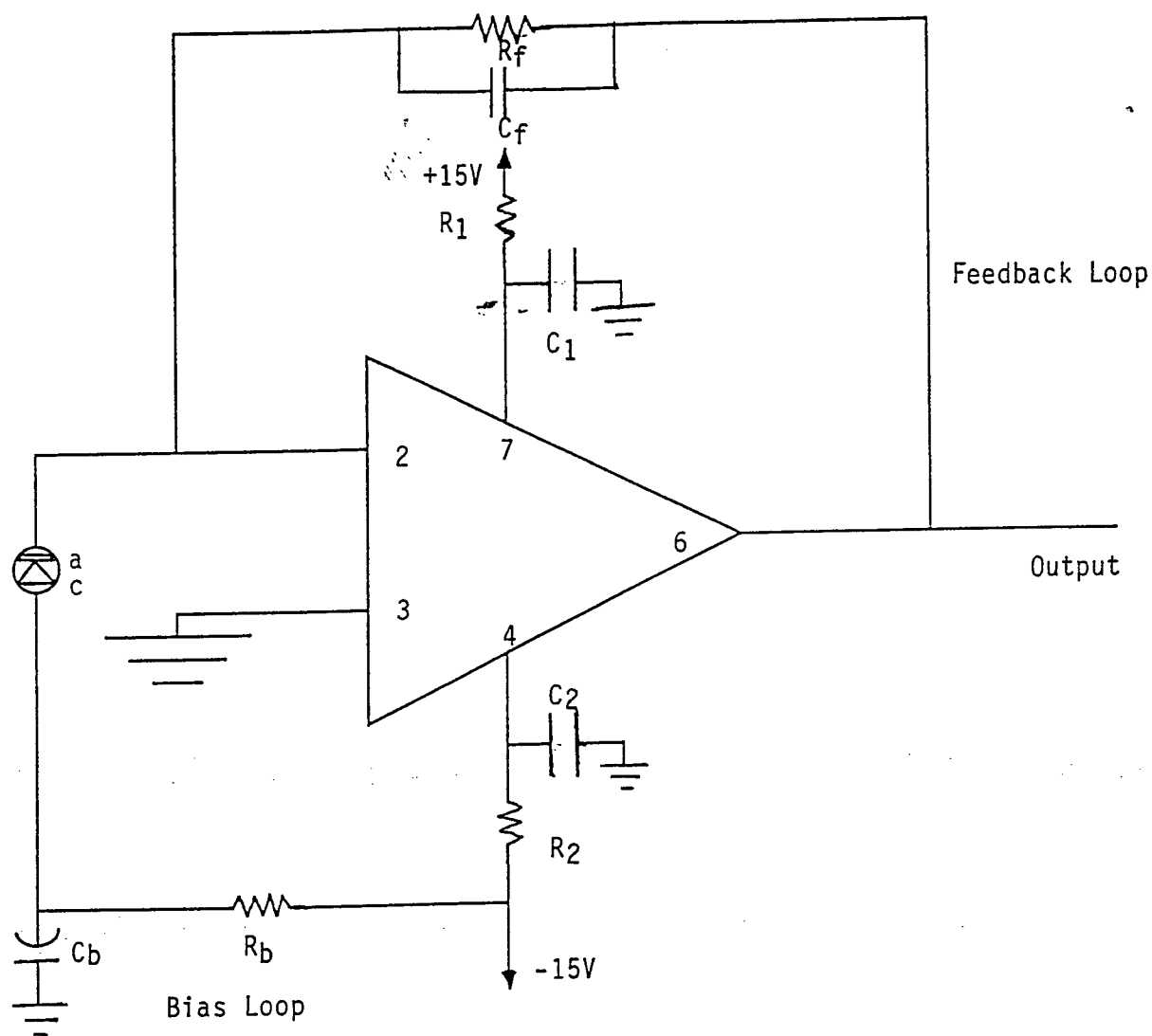
Figure 1

COMPONENT	C1	C2	R1	R2	Rf	Cf	Rb	Cb
VALUE	.1uF	.1uF	100 W	100 W	1 MW	1pF ch. 1, 2pF ch. 2	10 KW	27uF
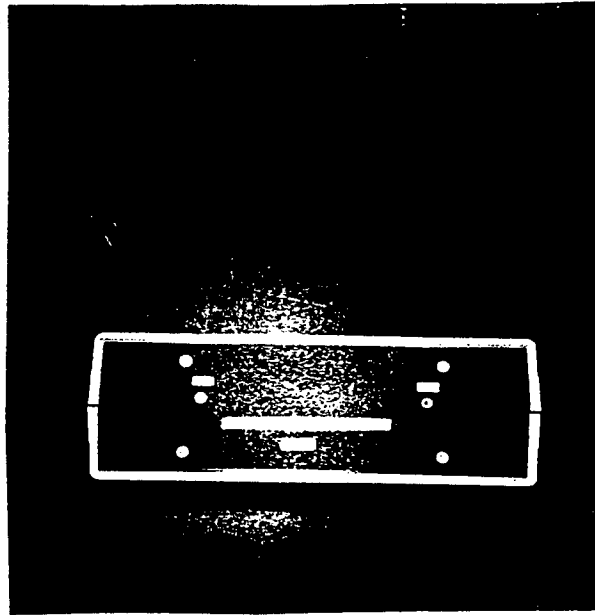
Figure 2

Figure 3
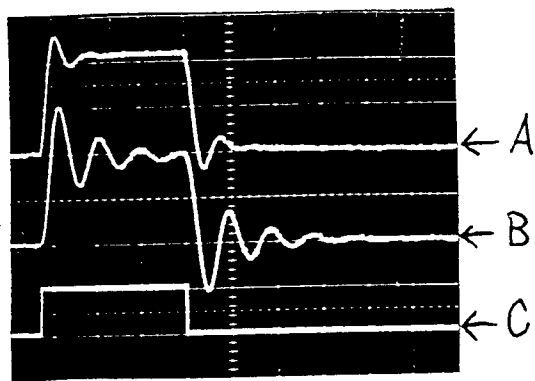
Figure 4
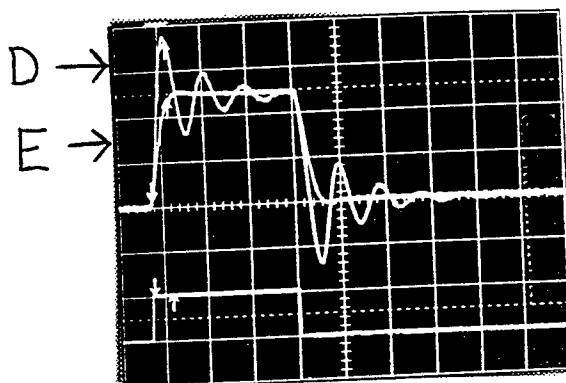
Figure 5
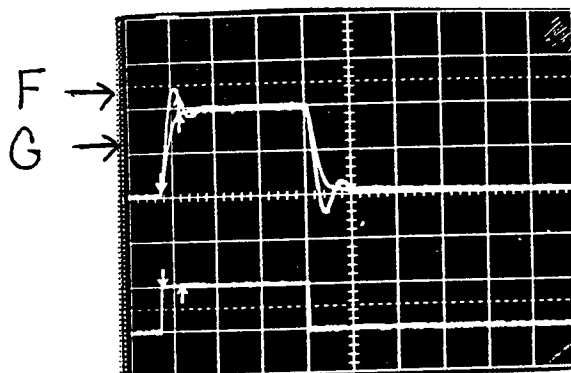
Figure 6

A STUDY OF LINER COMPOSITIONS
FOR SOLUTION PROPELLANTS

Bridget C. Engelhardt

Paraclete High School
42145 North 30th Street West
Lancaster, CA 93536

Captain Bernard Wilkerson
Dr. Tom Hawkins
Mentors

Final Report for:
High School Apprenticeship Program
Phillips Laboratory

A STUDY OF LINER COMPOSITIONS
FOR SOLUTION PROPELLANTS

Bridget C. Engelhardt
Apprentice
Paraclete High School

Abstract

The strength of adhesion of epoxy resin liners to solution propellants was studied. Test specimens (R-BITS) were prepared by coating aluminum plates with various liner materials then placing a solution propellant (composed of hydroxyl ammonium nitrate and polyvinylalcohol) between the liners. The strength of the adhesion of the liner to the solution propellant was tested using rectangular bond-in-tension samples on an INSTRON test machine. The results indicated that neither conventional liner nor epoxy formulations (utilizing Trimer acid and ERL 4221) adhered to the solution propellant sufficiently to be useful as rocket motor liners.

A STUDY OF LINER COMPOSITIONS
FOR SOLUTION PROPELLANTS

Bridget C. Engelhardt

Introduction

Liners have been used for years to ensure adhesion between motor cases and the propellant. However, recently a new type of propellant called solution propellant has been developed. When tested with a conventional (T3-AS) liner (control), it proved a new liner system was needed. Conventional propellants typically have a hydrophobic matrix and the liner also tends to be hydrophobic and chemically reactive to the propellant. This is not true in the solution propellant case. The hydrophilic matrix of the solution propellant requires a compatible liner. Therefore, different approaches are being taken to find functional lining systems for solution propellant. An epoxy approach which involves chemical bonding is shown by Equation 2. Another approach, physical bonding by embedment, is considered and demonstrated in Equation 1.

Methodology

Six different liner formulations were tested using rectangular bond-in-tension specimens (R-BITS). Two liner controls were used- a T3-AS liner which represents liner normally used for conventional propellants, and a Kraton 1102 liner. The T3-AS Liner consisted of R-45M (a hydroxyl terminated polybutadiene), titanium dioxide (TiO_2), Carbon black (C), DDI (a reactive Aliphatic Diisocyanate), and dibutyl tin dilaurate (DBTDL). The Kraton 1102 liner consisted of 80% Dichloroethane and 20% Kraton 1102. Both of these liners were applied to the R-BIT aluminum plates, but the T3-AS liner was cured for 3 to 5 hours at 140°F before the 80% HAN / 20% PVA solution was injected into each R-BIT. The Kraton 1102 liner was cured at ambient temperatures overnight, after which the 80% HAN / 20% PVA solution propellant was injected into the specimen.

Five specimens were made for the T3-AS liner, and one specimen of the Kraton 1102 liner was made. After one week, the T3-AS and Kraton specimens were tested on the INSTRON.

Embedding PVA into Kraton is an approach to making a liner which utilizes physical bonding. Equation 1 shows this approach. The drawing on page 4-6 shows the two liner approaches. The second one titled "Physical Bonding" also illustrates the solution propellant bonding to the PVA and Kraton liner.

Equation 1

Physical approach

$$S\text{---}B\text{---}S \quad + \quad CR_2\text{---}CH\text{---}OH \quad \longrightarrow \quad \text{No Chemical Reaction}$$

$$\text{Kraton} \qquad\qquad \text{POLYOL}$$
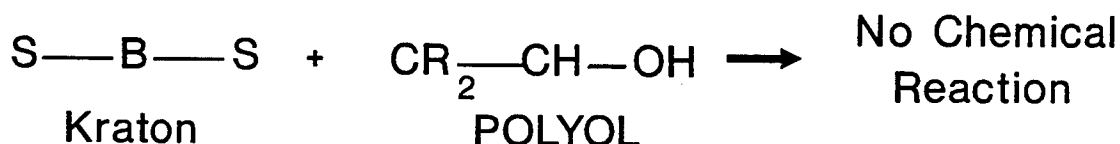
A liner used for 2 x 4 motors was also made and tested. When lining the 2 x 4 motors, 20cc of the Kraton 1102 solution are applied to the motor wall as it rolls on a roller. After waiting approximately twenty-seven minutes, 10cc to 15cc of PVA can be injected into the rolling motor. Wait for 2 to 3 hours before taking the motor off the roller. Allowing it to roll for this amount of time helps the PVA become embedded into the Kraton, but at the same time keeps it from being absorbed by the Kraton. This liner was used successfully for motor firings up to 1200 psi. The illustration on page 4-5 shows a motor case with both the liner and the propellant.

This approach was also tried on the R-BIT aluminum plates in hope of preparing R-BITS with the solution propellant. While 0.5g of the Kraton 1102 was

applied to each of the plates, followed by a two minute time delay, approximately 1g of PVA was added to the Kraton. After sitting in the desiccator for an hour, the Kraton absorbed some of the PVA that was added. This made the liner break apart more easily. It did not show the elasticity that the liner in the 2 x 4 motors have. To create better R-BITS, more work with the Kraton liners will need to be done. This includes figuring the perfect amount of time to wait before the PVA is added. The drawing below contains a R-BIT specimen.

Liner Locations

Motor Case

Liner

Propellant

Aluminum Plate
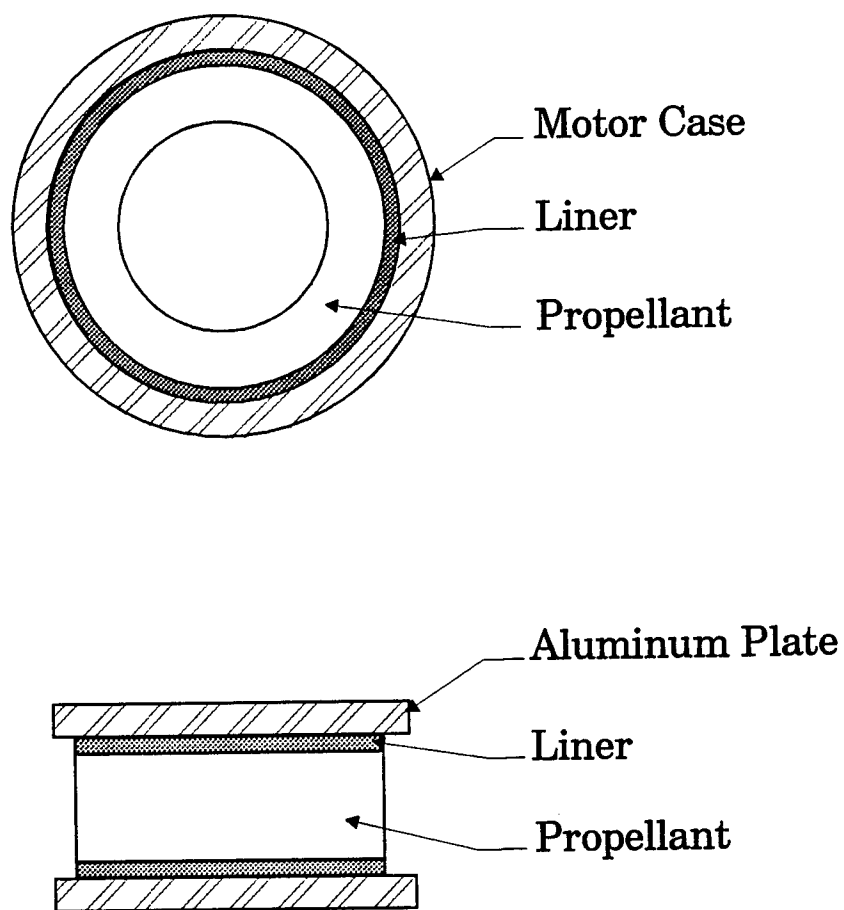
Liner

Propellant

Liner Approaches

Chemical Bonding
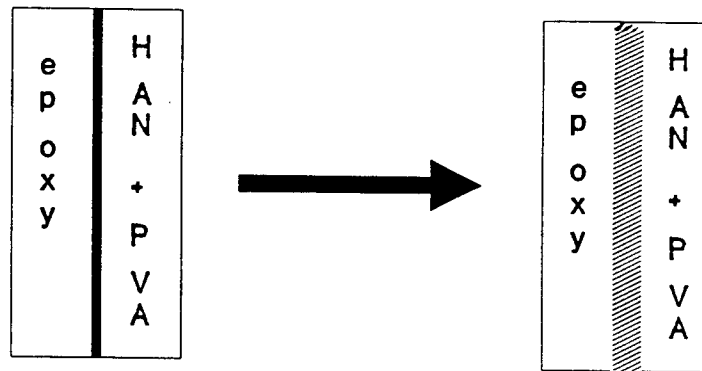
Physical Bonding
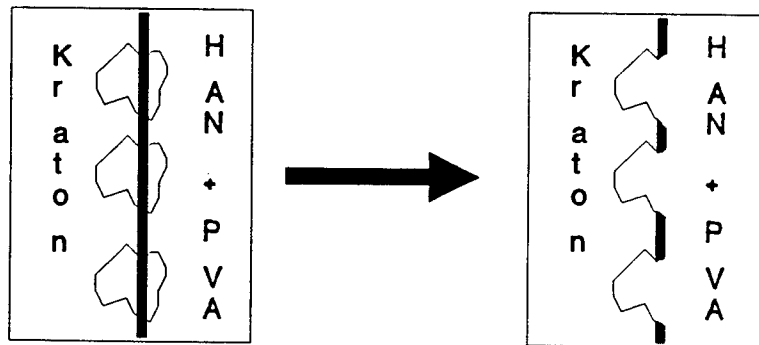
The epoxy approach is another attempt that was tried with the solution propellant. Equation 2 shows the pertinent reaction while the "Liner Approaches" also illustrates this reaction shown above. Two different weight ratios of Trimer Acid to ERL 4221 were tried. A 3 to 2 Acid / ERL 4221 ratio and a 2 to 1 Acid / ERL 4221 ratio were tried. Both were cured at 60°C for 2.5 hours. For the 3 to 2 ratio, the 80% HAN / 20% PVA solution was injected between the two aluminum plates. However, the 2 to 1 ratio is not as sticky as the 3 to 2 ratio

so a thin layer of the ERL 4221 was applied just before the solution propellant was injected into the teflon mold between the two aluminum plates. Five R-BIT samples of each of these liner formulations were made and tested on the INSTRON after waiting for the propellant to cure at ambient temperatures for one week.

Equation 2

Chemical approach

$$R-CH \underset{\displaystyle \diagdown \,O\, \diagup}{\overline{\hspace{1.2cm}}} CH_2 \; + \; H-R \; \longrightarrow \; R-\overset{\displaystyle OH}{\underset{|}{CH}}-CH_2-R$$

Epoxy   OXIDIZER
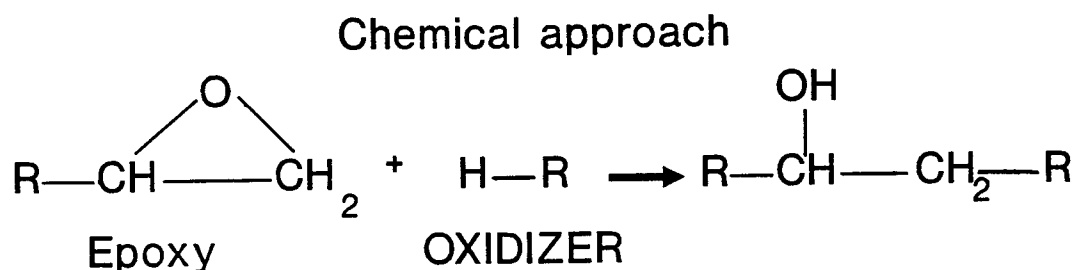
The sixth set of R-BIT samples consisted of a polymer (Poly vinylamine-co-vinylalcohol with 12 mol% vinylamine) embedded into the epoxy resin. This was attempted using a 3 to 2 Trimer acid / ERL 4221 ratio and the polymer was added before the liners were cured for 2.5 hours at 60°C. After curing, the 80% HAN / 20% PVA solution propellant was injected between the two aluminum plates. Then after the propellant had a chance to cure for one week at ambient temperatures, the 5 specimens were tested on the INSTRON.

The R-BIT test specimen illustrated on page 4-8 is composed of two aluminum plates, the liner to be tested applied to both aluminum plates and the solution propellant (HAN+PVA) between the liner. These specimens were tested on the INSTRON machine by sliding the ends of the plates into the slots of stationary and moveable heads. At a crosshead speed of 0.2 in./min., the samples were pulled testing the bond strength between the propellant and the liner. The Maximum Load was recorded using the fifty pound scale. The Maximum Load (lb) can

be converted to Maximum Stress (psi). By dividing the 0.8 sq. in. area of the R-BIT into the Maximum Load reading of each sample. The failures observed in the test specimens were all either adhesive liner failures or cohesive liner failures. The solution propellant never failed (it fails at about 100 psi while the test liners failed between 3 and 14 psi).

Liner Test Method

Approach

Rectangular Bond in Tension specimen
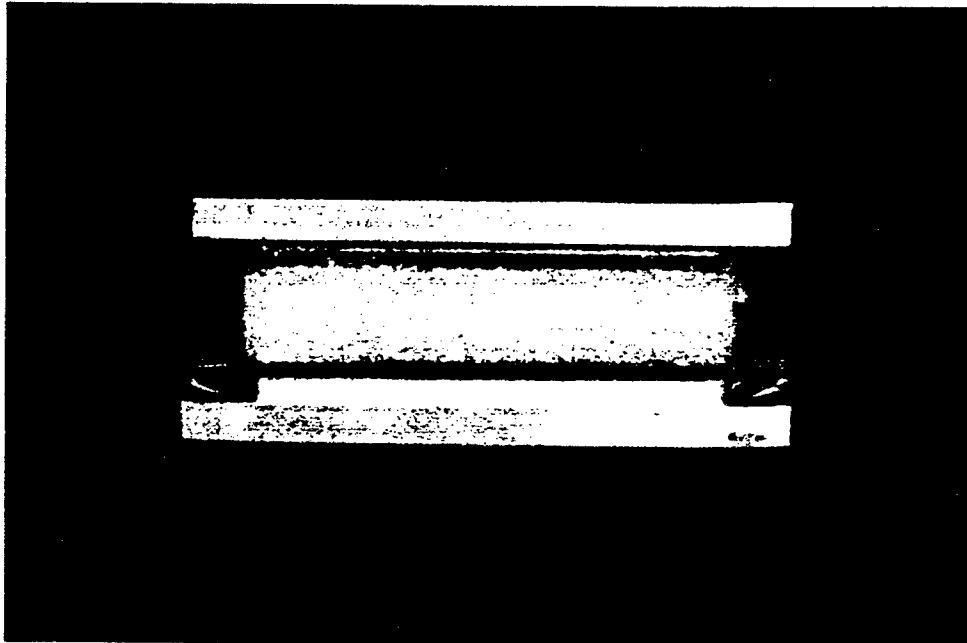
Results

Maximum loads causing failures of various liner formulations tested on the INSTRON are shown as averages on the bar graphs on pages 4-12 and 4-13. Both graphs display the conventional T3-AS liner as a comparison for the chemical approach taken with the 3 to 2 and 2 to 1 ACID/ERL 4221 ratio and the physical approach taken with the embedment of the poly (vinylamine-co-vinylalcohol) into the epoxy resin.

The conventional liner was tested on the INSTRON at a 0.2 in./min. crosshead speed. The Maximum Load (lb) of the samples ranged from 2.5 to 4.7 lbs while the Maximum Stress (psi) after being calculated ranged from approximately 2.6 to 5.9 psi. The average of the Maximum Stress was 4.1 psi as shown on the graphs (pages 4-12 and 4-13).

TABLE 1

Sample x Section Area = 2 in. x 0.4in. = 0.8 sq. in.

Sample	Max. Load (lb)	Max. Stress (psi)	Average Max. Stress
CL 1	3.9	4.9	
CL 2	4.7	5.9	
CL 3	2.3	2.9	
CL 4	2.1	2.6	
CL 5	Fell Apart		4.1

CL (Conventional Liner)

The Kraton 1102 liner alone was not tested on the INSTRON since the single specimen prepared fell apart before the teflon mold was completely removed. This demonstrated no significant adhesions of the Kraton to the propellant.

The 3 to 2 epoxy liner failed cohesively on three of the R-BITS, but failed adhesively on the fourth. The reason for the cohesive liner failure was believed to be due to a short cure time of 2 hours. Thus, cure time was extended to 2.5 hours to avoid future cohesive failures within the liner. However, the liner did

give fair results ranging from 6.7 lbs. to 13.1 lbs. for the Maximum Load while the Maximum Stress ranged from 8.4 psi to 16.4 psi considering the short cure time. The average of the Maximum Stress was calculated to be 11.6 psi. The graph on page 4-12 illustrates these results.

TABLE 2

Sample	Max. Load (lb)	Max. Stress (psi)	Average Max. Stress
EL 1	7.8	9.7	
EL 2	9.4	11.7	
EL 3	6.7	8.4	
EL 4	13.1	16.4	
			11.6

EL (Epoxy Liner)
3 to 2 Trimer Acid/ERL 4221

The adhesive performance of the 2 to 1 epoxy liner appears somewhat better than the 3 to 2 epoxy liner although the deviation in the data makes it difficult to be definitive. This may have happened due to the fact that another layer of the ERL 4221 was applied to the 2 to 1 liner for more adhesion without additional curing. Specimens should be prepared and tested without the layer of ERL 4221 to make this determination. The Maximum Load and Maximum Stress for these two R-BITS is shown on Table 3 while the average Maximum Stress is shown on the graph on 4-12.

TABLE 3

Sample	Max. Load (lb)	Max. Stress (psi)	Average Max. Stress
2 EL 1	9.4	11.7	
2 EL 2	12.1	15.1	
			13.4

2 sets of Epoxy Liners tested
2 to 1 Trimer Acid/ERL 4221

The performance of the epoxy liner embedded with poly (vinylamine-co-vinylalcohol) proved to be as poor as the T3-AS liner. Again, the liner failed adhesively as seen on the graph (page 4-13) while the other epoxy liners failed

two different ways. This was meant to be a physical bonding approach to liner adhesion; however, there was evidence that the embedded polymer was solubilizing and reacting with the epoxy liner and weakening it. Consequently, the physical bonding approach was not modeled well with this epoxy/polymer pair. The Maximum Load and Maximum Stress for these specimens ranged from 0.8 to 6.6psi. The average Maximum Stress is also shown on the graph on page 4-13.

TABLE 4

Sample	Max. Load (lb)	Max. Stress (psi)	Average Max. Stress
EV 1	3.3	4.1	
EV 2	0.8	1.0	
EV 3	1.5	1.9	
EV 4	3.0	3.8	
EV 5	5.3	6.6	3.5

EV (Epoxy w/ vinylamine/alcohol)

Solution Propellant
Liner Test Results

Max. Stress (psi)   Chemical Approach

| | Set 1
epoxy
3/2 acid/epoxy | Set 2
epoxy
2/1 acid/epoxy | Set 3
conventional
liner |

Solution Propellant
Liner Test Results

Physical Approach

Max. Stress (psi)
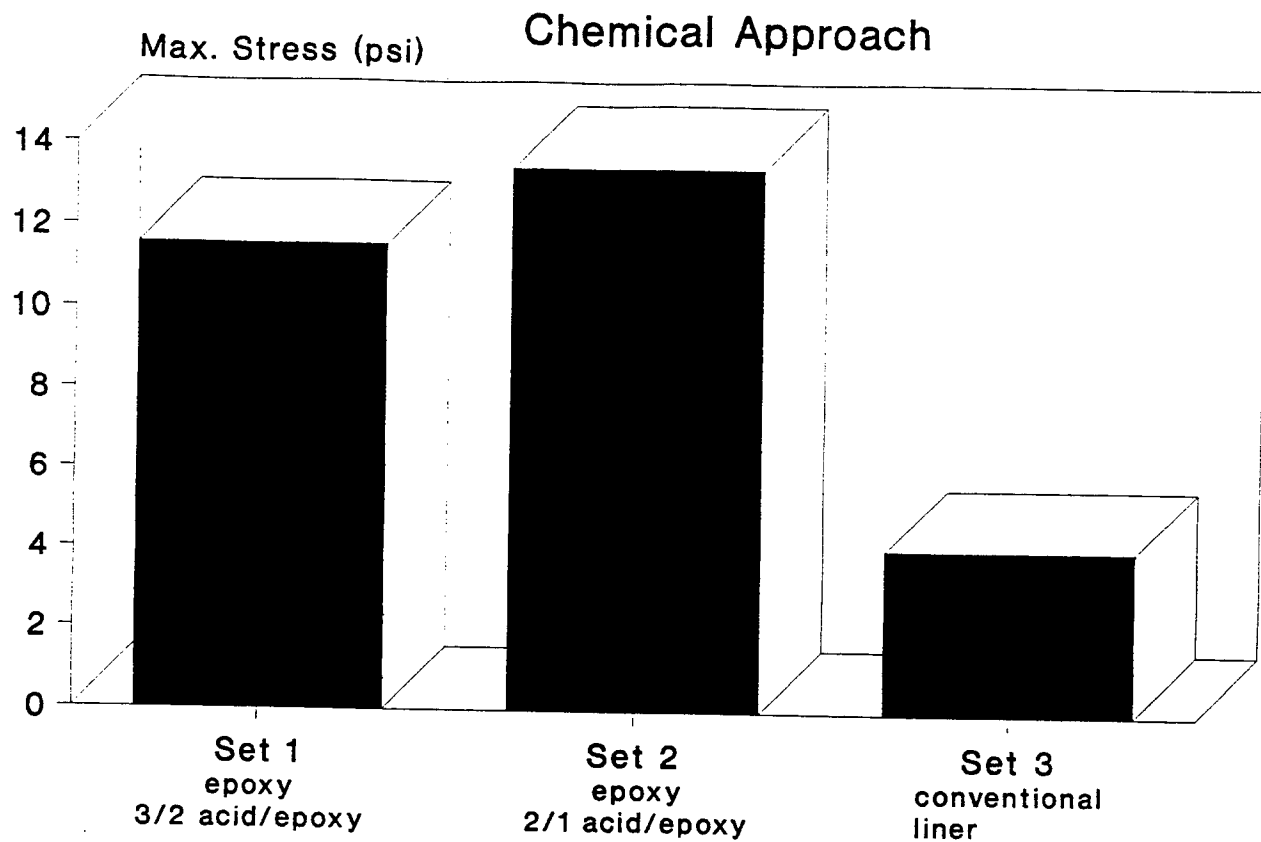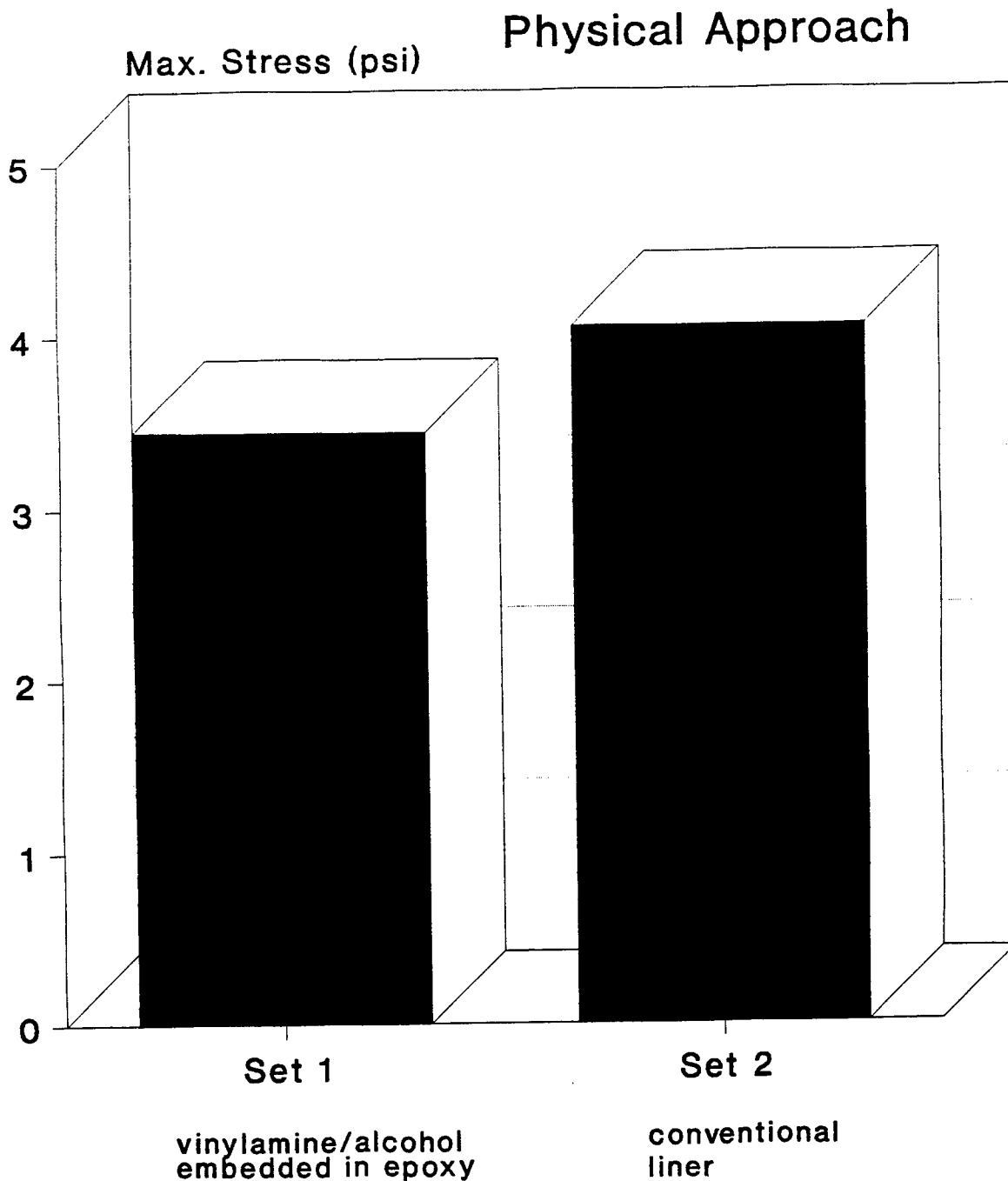
Conclusion

The epoxy liner approach taken with the R-BITS looks promising and research in this area will continue. Possibilities for improving the epoxy liner are: varying the acid/epoxy ratio, and trying different epoxy resins. The physical approach taken with the vinylamine-co-vinylalcohol polymer was not satisfactory. This is because the polymer was partially miscible in the epoxy. INSTRON test results brought about the idea of making use of both the chemical and physical approach. Research in changing the epoxy type or increasing the epoxy concentration will be done. The physical bonding approach taken with the Kraton liner tests will be continued. This work has laid a foundation for evaluation of liner candidates for solution propellants.

References

Nicholson, J. W. The Chemistry of Polymers.

    Cambridge: The Royal Society of Chemistry, 1991.

Timnat, Y. M. Advanced Chemical Rocket Propulsion.

    San Diego: Academic Press, 1987.

THE CONSTRUCTION OF A MODEL
SOLAR POWERED CAR

Daniel C. Ghiglia

Sandia Preparatory School
532 Osuna Road N.E.
Albuquerque,NM. 87113

5-1

THE CONSTRUCTION OF A MODEL
SOLAR POWERED CAR

Daniel C. Ghiglia
Sandia Preparatory School

Abstract

A model solar powered remote control car was constructed to run only on the power of the sun. The power of the car was supplied by a solar array consisting of four strings constructed of eleven cells in parallel. The object was for the car to not only run on the power of the sun, but also to allow the operator to control the speed and the steering of the vehicle. Because several of the parts were purchased at a local hobby shop, the car had to be constructed to fit them.

THE CONSTRUCTION OF A MODEL
SOLAR POWERED CAR

Daniel C. Ghiglia

Introduction

The idea of using the energy of the sun to power vehicles is not a new one. Building a remote control model that runs on the energy provided by the sun is an effective way of proving that it is possible. When first approached with the idea of constructing the model, I felt it would be an interesting challenge. The idea was for my partner,Julie, and I to build a remote-controlled vehicle that would run to our mentor, Randy's, specifications in a matter of two weeks. We were supplied with the array of solar cells and were asked to design and figure out the cost of building such a thing. By building the model, we could prove that the sun could provide sufficient energy to drive perhaps a life size vehicle with efficiency in the future.

Problem

When the idea of constructing a remote controlled vehicle that was solar powered was first mentioned it sounded like something that would be fun to do and experiment with. However, when we were shown the materials that we had to work with, I became somewhat skeptical. We were given two broken down models that had been put together at a local high school as a part of another project. The frame work was very poorly done, the wheels were made out of balsa wood and because of its high profile, the cars were very unstable. Because the frames from the first cars were not of much use, all that we had to start with were the arrays of solar cells. Each of the arrays consisted of 44, ten by ten centimeter cells that were soldered together. Randy wanted us to get one of the cars into working order. He only asked that the cars be controllable by the user, meaning that he wanted to be able to control the speed and the steering. The rest was left for my partner and I to figure out.

Procedure

Randy told us that he wanted the plans drawn up along with a price list before we could start construction on the vehicle. So as we discussed the way that the frame would be constructed,

we decided that stability and weight would be the two main factors in determining how well the car would perform. Stability was a problem because of the size of the array. It measured 26.5" by 36.5" and therefore needed a frame that would distribute the weight of the frame. The car was to be driven by a small, electric, hobby motor. Because the motor being used was intended for Radio controlled. cars that typically weigh three pounds, we had to design a vehicle that the motor could push. Another concern, with the motor, was the current that it needed to run properly. The array under direct sun put out about nine volts and six amps. This current was slightly less than normal for a motor of that type. Fortunately, there would be some slight leeway with the torque of the motor since the gear ratios could be adjusted. In all, there were three major problems that we had to start with.

While drawing up the design for the frame, we contemplated the materials to use. Because we had to keep the weight of the vehicle down, we settled on balsa wood. For the main frame we decided on using 3/8" by 1/2" pieces cut to the needed lengths and doubled side by side for strength. As we started to figure out how to mount the wheels, we ran into even more problems. Originally, we wanted to use a wide wheel base for maximum stability. However, the drive shafts that were on the motor didn't allow for the wheel base to be expanded. Now we were stuck with a seven inch wide wheel base to fit with a 26.5" wide array. Because of this, the shape of the frame became more and more important. We tried triangle shapes and box shapes and finally settled on an "I" shaped frame. This frame had many advantages. Since the wheels were fairly high, we had wanted to somehow mount them out from underneath the solar array to give it a lower profile. This design would allow for this type of mounting. The I shaped frame also gave the desired support to the array because of triangle shaped struts expanding from the center. In our plans and drawings of the car, we had drawn the main frame and the housing for the wheels as two different parts. We had designed the car on the idea that the array would sit on the main frame and in turn, the array and frame would sit on the wheel mounts thereby distributing the weight on the wheels.

The next problem that we ran into was finding the parts and pricing them. We also had no idea what specific parts were needed to get the motor and steering into running order. We knew what we wanted to do but we needed help in finding the parts. Fortunately, Another employee had a son,Chris James, who was very knowledgeable in Radio controlled. car racing. We set up a meeting with him to see if he could help with some of our problems. When Chris arrived, he

seemed to instantly know what was needed for the motor and steering. In fact, he had many of the parts that we needed and donated them to us. Among them was a speed control that would regulate the flow of the current to the motor allowing control of the speed. It was even equipped with a reverse.

We knew that the place to get the parts was at local hobby shops so the next move would be to find the costs of the parts that were needed. Because Randy had said that he didn't want to spend a great deal on the parts, we had to shop around and find the best prices.

Chris knew what to get and we ended up with a price of about 50 dollars. When we presented this and the drawings for the car to Randy he thought it sounded reasonable and told us to go ahead with our plans. The process of drawing the plans and getting a price estimate took us about a week. The only thing that was left was to complete the actual car by the end of the second week.

Construction

After obtaining the parts for the car, we drew up a schedule of how we would assemble the car over the following five days. The first thing that was done was to complete the main frame. For the frame, we had purchased wood screws and glue to fasten the frame together. The reason for completing the frame first was that it needed to be longer then the array in order for the wheels to fit out from underneath it. We would do this in case our plans didn't work as planned. If everything went as planned we figured that the frame would take about two days to complete. After completing the frame, we would assemble the wheel mounts, and finally we would finish by fixing the array on the frame so that it could be removed for easy transportation.

The assembly of the main frame went along smoothly with the exception of the odd angles that were created by the triangular struts. The problem with the struts was that the angle didn't allow for them to be glued together. Instead, using scraps of sheet metal, we fashioned brackets bent at the right angle to fasten the pieces together. Because the main frame was made up of only straight pieces, it was easy to assemble and was finished in a day.

Putting together the steering and motor mounts was a bit trickier. In the front, a servo had to be mounted so that the steering could operate. This was a tedious procedure because we had to figure out how to mount the servo with small pieces of balsa wood. Several modifications were made from the original drawing because we hadn't accounted for certain things. The size of the tires in the front forced us to taper off the ends of the mounting block to allow them to turn. another problem was that the steering arms needed room to span across the mount to the wheels. With the frame laying on top of the front wheel mount, this was not possible to do as well as keep the

5-5

low profile that we had wanted. after finishing the front wheel and steering mount, we ended up adding small blocks for height to give the steering arms clearance to move. By doing this, we had not changed the overall height of the car to dramatically.

On the rear wheel and motor mount, we had similar problems with the drive shafts. because our original design called for the frame to sit on the rear and front wheel mounts, the drive shaft had to somehow sit underneath the frame. To solve this problem, we simply ran two parallel pieces of balsa wood that would act as a groove for the shaft to sit in. In turn, the frame would sit on these pieces making the panel on the frame almost flat. This turned out for the better because the panel needed to be as flat as possible in order to get the most direct sunlight. Another problem that we had to face was mounting the motor to the wood plate. This was because of the number of screws that it required. We were unsure if the balsa wood could handle the screws and maintain its strength. However, the wood held up after the motor was mounted.

The last thing that was left to do was wire the panel to the motor and speed control and to fine tune every thing so that the car would run. Because Randy had wanted the array to be removable, the wiring was all done with clips that could be easily removed. The motor had a pinion gear and a large spur gear that was rigged for torque. once we had this put together, the car was ready for its first trial run.

Fortunately, by the time the car was complete, the sun was directly over head and would supply maximum light. After everything was switched on, a press of the trigger on the transmitter proved that the car didn't have e the correct gearing to move its weight. This was along with the large size of the wheels. By downsizing the wheels and making the gear ratio larger, the motor would be able to push the car. Unfortunately, Chris didn't have a larger gear ratio so we had to go back to the hobby shop and purchase the gears. We ended up with a gear ratio of 6.4:1 and used wheels that were one inch smaller in diameter.

Results

By changing the ratio and the tire size we had created a solar powered vehicle that was remote controlled. To our surprise, the car moved faster than expected and was very easy to control. It also had a reverse on it. Unfortunately, several problems arose. As we had feared, the rear mount had too many screws in it and eventually split because of the rough pavement. Also, because of the nature of the type solar cell that we were using, the heat caused the current flow to drop and as a result, the motor would lose power and slow down tremendously. One other engineer suggested that we put reflector panels on the sides of the array in order to increase the current flow by over 30%. We decided not to do this because we were concerned with the

effects that the panels would have on that stability of the car. Overall, there were many problems that were faced with the car throughout the planning, construction, and testing. However, because it was a leaning experience, we had discovered thing that we would do differently if we had to build the car again

<u>Conclusion</u>

Building and running the solar powered was a fun and interesting task. It helped give a touch of engineering that goes into the design of any vehicle. First there was the planning, then the construction, and then discovering what should be done differently in the future to make a better running vehicle. Making the solar powered car opened Julie and myself up to that. Although it was a simple project on a large scale, it taught me some things that I won't forget when I design new and bigger things.

Acknowledgments

I would like to thank Leigh Thompson for the recomendation letter that she wrote for me which aided in my recieving of the job. Next, I would like to thank my parents for pushing me to apply because now I see what a valuable experience it has been. Finally, I would like to thank those at Phillips Labs, Randy Boswell my mentor, Captain Kelly Gaffney my lab focal point, and finally Rob Wolverton who assisted me with the solar car. I look at all of these people as my friends and I will not froget any of them.

THEORETICAL STUDY OF RADIATION AND HEATING
EFFECTS IN ACOUSTO-OPTICAL DEVICES

Tad L. Goetz

Sandia Preparatory School
532 Osuna Rd, NE
Albuquerque, NM 87113

Final Report For:
High School Apprentice Program
Phillips Laboratory

August 1994

THEORETICAL STUDY OF RADIATION AND HEATING
EFFECTS IN ACOUSTO-OPTICAL DEVICES

Tad L. Goetz
Sandia Preparatory School

Abstract

The thermal and acoustic properties of various acousto-optic semiconductors and oxides were researched. The Photonics Research Group at Phillips Laboratory at Kirtland Air Force Base provided experimental data on spatial intensity deflection for crystals that were exposed to radiation. A theoretical study was conducted to ascertain the ability to predict the acousto-optic spatial intensity deflections due to the nature of the materials and their thermal properties. Practical applications for such devices and a brief explanation why this research is valuable are outlined.

THEORETICAL STUDY OF RADIATION AND HEATING EFFECTS IN ACOUSTO-OPTICAL DEVICES

Tad L. Goetz

Introduction

The use of crystals in acousto-optic modulators has become a vital part in communication and processing technologies. How they withstand variable and adverse environments has only recently become an important area of study. Many space applications for these devices will have a low-earth orbit environment and therefore will be subject to radiation dosage and heat fluctuation [1]. The collection, interpretation, and conversion of data collected on oxide and semiconductor crystals such as TeO_2, $PbMoO_4$, $LiNbO_3$, GaP, and InP to predict and subsequently test how they react is a major hurdle that must be cleared in order for the data to be put into a useful form.

Acousto-optic devices are devices where the interaction of sound and light are of key importance. An acousto-optic deflector is a device that, using a crystal, a radio-frequency (rf) modulator, a laser, and some sort of sensor, is able to deflect the diffracted beam from the laser by changing the frequency of the rf modulator. An acousto-optic modulator does the same thing but is also able to change the intensity, or the amount of light that is diffracted. The rf modulator produces within the crystal perturbations to the index of refraction moving at the speed of sound that can look like a sine wave. This, when operated within a finite frequency range, causes light to be diffracted under the Bragg-angle diffraction condition. The Bragg condition allows light to be diffracted at the same angle as it enters the crystal (see figure 1a).

Procedure

The first step in performing research upon these crystals is to determine what data has already been collected by other researchers, the validity of their data, and under what conditions those tests were performed. In the case of TeO_2, many older sources that recorded things such as the refractive index do not specify whether or not it is ordinary or extraordinary, at what wavelength of light, or at what

temperature the crystal was at, all of which have slight effects on the refractive index [2]. While the collection of this information is often a time-consuming paper-chase, it will most likely be quicker and cheaper than determining these factors in the lab.

The second step taken must be to convert the data into a standard form so that the units in the equations match up. More often than not, data collected from other sources will be represented in different ways. The Kelvin, Celsius, or Fahrenheit temperature scales may be used when representing things such as (dn/dT), the rate of change of the refractive index (n) as the temperature (T) changes. If the conversion between scales is not done properly, even the slightest difference may make calculations invalid. This is why it is necessary to check the work done and even have associates do the calculations as well. A theoretical prediction does no good if it is not done with the correct units and values for the materials worked with.

$$\eta = \frac{I_1}{I_0' + I_1}$$
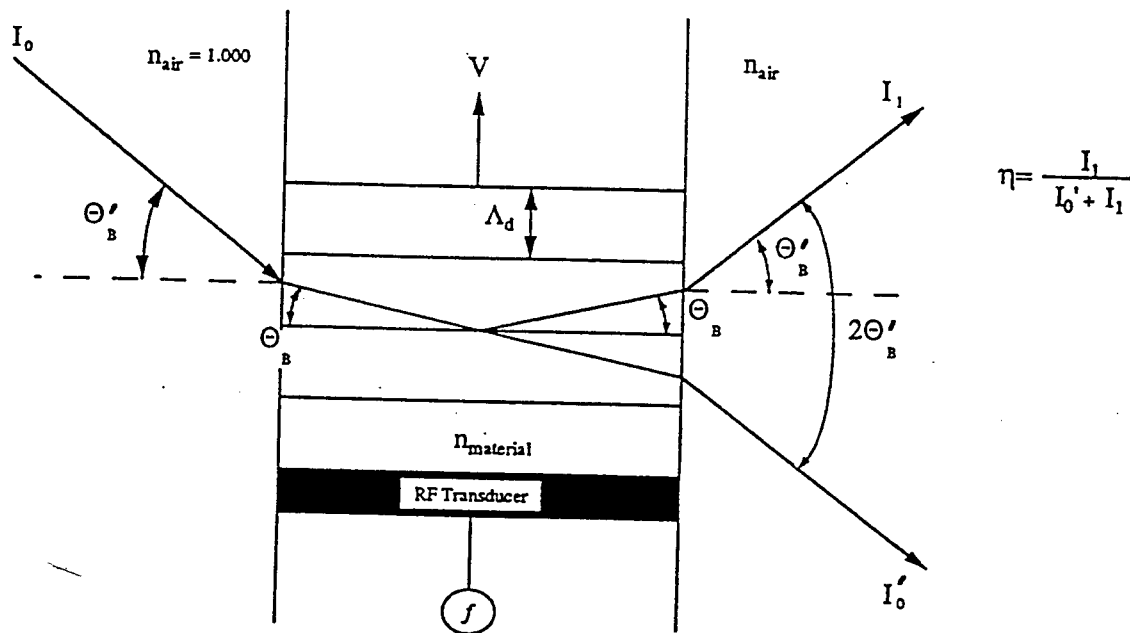
[6]

Figure 1a. Acousto Optic Bragg Deflector. This is the special AO interaction which results in a single side order spectra (I_1) by operating the deflector at the Bragg angle (Θ_B). In this instance, the separation between the two optical beams is given as $2\Theta_B'$. The diffraction efficiency (η) of the deflector is defined as the ratio of the magnitude of first-order spectra (I_1) to the sum of the magnitudes of I_1 and the emerging main beam (I_0'). The grating spacing is indicated by Λ_d and is defined by $\Lambda_d = f/V$, where f and V are the applied modulation frequency and material acoustic velocity, respectively

6-4

The third step is the favorite part for many scientists; the hypothesis. After collecting all the data needed, then devise a hypothesis as to what could happen when the device is exposed to radiation or a change in temperature. Here two important things must be realized. One is that it is often extremely difficult to include and calculate in a theoretical problem all the anomalies that are experienced in a lab setting. The second is that, in the case of acousto-optic modulators in orbit, the sudden changes and radiation doses that the device might experience in the case of a solar flare as well as the relatively nominal constant background radiation must be considered.

The last step is testing and comparing the data to results taken in the lab. Here is where the unexpected factors will appear, such as vibrations other than the acousto-optic modulator, heating induced by radiation, the unstability of the optical power, the sensitivity of all detectors used, etc.

In my 8 week research program, I was able to experience the first three steps of this process and a part of the fourth. I began by looking at all five materials and eventually concentrated on $PbMoO_4$. My first task was to collect all the information I could on TeO_2, the material that seems to have the least pooled information. I then found the thermal properties of all the materials and was given a chance to guess at what might happen when the modulator was heated. The Photonics Research Group at Phillips Laboratory on Kirtland Air Force Base in Albuquerque, New Mexico then provided me with experimental data from their tests with neutron, electron, proton, and gamma radiation, allowing me to compare their results to what I predicted might happen. I then attempted to determine whether or not the effects they produced could, at the least, be generalized or if a trend could be seen between the properties of the materials and the displacement they experienced. I then considered the acoustic properties of $PbMoO_4$ and was given a chart of what had happened with the crystal under different amounts of radiation [3]. I was asked if I could explain what was happening to the main beam and the diffracted beam. In addition to looking at the crystals, I was fortunate enough to have an opportunity to experiment with a few methods used for measuring the temperature of the crystal cells.

I began by collecting the values for dn/dT, heat capacity, and thermal conductivity for the five optical crystals I was studying. After converting these values to common units, I was given a

measurement of radiation dosage and a spatial intensity deflection value as recorded by the Photonics Research Group. I plotted several charts with the spatial intensity on the y-axis to see if a trend existed between any of the materials and their reaction when exposed to the radiation. When the graph of thermal conductivity versus spatial intensity was plotted, there did appear to be a roughly hyperbolic trend. This showed that the lower the thermal conductivity was for a material, more spatial intensity shifts were observed.

To prevent making a hasty generalization, my mentor suggested that I look at the acoustic properties and the polarization of some of the materials as well. When I researched $PbMoO_4$, I realized that not only one factor determined how the crystal would react when heated. There were many other possible reasons for the way it responded. For example, the temperature dependence of the polarizability is another factor that strongly influences how the materials react.

I came to the conclusion that while thermal conductivity is a major factor for determining how the materials react when exposed to heat, there are several other factors that are not apparent unless you look at a larger range of materials. Of the five that I studied, only $LiNbO_3$ revealed that something else was happening that affected the spatial displacement. If looked at closely, the results show subtle changes that cannot be attributable solely to two or three factors; I believe that there may be many more factors that make subtle differences that probably are not important when the acousto-optic detector is used within a range of a few meters, but when the laser is directed over longer distances these subtle perturbations must become a vital consideration.

One major limitation in sensor technology is the ability to measure temperature precisely. When a stream of radiation hits a part of a square face of a crystal ($1cm^2$), it is difficult to determine the temperature at that point and even more difficult to determine temperature inside the crystal. Among the methods attempted by the Photonics Research Group were infra-red thermocouples and thermistors. Neither offer an accurate or precise temperature measurement. In the case of the thermocouple, the field of view is too large. It ended up averaging all that it saw, and was not able to focus in on a certain point as was needed. The smallest area that it was able to measure (when it was as close to the crystal as

possible) was unfortunately wider in area than what is needed for accurate calculation. With the thermistor, which uses resistance changes to calculate temperature, the response time was too slow. It also appeared to be non-discriminating in which side it took temperature from. The face that was against the crystal could measure the temperature at that point, but it also took a measurement of the air on the other side of the thermistor. There is no effective way to block that side from measurement, as it is likely to change at a different rate than the crystal. These problems may be solved in the near future with the introduction of a relatively new method to measure temperature using light to calculate the density of the material [4].

Conclusion

The future of acousto-optic devices is an exciting one. Acousto-optic modulators are presently used in such things as photocopiers, signal processors, communication satellites, and some new experimental types of televisions and personal computers [5]. As communication technologies become more available, versatile, and important to society, more computation of the binary signal that serves as the fastest and clearest way to send information will be conducted in satellites that will be in space to cover a larger area of the earth than conventional radio-wave towers and electronic wires can. Along with that comes the exposure of these devices to hostile environments. In order to increase speed and to decrease cost to companies and consumers alike, the effects of these environments must be studied prior to wide-spread use of acousto-optic devices in space.

[1]   Taylor, E.W., "*Overview of Photonic Components for Space Applications: Radiation and Temperature Responses*"; SPIE Proceedings vol. 1953, April 1993.

[2]   Ediger, Marwood & Waynat, Ronald, <u>Electro-Optics Handbook</u>; McGraw-Hill, Inc., New York 1994, Chapter 11

[3]   Taylor, E.W., "*Radiation Induced Effects in Acousto-Optic Devices*"; SPIE Proceedings vol. 1994, p. 220, September 1992.

[4]   Lipkin, Richard, "*The Unbearable Lightness of Heating*"; Science News vol. 145 no. 13, p. 206, March 26 1994.

[5]   Higgins, Thomas V., "*There is a lot more to an A-O modulator than meets the eye*"; Laser Focus World, p. 133, July 1991.

[6]   Taylor, E.W., "*Radiation Induced Effects in Acousto-Optic Devices*"; SPIE Proceedings vol. 1994, p. 218, September 1992.

PROGRAMMING DATA CLASSIFICATION PROCEDURES,
TIME MANIPULATION FUNCTIONS,
AND IMAGE PROCESSING PROGRAMS FOR THE
AIRBORNE LASER EXTENDED
ATMOSPHERIC COMPENSATION EXPERIMENT

DeLesley S. Hutchins

Albuquerque High School
800 Odelia NE
Albuquerque, NM 87110-4924

Final Report for:
High School Apprentice Program
Phillips Laboratory

PROGRAMMING DATA CLASSIFICATION PROCEDURES,
TIME MANIPULATION FUNCTIONS,
AND IMAGE PROCESSING PROGRAMS FOR THE
AIRBORNE LASER EXTENDED
ATMOSPHERIC COMPENSATION EXPERIMENT

DeLesley S. Hutchins
Albuquerque High School

Abstract

Due to their long range and extremely high speeds, lasers would make an ideal defense against missile attack. One design for a laser defense system is to use adaptive optics technology to negate the effects of atmospheric turbulence so that a laser mounted on an airplane can destroy enemy missiles. The ABLE ACE experiment at Phillips Laboratory will measure the propagation of a laser through the atmosphere, to further the design of such a system. Three programs were written as a part of this experiment.

The first program encodes and decodes identification bytes, which can be used to classify the different types of data recorded during the experiment.

The second program provides a variety of functions for manipulating the way time is recorded during the experiment.

The third set of programs will be used to decode the digitized raw video data into a form that can be analyzed by scientists at the laboratory, after the experiment is completed.

1.0   Background

One of the areas on the forefront of military technology is research into lasers. Lasers can strike objects with great accuracy over long distances at the speed of light. They are perhaps the best means of defense available against missile-based attack. For instance, the NORAD air defense system at Colorado Springs monitors U.S. and Canadian air space, and can identify an incoming ICBM (Intercontinental Ballistic Missile) within four minutes. Once a missile has been identified, however, there is currently no way to stop it from hitting its intended target. The only defense we have against a nuclear attack is a counter-attack, and the start of a nuclear war. A laser-based defense system however, could easily target and destroy an ICBM from hundreds of miles away. Likewise, in a Gulf War type of situation, an aircraft equipped with a laser defense system could shoot down Iraqi SCUD missiles from far away, thus eliminating the need for the costly Patriot Defense Systems.

Unfortunately, due to atmospheric turbulence, focusing a laser beam over hundreds of kilometers using ordinary lenses and mirrors becomes a practical impossibility. These problems can be overcome by using an adaptive optics (AO) system. A systems make use of the fact that any atmospheric disturbances have the net effect of a single lens (however warped) on a beam of light. In an A system, readings are taken to calculate the net effect of atmospheric interference, and the results are sent to a flexible mirror. The shape of the flexible mirror is then altered so itis the exact opposite of the shape of the atmospheric turbulence.

The mirror cancels out almost all atmospheric effects on light that is entering, or leaving the adaptive optics system.

2.0 The ABL Program

2.1 Introduction

The United States military is currently investigating the use of lasers and adaptive optics systems to identify, acquire, track, and disable hostile missiles from the air. Phillips Laboratory has been involved in these experiments for more than three years under the ABL (Airborne Laser) program.

Under the ABL system concept, a Large Aperture Telescope, a Small Aperture Telescope, acquisition tracking and pointing (ATP) devices, and A systems are used to passively sense and acquire the IR signature of a missile up to 400km away. The location of the missile is then estimated and a low-power illuminator laser is reflected off the missile to get its active signature. One the missile has been successfully located, a beacon laser is reflected off the missile to get a picture of the atmospheric distortion. This data is sent to an adaptive optics system in which a High Energy Laser (HEL) is used to destroy the missile.

2.2 Phillips Laboratory Experiments - ABLE ACE

Currently Phillips Laboratory is the design and development stage of ABLE ACE (Airborne Laser Extended Atmospheric Compensation Experiment). Like its predecessor, ABLEX (Airborne

Laser Extended Experiment), the goal of ABLE ACE is to obtain atmospheric characterization data to further the development of an ABL system. ABLE ACE uses three different pieces of equipment. The first part is a weather balloon, which takes atmospheric readings. The second part is the transmitter, a small airplane which transmits a low power laser beam at the receiver. The majority of the hardware for the experiment is on the receiver: the third part. Argus, the plane which will beused as the receiver, is a military version of the Boeing 707. In addition to a carrying a wide variety of sensory and recording equipment, virtually all of what would be the passenger section of the plane is taken up by numerous computer platforms.

3.0   The Idbyte and Irig Utility Programs

3.1   Introduction

The ABLE ACE experiment itself will record 80 hours of many different kinds of data. Instruments on board Argus will split the incoming laser beam into two parts: the Pupil Plane image (PPI) and the Far Field image (FFI). Other instruments such as anemometers and scintelometers, positioned at the front and rear of the plane, will record atmospheric data along Argus's flight path. In order to keep track of all this data, a method of encoding the data into identification bytes was developed. These bytes will be placed in a header at the beginning of each piece of data. Depending on the requirements for each portion of the experiment, either one, two, or four identification bytes will be

used. The *idbyte* program encodes and decodes this data.

The identification bytes, however, are only one of the things stored in the header. It is also necessary to know at what time each piece of data was recorded. An IRIG card supplies a 9-byte time stamp describing everything from which day it is down to microsecond accuracy. Unfortunately, much of the data isbeing recorded extremely quickly; the anemometer for instance records data at 12,000 Hz. It is not necessary to record what day and hour it is several thousand times per second. Likewise, for slower or less precise recordings, it is unnecessary to record the millisecond or microsecond that the event took place. Therefore 15 different time formats were developed to cover all the different kinds of experiments which utilize the IRIG time stamp. The *irig* routines were written to convert between the various kinds of time stamps, and to manipulate the IRIG time stamps themselves.

3.2   The Idbyte Program

There are four different values that must be encoded in the identification byte(s). These four values are the recorder number, the recorder identification number, the time format, and the data format. The encoding scheme depends on the number of bytes used for the identification number. This number is actually stored in the number itself. The bytes are read in reverse order. If the first bit of the first byte read is clear, the number is one byte long. If it is set, then the number is two or four bytes long. If first bit in the second byte is also set, the number is

7-6

four bytes long, otherwise it is two bytes long. For the one byte
ID number, the time format and data format are omitted, since
seven bits do not hold enough information to store four meaningful
numbers.

The formats are as follows:

```
    Format using 1 byte:
         bits: 7-5              4-1                 0
         meaning:  recorderID record       set to 0
    Format using 2 bytes:
         bits: 15-11       10,9,7             8
         meaning:  record             recorderID set to 1
         bits: 6-4              3-1                 0
         meaning:  time format    data format    set to 0
    Format using 4 bytes:
         bits: 27-25       23-17        24
         meaning:  time format    data format    set to 1
         bits: 15-10       7-0                 16
         meaning:  recorderID record          set to 1
```

3.3 The Irig Routines

One of the fields of the idbyte program is the time format.
The time format specifies how much information, and what type of
information will be imbedded in the time stamp that comes after
the identification number. This time stamp is based on the
information supplied in the 9 byte IRIG code:

```
Format of the 9 byte IRIG code:
     byte 0: seconds (tens/units)
     byte 1: minutes       (tens/units)
     byte 2: hours         (tens/units)
     byte 3: days          (tens/units)
     byte 4: bits 7-6: hundreds of days;
             bits 5-0: data bits C20-C16
     byte 5: data bits C07-C00
     byte 6: data bits C15-C08
     bytes 7-8: offset bytes used to augment data bits C20-C00
```

Data bits C20-C00 are used to hold the value of a 21-bit binary number, which gives the number of half-microseconds. Bytes 0-4 are split into two halves, which contain the value of the two digits of a decimal number. The two offset bytes are used to correct any inaccuracies in the time data.

As mentioned previously, this IRIG code can be compressed into 1 of 15 different time formats in order to save space. A header that is a just few bytes smaller can result in a significant increase in storage space if it is saved multiple times a second. The formats are as follows:

```
format 0:   bytes 0 1 2 3 4 5 6 7 8   (full IRIG)
format 1:   bytes 0 1 2 3 4           (no microseconds)
format 2:   bytes 0 1 2               (hour, min, second)
format 3:   bytes 0 1                 (minutes, seconds)
format 4:   bytes 0 1 2 4 6           (hour, min, sec, milisec)
format 5:   bytes 0 1 2 4 5 6         (hour, min, sec, micro)
format 6:   bytes 0 1 2 4 5 6 7 8     (everything but days)
format 7:   Specifies one of 8 additional formats.  A second
code must be supplied to use these formats.
            code 0: bytes 4 0 1 6       (min, sec, milisec)
            code 1: bytes 4 0 6         (sec, milisec)
            code 2: bytes 4 0 6 5       (sec, microsec)
            code 3: bytes 4 5 6         (microseconds)
            code 4: bytes 4 0 1 6 7 8   (min, sec, milisec, offset)
            code 5: bytes 4 0 6 7 8     (sec, milisec, offset)
            code 6: bytes 4 0 6 5 7 8   (sec, microsec, offset)
            code 7: bytes 4 5 6 7 8     (microseconds, offset)
```

The first two routines contained in the irig program convert between a full 9 byte IRIG code and one of the compressed time formats. When converting from a compressed format back to the IRIG code, the routine uses a default IRIG supplied by the user to fill in the missing information.

The next two routines convert IRIG codes to and from the number of floating point seconds they represent. To ensure maximum accuracy, these routines use the values of the offset

7-8

bytes in their calculations.

The following two routines add and subtract two IRIGs. In the first routine, one IRIG is subtracted from another, and the difference returned in floating point seconds. In the secondroutine, a number of floating point seconds is added to and IRIG, and the sum returned as a IRIG.

The last two routines convert IRIGs to and from ASCII (text) strings. Depending on a user supplied flag, they use either the format DDDHHMMSS.mmmmmmm, or DDDHH:MM:SS.mmmmmmm. D = number of days; H – number of hours; M = number of minutes; S = number of seconds; m = number of microseconds. These routines are primarily used for imputing and displaying IRIG codes.

4.0   Reading and Converting Image Data from an IMC Card

4.1   Introduction

Almost 95% of all the data that will be recorded in the ABLE ACE experiment will be fast FFi (Far Field image) data. Out of the 38.7 gigabytes of data that will be recorded every hour, 36.5 gigabytes will be fast FFI data. During the experiment, a laser beam firing at 20 Hz from the transmitter will be sent to a video camera on board Argus, and recorded onto high quality tape by a DCRSi video recorder. The DCRSi recorder is connected to a custom built IMC card, which digitizes the video data and allows a programmer to transfer the data onto a computer. Back at the lab, scientists will take the point spread function of the data, and compute the statistical average of atmospheric conditions over

7-9

long distances and long periods of time. Hopefully this will enable us to understand statistically how a laser beam propagates through the atmosphere.

Unfortunately, the data is not stored in a format which can be easily used. It is stored in digitized RS-170 video format, which is fine for sending to an analog video player, but not useful for much else. Moreover, the computer systems which will be used to analyze the data do not accept the tapes used by the DCRSi recorder. Before any analysis at all can be done, the data must be decoded from the RS-170 format, and written to DAT tape.

4.2 RS-170 Video Format

The RS-170 video format is simply a digitized version of the signal which is sent to a CRT monitor, following the dictates of NTSC standard 2:1 interlaced video. In a CRT monitor, a beam of electrons, controlled by magnetic fields, sweeps back and forth and up and down the screen, causing bits of phosphorus that it hits to glow. By modulating the voltage of the electron beam, an image can be painted on the CRT screen. The video signal however, consists of more than a simple set of values representing the electron beam modulation. Every time the beam comes to the end of one scan line and moves to the beginning of the next, the beam must be shut off to avoid cutting across the newly created image. Likewise, when the beam reaches the bottom of the screen and moves to the top, it must be shut off. These are called blanking intervals, and the image data is understandably filled with them.

In addition, there are a number of sync pulses in the data.

The sync pulses make sure that the timing of the CRT matches that of the video signal. Horizontal and vertical sync pulses signal the CRT to perform horizontal and vertical retraces, and equalizing pulses maintain the video signal level, and provide synchronization information. On top of all this, the screen is not redrawn all at once. In an interlaced video signal, the even scan lines are drawn first, and then the odd ones are drawn.

A program which extracts the image data from an RS-170 file must do through software what a CRT monitor does through hardware. It must respond to sync signals and blankingintervals, but must write the data into an array, instead of writing it to the screen.

4.3 Writing the RS-170 Decoding Software - Introduction

Fortunately, some of the programming necessary to access the recorder data, and decode it into usable images was already available. Kirk Powell from MetroLaser inc. provided a set of programs that utilized the bit3 library to access the IMC card, which digitizes the video data from the DCRSi recorder. He also provided some code that a previous employee had written to decode RS-170 video format. Unfortunately, both sets of programs were intended for use on another project and had to undergo significant adaptation for use in ABLE ACE. The most serious problem with the programs was that they were not really designed to be used together. The programs that accessed the IMC card just dumped the RS-170 video data from the DCRSi recorder to a hard drive. Then the RS-170 decoding program read the data from the hard drive, decoded it, and either dumped the extracted data to the hard

drive, or piped it to an X-Windows viewing mechanism. Clearly, since the Fast FFi experimental data will take up 36.5 gigabytes per hour, and the experiment is expected to last 80 hours, using this method is a practical impossibility. The solution decided on was to download the data from the DCRSi recorder directly into memory, while simultaneously decoding it into usable image data, and writing that data to DAT tape.

4.4   The Buffers Routines

The *buffers* program was written to help connect the IMC programs and the RS-170 decoding programs. By using the routines contained in this program, another program can create a wraparound buffer in memory of any size, and access that buffer as if it were a normal file. The wraparound feature means that any data written past the end of the buffer will be placed at the beginning, to insure continuity.

In the buffers program, a memory buffer is defined as a block of memory, with two pointers pointing to some location within the block. One pointer records the position where the information stored in the buffer begins, and the other records where it ends. Whenever information is read from the buffer, the pointer at the beginning is incremented the proper amount, and when information is written to the buffer, the pointer at the end is incremented the proper amount. A number of other variables handle bounds checking and the wraparound function.

The first two routines in the buffers program deal with the buffer's creation and subsequent disposal. The first procedure

allocates memory for the buffer, and initializes a number of variables used internally by the program. The second procedure deallocates the memory used by the buffer.

Unlike a file, a memory buffer can have varying amounts of information stored in it at various times. If a program reads from the buffer faster than it writes to it, it will run out of information. Likewise, if a program writes faster than it reads,it will run out of space. The second two procedures check how much information is currently in the buffer, and how much space remains in the buffer.

The last two procedures simply read and write blocks of memory to the buffer. If there is not enough space in the buffer to write to, or there is not enough information to read the requested amount, the procedures will read or write as much as they can, and return the amount they read or wrote.

4.5 Connecting the IMC and RS-170 Decoding Programs

The first step in splicing the three separate pieces of code (the IMC routines, the RS-170 decoding routines, and the buffers program) was to consolidate the pieces of code into three distinct programs. The buffers program was already a distinct program, having been written that way. The IMC and the RS-170 routines were not.

4.5.1 The imcstuff program

The IMC routines were written as several distinct programs

that had been designed to run separately. These programs were re-written to remove redundancy in the code, and placed in a single program called *imcstuff*. The imcstuff program contains four procedures, all of which use the bit3 library developed to access the IMC card.

The first two procedures turn the IMC card on and off. The card is not initially on; it must be activated by software means before any of the information on the DCRSi recorder can be accessed.

The third procedure sets up the IMC card for reading, and initializes all the internal variables used to access the IMC card. This includes allocating a memory buffer of the proper size to store the video data.

The fourth procedure is used to actually read data from the card. The IMC card sends data in blocks of 8380 bytes. As soon as one block of data is read, the card automatically activates to read another 8380 bytes of data from the DCRSi recorder. This procedure reads a block of data from the IMC card and writes to the memory buffer.

4.5.2 The rsdecode program

Although the IMC routines were initially separate programs, they were relatively simple, and required little modification to consolidate them into one program. The RS-170 decoding routines were much more difficult. First of all, the individual procedures were contained in a number of files, and all of them seemed to call on most of the others, following often obscure threads of

logic. Once this problem was unraveled, another sprang up. Much
of the code had no bearing on the decoding mechanism; it was a
remnant of an earlier project. One of the problems in getting rid
of this undesirable code was that oftenthe code made direct
modifications to the image data, so it became difficult to tell
what was just some obscure part of the decoding process, and what
was code that should be removed. After considerable effort, the
decoding mechanism was isolated from the rest of the code. The
resulting program, named *rsdecode*, was then re-written and
condensed into six procedures.   One of these procedures, the
next_pixel function, handled all file access. This function was
mostly re-written to use a memory buffer instead of a file.
Whenever the function is called it reads a pixel from the memory
buffer. As soon as the memory buffer runs out of pixel
information, it calls the procedure from the imcstuff program to
read in more data. As soon as the buffer is filled with the
desired amount of data, decoding of the video signal resumes.

The next three procedures deal with the decoding mechanism
itself, and are used internally by the program. They are not
intended to be used outside of the program under any
circumstances.

The fifth procedure calls upon the first four procedures to
decode a single frame of video information. It returns two
fields, which contain the interlaced image data for the frame.
This procedure is the primary interface to the decoder.

The sixth procedure takes the two fields, and interlaces them
together to form a single image.

Once the imcstuff program, the buffers program, and the rsdecode program were completed, it was a relatively simplematter to write a master program to tie them all together. The program imc2dat initializes the IMC card, and then decodes the video signal stored on the DCRSi recorder, saving each frame as a separate file on the hard drive. When the ABLE ACE experiment gets underway, it will be no more than a few minutes work to modify the program so it writes the data to DAT tape instead.

4.6 Testing the Programs

The final step in the process was to install the programs on Argus itself, compile them, and test them with the DCRSi recorder and the IMC card. The programs were written on Aquila, a Silicon Graphics machine back in the office, and although they compiled with no problems, there was no way to test them in the office.

The programs were installed on an IBM RS6000 running X-Windows aboard the airplane. After a number of the small, trivial bugs that invest any new program were removed, the program still didn't work. Kirk Powell and I spent a full day attempting to resolve the problem.

After repeated attempts with two different tapes under a variety of conditions, we finally managed to decode a small portion of the video data. We tried to recreate the experiment to discover why the program managed to decode the data under one set of circumstances, and not under any of the others, and found that we were unable to do so. On this second attempt, the program wouldn't decode the data under any circumstances. We finally

discovered that the one time we managed to decode thedata was the one time we ran the original IMC program to turn the card on. Apparently, the code I received that turned the IMC card on was in fact nonfunctional. When the *on* program was run before activating the imc2dat program, everything worked perfectly.

5.0 Conclusion

Currently, the United States has little defense against an air strike which makes extensive use of long range ballistic missiles. In case of a nuclear attack, this weakness could cause the deaths of millions of people. A working ABL system would provide a strong defense against such an attack. The ABLE ACE experiment is therefore very important to our national security.

The two utility programs I wrote will provide a method by which the enormous amounts of data generated by ABLE ACE can be more easily organized and manipulated. In addition, the programs I developed to decode the video data on the DCRSi recorder and transfer that data to DAT tape, will enable scientists at Phillips Laboratory to access the Fast FFi data, which compromises 95% of all the data recorded by the ABLE ACE experiment. Although the programming was not unduly difficult, being able to use the data from an experiment is obviously of primary importance.

In addition, I received extensive career training which is valuable to me personally. I gained greater familiarity with the Unix operating system, the most widely-used operating system inthe professional and academic world. And perhaps most importantly, I learned the C programming language, which is the primary tool of

any programmer in today's world.

I believe my experience in the High School Apprenticeship Program has been valuable to the Air Force, the United States, and to my own personal development.

Spacecraft Charging and Discharging Problem

Caroline H. Lee

Lexington High School

21 Waltham Street

Lexington, Massachusetts 02173

The Spacecraft Charging and Discharging Problem

Caroline H. Lee
Lexington High School
21 Waltham Street
Lexington, Massachusetts 02173

Abstract

In this report , I briefly describe the spacecraft charging and discharging problem which has been actively investigated by scientists at Phillips Laboratory and other places. The problem can be understood phenomenologically such as collisions, backscattering and emissions that lead to adhesion of electrons to the spacecraft or release of electrons from the charged spacecraft. A widely used probe, known as a Langmuir probe, for the studies of the addressed problem is discussed. Several new techniques to reduce or prevent spacecraft charging are elucidated.

The Spacecraft Charging and Discharging Problem

Introduction

In launching spacecraft, some considerations are needed to insure the "safety" of the

spacecraft, successful operations, and accurate measurements on the spacecraft. One of the most

important problems is the mitigation of charge build up on the spacecraft surface as this would

contribute to navigational problems and incorrect measurements from electronic instruments on

board. This brief article attempts to give an introductory overview of what this phenonmenon is

all about.

How does a Spacecraft become Charged?

In space, the environment is made up
of plasmas, which consist of charged particles
such as electrons and ions, and neutral
particles. These charges move about within
this vast area, and upon the arrival of an alien
object, such as a dust grain or a spacecraft,
some of the charged particles may collide

Figure 1: The Charging of a Spacecraft

upon its surface and "stick" to it. Negative charging is more likely than positive charging because

electrons, being much lighter and faster than ions, are more probable to collide with objects. Upon

collision, the electron (or ion) may "stick" on or penetrate into the surface material, thereby

adding negative (or positive) charge to the material. Whether an electron is likely to penetrate and bounce off the surface back into space depends on the electron energy and the material properties. This describes, essentially, how a spacecraft becomes charged. Charging is a problem that must be solved in the development of space research.

Photoemission, Secondary Emission, and Backscatter

There are some "natural" ways in which the spacecraft surface may reduce its charge. The sun's ultra-violet rays may be energetic enough to knock out some electrons from surfaces. This is photoemission. Usually, charging is worse at night. During the day, the sun's UV rays are present to release some
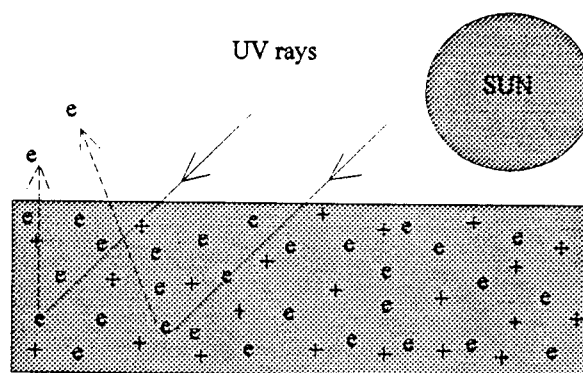
Figure 2:   Photoemission

electrons from the spacecraft surface into space. This reduces negative charging in sunlight; but as the sun slowly descends presenting the night, negative charge is again able to accumulate.
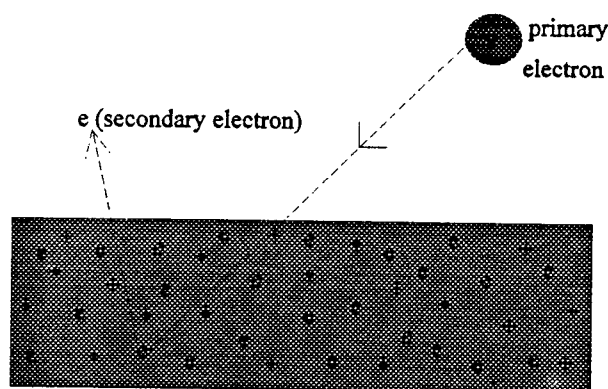
Figure 3:   Secondary Emission

Occasionally, sunlight may even charge a spacecraft to a few volts positive. There are a few other ways in which electrons are released back into space "naturally". Similar to photoemission, in which there is an action by UV rays to energize and eject electrons, secondary emission requires an incoming

electron, in place of UV rays, to penetrate the surface. The incoming electron is called the primary

electron. It penetrates through the surface and energizes other (relatively stationary) electrons

(already lodged in the material) into vigorous motion. The energized electron may leave the

material surface. The electron so released is called a secondary electron. In order for this to occur

however, it is necessary that the primary electron does not travel too fast or too slow. Both of

which would simply result in adding (not reducing) extra negative charge to the spacecraft. By

travelling too fast, the primary electron lodges deeply within the material; so deep that the

probability of escaping for its energized electrons is low. On the other hand, travelling too slowly,

the electron is not energetic enough to generate secondary electrons. Velocity (v) is related to

energy (E) and mass (m). ($1/2mv^2 = E$)

If the primary electron's energy (E) is too low

or too high, the probability P_S of secondary

electron emission is low. In the intermediate

energy range (usually between $E_1 = 70$ eV to

$E_2 = 1200$ eV depending on the surface

material), the probability of secondary

electron emission is higher. For some

materials, the probability P_S of secondary

electron emission in the primary electron

Figure 4:   Backscatter

energy range ($E_1 < E < E_2$) may exceed one. That is, for every primary electron coming in,

there are likely more than one secondary electron going out.
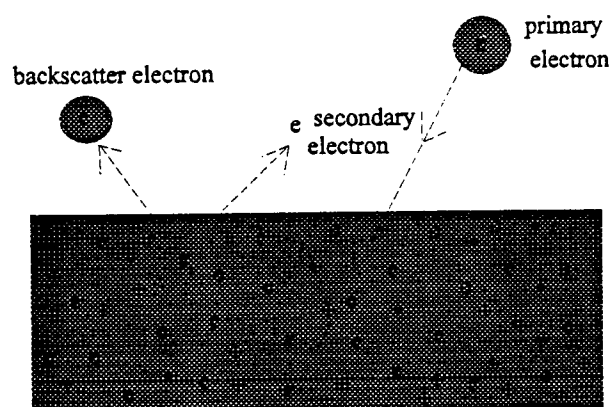
When a primary electron is scattered by the electrons and ions in a material, the primary electron may eventually lose most of its energy and stay inside the material, or it may go out. If it comes out, it is a backscattered electron. Unlike secondary
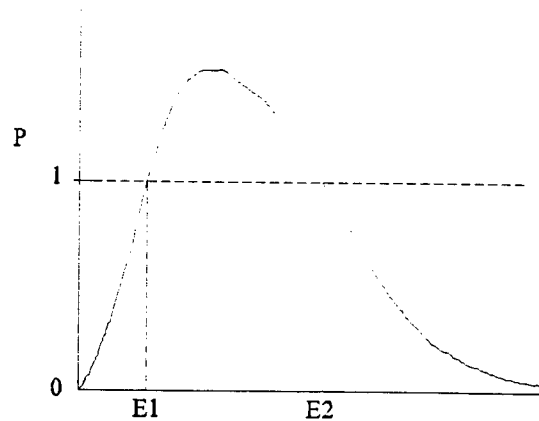
Figure 5: Probability of Outgoing Electrons

electrons, it is the same electron (primary) that came in. The probability P_B of backscattered electron emission can not exceed one. Since both secondary and backscattered electrons are going out, they contribute similarly. The total probability of outgoing electrons is $P = P_S + P_B$. P depends on the primary electron energy and also the material properties.

What is a Langmuir Probe?

In studying the problems of charge buildup upon spacecraft, it is useful to have mathematical models relating the spacecraft potential to the currents of the ambient plasma environment. A very useful one is the Langmuir probe model, developed by Mott-Smith and Irving Langmuir (1926). Langmuir probes are common in the laboratory. A typical Langmuir probe is a small metallic
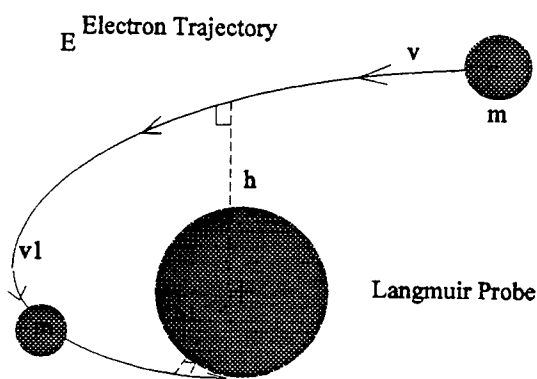
Figure 6: Angular Momentum

electrode put in a plasma. The probe is attached to a power supply capable of biasing it at various voltages positive and negative relative to the plasma. In response to the voltages applied, the currents collected by the probe varies. The currents then provide information about the condition (density and temperature) in the plasma. When the probe is set to the same potential as the plasma, there is no electric field between the plasma and the probe, and some of the charged particles of the plasma simply migrate to the probe because of their thermal velocities. Due to their significantly less mass in comparison to ions, electrons tend to move much faster, the current collected by the probe is predominantly electron current. When the probe voltage is made positive relative to the plasma, electrons are attracted toward the probe while ions are repelled. When the probe voltage is set negative, the plasma electrons are repelled while the ions are attracted. In summary, the currents collected depend not only on the plasma conditions but also on the potential (voltage) of the probe.

The Spacecraft as a Langmuir Probe

In space plasmas a spacecraft itself behaves like a Langmuir probe. Unlike a Langmuir probe in the laboratory, one cannot apply a potential (voltage) to a spacecraft. The spacecraft potential responds to the currents collected by the spacecraft. When the currents vary, the potential varies accordingly. The variations of the currents may be due to variations of the (natural) space plasma conditions such as densities and temperatures of the electrons and ions. They may also be due to emissions of photoelectrons and (artificial) charged particle beams.

In figure 6, there is an electron being attracted by the Langmuir probe. Note how its path isn't direct or straight, but in a spiraling curve. This is because of the conservation of angular

momentum. The angular momentum is, "mvh", m being the mass, v being the velocity and h, representing the impact parameter of the elecctron. According to nature, even as the electron gets closer and closer to the probe, the angular momentum should always be the same. In otherwords, $mvh = mv_1h_1$.

Looking at this equation, the "m's" cancel out leaving just the $vh = v_1h_1$ Since the impact distance "h" is getting smaller, as the electron approaches the probe (center of attractive force) "v" is getting larger, or faster. From this equation one can deduce that the closer an electron gets to the probe the faster it travels.

The Langmuir Probe Equation

The kinetic energy E of a free charge particle (for example, an electron) with mass m and velocity v is given by

$$E = mv^2/2 \tag{1}$$

The thermal energy H of the charge particle of temperature T is approximately

$$H = kT \tag{2}$$

where k is the Boltzmann's constant.

In the absence of external interactions, the kinetic energy equals the thermal energy, a

constant:

$$mv^2/2 = kT \qquad (3)$$

In the presence of an electrostatic potential $\phi(r)$ where r is the distance from the center of force, the total energy is:

$$mv^2(r)/2 - e\phi(r) = mv^2/2 \qquad (4)$$

which is a constant given by eq(3). In eq(4), v(r) means the velocity as a function of r and the minus sign implies the potential considered is attractive (in analogy to a well). As discussed in the previous paragraph, as the charge particle gets nearer the center of force, the velocity v(r) gets faster because of the conservation of angular momentum.

$$mvh = mv_a a \qquad (5)$$

where h is the impact parameter, which means the shortest distance of the trajectory from the center of force, a is the radius of the spherical probe (attractive) and v_a is the velocity v(a) when the charge particle reaches the probe surface (r=a).

From eq(5), the m's cancel out and we have

$$h = a(v_a/v) \qquad (6)$$

From eqs(3,4), the velocity v(r) at r=a is given by

$$v_a = v \left(1 + e\phi_a/kT \right)^{1/2} \tag{7}$$

where ϕ_a is $\phi(a)$, the probe potential at r=a.

Therefore, eqs(6,7) give

$$h = a \left(1 + e\phi_a/kT \right)^{1/2} \tag{8}$$

The current I collected by the probe is given by

$$I = 4\pi h^2 nev \tag{9}$$

where $4\pi h^2$ is the area of the spherical surface of collection (radius h), n is the charge density, e the unit of charge, and v the charge particle velocity at infinity (thermal velocity).

From eqs(8,9), the current I collected is given by

$$I = 4\pi a^2 nev \left(1 + e\phi_a/kT \right) \tag{10}$$

If the probe has no attraction at all (that is, if $\phi_a = 0$), then the current I_o collected by the probe would be

$$I_o = 4\pi a^2 nev \tag{11}$$

From eqs(10,11), we obtain the Langmuir probe equation:

$$I = I_o (1 + e\phi_a/kT)$$ (12)

If one includes the repelled charge species, eq(12) becomes

$$I = I_o (1 + e\phi_a/kT) - J_o \exp(-e\phi/kT)$$ (13)

where J_o is the collected current of the repelled species when $\phi=0$. Eq(13) is given without derivation, because such a derivation would require Boltzmann's law which is not simple.

If the sign of probe potential is reversed, then the roles of electrons and ions would be reversed accordingly.

Ways to Reduce or Prevent Spacecraft Charging

When different surface materials on a spacecraft are charged to different potentials, the situation is called differential charging. Differential charging is undesirable because it may form local potential wells and barriers, and also it may generate electrostatic noise or even sparks when occasional discharging occurs. The easiest way to prevent differential charging is to cover a

spacecraft entirely with a conducting surface material, thus letting the potential to be uniform all over. A conducting material is able to do this since the electrons and ions can move freely within it. However, it is impossible to have all the outer parts of a satellite made out of conducting material, with
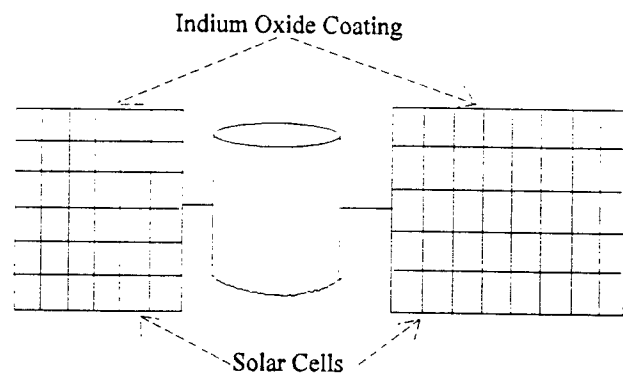
Figure 7: GEOS, a geosynchronous Satellite

various electronic instruments on board. Electronics and circuits have to be isolated from each other by means of plastics or dielectrics. Therefore, this method of prevention of differential charging by means of conductive coating is usually impractical. However, partial coverage of spacecraft surfaces with conducting materials has been used with some success. Indium oxide coating on some parts of the surfaces of spacecraft has been successful. On GEOS satellites, indium oxide coated on the solar cells basically transforms the cell surfaces into a conductive surface while still allowing the solar cells to remain quite functional (indium oxide is a transparent enough substance). This method has two limitations: (1) Coating with conducting material, such as indium oxide, can be applied to small areas only and not the whole spacecraft, (2) even with the coat, little cracks between panels may still develop resulting in charging.
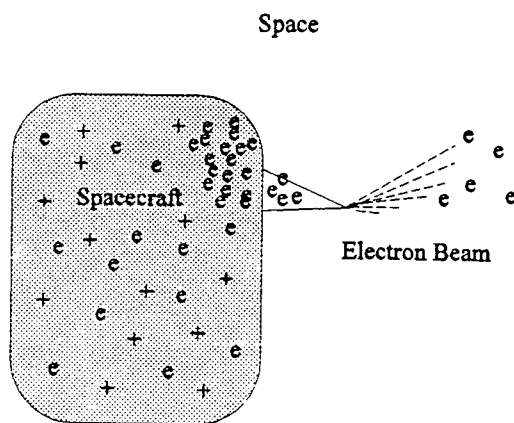
Figure 8: Electron Beam Emission

Artificial beam emissions can discharge (i.e. reduce the charging level of) a spacecraft to some extent. There are, in general, four types of beam emissions: electron beam, low energy ion beam, neutral beam, and

combinations of the above.

An electron beam emits electrons from the conducting ground into space. This is analogous to photoemission but with controllable energy or current. However, electron beam emission can only discharge the conducting ground but not the dielectrics.

Low energy ion beam emission is more effective. At first, this may sound ludicrous. If the positive charges within the material are removed, then wouldn't this cause the material to be even more negatively charged? This was not so when an ion beam emission experiment was conducted on the SCATHA satellite. When ions are emitted with low energy, they would be attracted back towards the highly, negatively charged spacecraft. Not only can the ions return and neutralize some negative charge, they are especially attracted to areas where negative charges are most abundant. This effectively reduces differential charging. Also, some electrons may be ejected as secondary electrons when the returning ions impact on the surface. The secondary electrons carry away negative charge from the spacecraft.

A low energy plasma (mixed electron and ion) beam is possibly the most effective spacecraft discharging method currently available. When such a beam is emitted from a negatively charged spacecraft, the negative charge attracts the low energy beam ions as described above, while the beam electrons are repelled away.

When a neutral beam with neutral molecules is emitted form a charged spacecraft, nothing normally happens to the charging level of the spacecraft. However, if the beam, or gas, is ionized
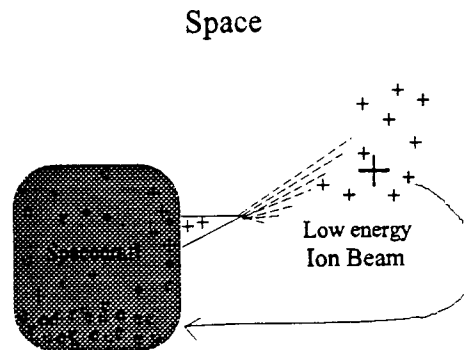
Space

Figure 9 : Low Energy Ion Beam Emission

(by electron impact or UV rays, for example), it would become a partially ionized beam (with electrons and ions) and be able to reduce the spacecraft potential.

REFERENCES

Garrett, H.B., The charging of spacecraft surfaces, *Rev. Geophys.*, Vol.19, 577-616, 1981.

Garrett, H.B., The charging of spacecraft surfaces, in *Handbook of Geophysics and the Space Environment*, J.S. Jursa (ed), AFGL, ADA 167000, 1985.

Lai, S.T., An overview of electron and ion beam effects in charging and discharging of spacecraft, *IEEE Trans. Nucl. Sci.*, Vol.36, 2027-2032, 1989.

Lai, S.T., An improved Langmuir probe formula for modeling satellite interactions with near geostationary environment, *J. Geophys. Res.*, Vol.99, 459-468, 1994.

Lai, S.T., Recent advances in spacecraft charging, *AIAA Aerospace Sci. Mtg.*, AIAA-94-0329, 11pp., 1994.

ramboise, J.G. and L.J. Sonner, Current collection by probes and electrodes in space magnetosplasmas: A review., *J. Geophys. Res.*, Vol.98, 337, 1993.

muir, I., The effect of space charge and residual gases on thermionic currents in high vacuum, *Phys. Rev.*, Vol.2, 450, 1913.

idell, M.J., I. Katz, G.W. Schnuelle, P.G. Steen, and J.C. Roche, The decrease in effective photocurrents due to saddle points in electrostatic potentials near differentially charged spacecraft, *IEEE Trans. Nucl. Sci.*, Vol.25, 1313, 1978.

Mott-Smith, H.M., and I. Langmuir, The theory of collectors in gaseous discharges, *Phys. Rev.*, Vol.28, 727-763, 1926.

C n, R.C., C.E. McIlwain, and E.C. Whipple, Obervations of differential charging effects on ATS-6, *J. Geophys. Res.*, Vol.86, 6809, 1981.

a, R.C., Experiments in charge control of geosynchronous orbit - ATS5 and ATS6, *J. Spacecraft & Rockets*, Vol.22, 254-264, 1985.

Olsen, R.C., Modification of spacecraft potentials by plasma emission, *J. Spacecraft & Rockets*, Vol.18, 462-469, 1981.

Purvis, C.K., H.B. Garrett, A.C. Whittlesey, and N.J. Stevens, Design guidelines for assessing and controlling spacecraft charging effects, *Rep. NASA-TP-2361, N84-33452*, 1984.

Scime, E.E., J.L. Phillips, and S.J. Bame, Effects of spacecraft potential on three-dimensional electron measurements in the solar wind, *J.Geophys. Res.*, Vol.99, 14769-14776, 1994.

Whipple, E.C., Potentials of surfaces in space, *Rep. Prog. Phys.*, Vol.44, 1197, 1981.
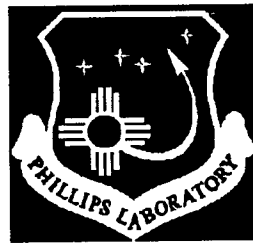
High Altitude Balloon Capabilities and Options

David Mirabal

West Mesa High School

6701 Fortuna Rd. NW
Albuquerque, NM 87105

Final Report for:
High School Apprentice Program
Phillips Laboratory

Sponsored by:
Air Force Office of Scientific Research
Bolling Air Force Base, DC
and
Phillips Laboratory

August 1994

9-1

Abstract

High altitude balloons and tethered balloons are different in many ways and are similar in others. They both must overcome the stresses primarily generated by ground winds at launch or wind shears in the troposphere. Because of high stresses due to ground generated wind shear, launch conditions are therefore usually limited to winds of 5 to 10 knots. Some of the missions which Phillips Laboratory runs are very sensitive and require a smooth ride or at least as smooth as possible. The high altitudes which are required sometimes make a smooth ride very difficult to accomplish. The answers to these problems are new and innovative technologies such as lighter balloon films and more durable payloads. For the tethered balloon, a lighter and stronger cable. The stresses do not isolate themselves to the balloon or its payload. The cable, which can sometimes exceed fifty thousand feet, has its share of stress. The wind at different levels of the atmosphere can blow in completely opposite directions and therefore shears the cable. some alternatives to high altitude balloons are remote controlled aircraft, high altitude self powered dirigibles, and newly developed long duration aircraft powered by energy supplied from microwave transmitters on the ground. These are all possibilities for high altitude surveillance of the battlefield and for high altitude experiments where tethered balloons just would not be feasible.

Anchored, and High Altitude Balloon Capabilities and Options

by David Mirabal

After careful research of the topic of the feasibility of anchored or high altitude balloons for battlefield surveillance, I have reached a conclusion. High altitudes require strong materials in both the balloon and the tether cable. High strength is also required in the anchoring device and the attaching point on the balloon. Although tethered balloons and high altitude balloons differ, they must perform the same function, their assigned duty, whatever it may be. The available materials have much of what is required but are still quite inferior. What is needed is either new materials or stronger existing materials. The cable is the main concern in the area of tethered balloons, and I tried to focus on it specifically.

The cable that is going to be used on our project is made of Kevlar, which is a high strength composite material capable of withstanding high pressures and shearing without failing. This is the most qualified material for this job, yet, it still lacks sufficient strength to withstand the pressures, shearing, and temperatures which we are going to subject it to. Work is now being done to strengthen the Kevlar so it will conform to our requirements. I have done extensive research into high altitude balloons and have found little information on anchoring capabilities. Some information is available but most reports on previous experiments are classified. Instead of going down a dead end road and trying to figure

some way to strengthen Kevlar, which I know nothing about, I decided to look for precedent to this experiment.   Some experiments followed nearly all of our guidelines but some were in different directions.   I will detail these reports to shed light on the situation.

The first report was from NASA.   It was titled, Mission requirements For Unmanned Airborne Platforms.   In this report, different types of airborne platforms were studied to find the best for high altitude and durability.   Cost was also a major factor.   The tethered balloon was one of the contenders.   It was found that the balloon concept made it hard to use for all-weather purposes.   Balloons are complicated, if not impossible, to launch in foul weather or high winds.   This factor severely limited the applications to which it could be used.

There are more options available to us other than the tethered balloon.   The RPV Powered Aerostat is another possibility.   Its specifications make it less of a possibility.   It requires too much observation and doesn't lift a sufficient payload to a workable altitude. It can rise to a maximum of 1,000 ft. for a period of 8 hours.   Its payload is restricted to 100 lbs. or less.   Its only advantage over the tethered balloon is its ability to escape in case of threat or foul weather.   This RPV is also lost to budget costs.   It sometimes requires a very expensive microwave power transfer unit.   The RPV might require a large amount of power to keep it in the air, depending on its payload.   The electronics

might require only a small amount of energy and therefore can be kept running at all times. Another restriction to this idea is the fact that the RPV unit must circle its power source and not stray too far or risk power loss and ultimately, loss of the vehicle. This is not an option for our project.

The next possibility outlined in this report is the mini-blimp. It is very similar to the balloon but is also remotely powered. The mini-blimp could carry a substantial payload to great heights but must still rely on the microwave power source. The blimp could also be powered by a ground power source which is carried up by a copper wire embedded in a tether cable. This can't work very well because of the use of a tether cable which will greatly increase the weight of the entire package. The blimp usually has a self-contained power source to drive the payload and the fans and blowers. The amount of fuel carried by the power source usually limits the endurance to one day. The copper wire in the tether cable will extend the endurance to seven days.

As stated in this report, the United States Air Force was working on procedures and hardware for deploying balloons from aircraft. The former Air Force Geophysics Laboratory tested a prototype system which was supposed to carry a 200 lb. payload at an altitude of 70,000 ft. The endurance of this project was dependant of whether a zero pressure balloon would be used or a superpressure balloon. The balloon would be

inflated by cryogenic hardware containing liquid helium. All of this equipment would be contained in a canister which is dropped from an aircraft at an altitude of 25,000 ft. The decent would be slowed by a parachute while the balloon inflates itself. After inflation was complete, a second parachute would carry the inflation device, containing the cryogenic hardware, safely to the ground for retrieval.

After the release of the cryogenic unit, the balloon and its payload would rise to an altitude of 70, 000 ft. The advantages to this system is the quick reaction to special events and the capability to launch over remote or inaccessible regions. The characteristics of the system are outlined in chart 1-3.

The next in the line of possibilities is the High Altitude Powered Platform (HAPP). This project was in the conceptual stage twenty years ago and two studies of the HAPP were conducted for NASA. Stanford Research Institute (SRI) analyzed the technical feasibility of the concept and Battelle Columbus Laboratories studied potential applications. This vehicle would have use an electric-driven propeller to keep over the desired location. The power, again, would be supplied by a microwave unit which would beam the needed power to the orbiting unit. The HAPP would fly in the region of minimum wind velocities to reduce the amount of power required by the unit. Over the United States, this would be a nominal altitude of about 21 km. or 70,000 ft.

The microwave system must supply a great deal of power for propulsion and the additional power required by almost any conceivable scientific payload would represent only a small fraction of the overall requirement. The SRI study of the HAPP concentrated on the four concepts with payloads up to 16,000 lbs. However, the study indicates that a payload ranging in weight from 8,000 lbs. to 10,000 lbs. might be possible.

The next in line is the Mini-Sniffer. This is an RPV (Remote Piloted Vehicle). It would be controlled from the ground by radar tracking and/or by telemetry from on-board computers and television cameras. Military RPV's tend to be very sophisticated and contain expensive avionics and other equipment. NASA was working on an inexpensive design based on simplicity and economy. It was known as the Mini-Sniffer. The NASA

prototype was originally developed as an atmospheric survey aircraft for sensing turbulence and measuring atmospheric constituents. The Mini-Sniffer could carry a payload of 70 lbs. to a height of 20,000 ft. or a 25 lb package to a height of 100,000 ft. The Endurance of the Sniffer was 3 hours. Propulsion was supplied by a large propeller at the tail which was

powered by a hydrazine monopropellant engine. In this type of engine, liquid hydrazine is expanded into a hot gas by passing it over a catalyst. The expanding gas then drives a piston connected to the propeller shaft. This idea combined a cost-effective solution to the problem of combining flexibility of operation of aircraft with the altitude capability of balloons.

Stress on Ascending Balloons

NASA did tests on the stress that a balloon encounters while ascending to altitude. These tests were run at the Goddard Space Flight Center/Wallops Flight Facility at Wallops Island, Virginia. The tests incorporated the flight vehicle known as the polyethylene zero pressure balloon. The conclusion was that the advances in scientific balloon technology haven't kept pace with the scientific requirements for increased duration, altitude, and payload capacity. Even though the Air Force has flown several thousand successful flights, balloons which were made after 1980 did experience an increase, only a slight increase, in the rate of catastrophic failures, slightly higher than those which were built

before 1980. These failures were attributed to the increased stresses placed on the balloons and the lack of sufficient advancement in balloon technology which would counter those stresses.

The current shape of natural shape zero-pressure balloons has not changed drastically since the extensive work by the University of Minnesota in the early 1950's, and Smalley of the 1960's. The fact that the balloons have increased in size and capability is due to scaling up the present designs. Most of this scaling up was successful only because of luck. The catastrophic failures still existed because of the inferior designs. The failure rate has doubled since 1980 and unless new designs or new materials are developed, those failures will continue. This failure to develop new designs and new techniques has been attributed to the lack of analytical models to predict balloon performance. Also noted was the non-existence of a specification for the wall/cap thickness distribution. NASA began to fix this problem by developing new models and programs to gauge the problems and help fix them. This all took place around 1984. This new model led to the correlation between balloon failure and the stress index.

At present, the natural shape of zero pressure balloons is not designed in the true sense of the word. The shape is predicted by solving the differential equations defining various loads acting on the element of the balloon. During the design process, the film's mechanical properties

are considered but sometimes underestimated, when determining its mass affect on the shape. Many simplifying assumptions are made with respect to the material and structure to make the solution tractable.

During the 1983 balloon failure investigation, it was determined that the balloon's internal caps did not appear to remain effective during the entire flight. Also, the majority of the failures were initiated from the top region of the balloon above the local maximum diameter, a region of increased thickness because of the caps.

Determination of the shape of an ascending balloon remains cumbersome even when using the simplifying assumptions addressed. As part of NASA's investigation into the causes of catastrophic balloon failures, the model was applied to a data base of over 550 balloon flights. One study determined the relative stress magnitudes along the gore of a balloon. During this application, the maximum magnitude of stress index predicted by the model occurred just above the shoulder of the balloon corresponding with the observed failure site. Immediately after launch, the magnitude begins to decrease. This is due to the pressure head decreasing at a higher rate than the balloon's radius is increasing. The magnitude continues to decrease until the cap drop off, at which time, the magnitudes increase due to the reduced effective thickness. Again, the magnitude will decrease until each cap drops off with a magnitude increase at those points. The maximum magnitude of the stress index

occurs at the last cap drop off for most designs. Also, this occurs at an altitude region of minimum temperature and where the majority of catastrophic failures occur.

After the last cap dropped off, the magnitudes continued to decreased until just prior to the balloon entering float where an increase is observed. Just prior to reaching float altitude, the gas is no longer expanding in a spherical bubble but in, what resembles, a cone. Because the balloon is nearly full, this has the affect of increasing the pressure head at a higher rate.

To determine if stresses have increased over the years, the balloons in this test were sorted by year of manufacture in an attempt to account for any design philosophy changes over the years. It was seen that stresses have increased slightly over the years with a corresponding increase in failure rate. This does not surprise anyone because payload weights have increased significantly over the years. The manufacturers used thinner film gauges to reduce balloon weight to achieve the same altitude with heaver payloads, therefore increasing the stresses. The stress in these balloons increased more dramatically in 1980. This corresponds to the time period when Raven was qualified to build larger balloons for the NASA balloon program. The competition between manufacturers apparently resulted in a stress increase due to thinner materials and heavier caps being used to reduce balloon size to capture the bid.

It can be seen that performance of the pre-1980 film maintained a relatively constant failure rate, probably due to the fact that the film was not taken to its limits.. It is also, in contrast, obvious that film made after 1980 has degraded performance, with the failure rate higher for the same magnitude of stress index. This supports the conclusion that the most probable cause for catastrophic balloon failures is the material.

A model was applied to the balloon design process in an attempt to lower stresses. Assuming that the internal caps were behaving as expected, one possible method of reducing stress in the balloon is to increase the length of the caps. This would allow the gas bubble to be contained in the capped region to higher altitudes and warmer atmospheric temperatures. Another alternative which appears in principle to offer great advantages, with few obvious detrimental affects, is the use of external caps. Current assumptions are that the external cap remains effective throughout the entire flight. As the wall of the balloon contains and resists the gas and its differential pressure, the wall material will strain until the load is introduced into the caps. This is true when the wall gore width is smaller than the associated cap width. If the wall gore width is greater than of the cap, then the cap material will experience the load first, straining until the load is picked up by the wall. Although this also occurs with internal caps, the weight of the external cap maintains contact and shape with the wall rather than dropping away from the wall once gas gets behinds the internal cap.

The stress-altitude history is identical until the first of the internal caps becomes ineffective and the stress index increases. In contrast, the magnitude for the external cap design continues to decrease until once again, an increase is noted upon just entering float altitude. In the case of the external cap design, a more substantial relative increase in magnitude occurs entering float. The reason for this is not obvious at first. However, the explanation for this is apparent when the designer looks at the stress distribution along the gore. In many instances, the maximum value of stress index remains within the capped region, therefore a magnitude increase entering float similar to the internal cap case is expected.

In this case however, the magnitudes in the cap region have reached such low values that the stresses below the caps may be approaching the same values. This is what happened in this case. The maximum value of stress, although small, occurs below the edge of the longest cap, thus appearing as a significant jump in stress due to the much reduced thickness. This could have been prevented if the external cap were slightly longer. This could be significant for some designs and conditions however, the magnitudes are such that a design change is not warranted.

OPTIONS OTHER THAN HIGH ALTITUDE BALLOONS

High altitude balloons have to be able to deal with the stresses placed on them by wind at launch or at float altitude. Some missions require reaching float altitude at times when launch wind conditions can exceed 30 knots, and thus threaten severe stress on the balloon material and causing launch postponement. This idea is not an option to high altitude balloons, but a step forward in developing a high altitude balloon which will withstand the strains and stresses placed on it by ground forces, gravity, wind, and temperature.

The polyethylene balloon was perfect for the uses which it was originally intended, but it has recently become too inferior for the new requirements placed on it. It is too weak, and too fragile. The new payload requirements require a balloon to carry weights which tear polyethylene apart. The option? Winzen International developed a material called StratoFilm. StratoFilm could take twice the stress which polyethylene could and would withstand abrasion which would literally tear polyethylene apart. This material, which revolutionalized high altitude balloon production, was designed by a joint team from General Electric and Winzen International. The material was tested in a wind field of 35 mph with gusting 45 mph at 20 degrees F ambient temperature on 17 Mar 83. The balloon was subjected to more than 30 min. of flagging and

abrasion on the asphalt apron before it was deflated. It was concluded that the film was an excellent material which was capable of surviving this type of launch environment.

Launching of thin film balloons in high winds has been avoided due to the high probability of failure especially with payloads weighing over 200 lbs. and with the large balloon volumes associated with these weights at high flotation altitudes.

The ability to launch scientific or military balloons with payloads of 100 to 500 pounds in winds up to 35 mph remains highly desirable. The Naval Air Development Center (NADC) Warminister, PA developed and successfully tested a light payload weight system (25 lbs) capable of shipboard launch in winds up to 50 mph. The NADC system utilized a two balloon (tow balloon) and gas transfer concept which was adapted to payload weights up to 450 lbs. StratoFilm has been the industry standard in single cell, high altitude, low-launch wind balloon flights for the past 20 years. We are quickly approaching the limits of StratoFilm with the larger payloads, reaching .5 to 5 tons, and the larger balloons, reaching from 10 to 70 M ft^3. The use of polyethylene was recommended in order to minimize gross floatation weight as higher payload weights are addressed. The smaller the inflation gas bubble and the balloon, the less concern is concentrated on the possibility of launch failure.

The following major factors significantly influence high wind launch consideration:

Chart 1-4

1. Wind speed and variability (gusting)

2. Balloon size

3. Balloon inflation time (gas volume/flow rate)

4. Ground launch-pad conditions

5. Balloon restraint/released methodology

By making the balloon weight as small as possible, and therefore gross weight and helium inflation requirements is an obvious first step

toward high wind design consideration. The Winzen has, therefore, developed a new material, which will replace StratoFilm as the more superior contender. The new film is designated StratoFilm-SFX. SFX is about twice as strong as the old StratoFilm and had significantly increased abrasion resistance which makes it very attractive for high wind launch applications. The only concern is control of the balloon once launched. Winzen International and General Electric, currently out of the high altitude balloon field, joined forces to produce a new launch concept. Basically, this concept utilizes an inclined and rotatable container with a single point tiedown. The balloon is restrained by this fixture during the 3 to 5 minute inflation where 60% free lift will assure high angle inclination and quick lift-off.

At launch the undeployed balloon section and payload are payed out by a mechanical, automatic, brake/tether until sufficient altitude is reached to release and allow the payload/balloon container to rotate under the balloon without contacting the ground. The lower balloon section, contained in a reefing sleeve to inhibit flagging, is deployed at or above an altitude of 1,000 ft. The outer payload shell can also be jettisoned at this time if required. See diagram on page next page.

The new StratoFilm-SFX was designed to withstand flagging in 35 mph winds and high ground wind abrasion. When tested, SFX performed satisfactorily. The basic high wind launch concept required only 3 to 5

9-17

minutes to inflate a balloon substantiated by hardware testing performed by GE/Winzen/Beech Aircraft. The test which was performed, exposed the balloon to 35 mph winds for over 30 minutes. After examination of the test balloon material, and considering this excessively long exposure time, the basic balloon design has been modified to specify using a .5 mil gas barrier and a 1.0 mil cap. This design will remain adequate to survive the rigors of inflation and launch in high wind and will provide a slightly smaller, lighter weight balloon at lower cost. This means that this design combined with the SFX will give a suitable balloon for battlefield surveillance. The cost of an expendable balloon for this propose is not known.

In conclusion, the new material, StratoFilm-SFX would be suitable to this mission. To send a balloon to an altitude of 65,000 ft. would induce great stresses on the envelope, gas bubble, tether, and other important components in the balloon set up. While gravity is doing its evil deed by pulling the payload back to earth, mother nature is doing her own evil deed by blowing the balloon sideways, up, and down. These two factors could cause a balloon to be lost or destroyed. In actuality, the payload is the most important component in the set up and is the most valuable item. The loss of the balloon might be acceptable, but the loss of some payloads could pose problems. The Department of Defense could send up a sensitive observation package and if the balloon fails or the tether

fails the package could be destroyed or lost. The loss means the balloon floating, untraced, to unknown places and maybe falling into the wrong hands.

The DOD is very cautious in matters such as these. Therefore, a more reliable balloon material and a stronger tether material is desirable. The StratoFilm-SFX is one consideration. This will make the balloons twice as reliable as the previous polyethylene types. The tether, however, is another matter completely. Kevlar is the strongest material that Phillips Laboratories has in inventory for tether cables. The Kevlar is strong but not strong enough for this specific mission. The good news is the possibility of strengthening the Kevlar to meet specifications. The off the shelf tether cable could also be coated to provide more strength without purchasing strengthen Kevlar which would severely deplete the budget. My suggestion, after careful research, is to rely on the coated, strengthened Kevlar cable. Have the off the shelf stock treated, do not buy new stock. The balloon is the most expensive part of the solution. The off the shelf models available to Phillips are not adequate to perform the required task. Therefore, I suggest finding a cheap form of the new material SFX, if not already in use. Polyethylene might not be strong enough to withstand the shearing and pulling put on it by this mission. Polyethylene might withstand the strains but a guarantee is not possible. If the payload is expensive, than the SFX might be the better choice for insurance

DEVELOPMENT OF THE PICLL (PARTICLE IN CELL LINKED LIST)
PREPROCESSOR

Nicholas Mitchell

Belen High School
1619 Delgado Road
Belen, NM 87002

DEVELOPMENT OF THE PICLL (PARTICLE IN CELL LINKED LIST) PREPROCESSOR

Nicholas Mitchell
Belen High School

Abstract

One technique for modeling a non-collisional plasmas is the particle in cell (PIC) approach. The domain of the problem is divided into spatial cells. The fields and currents within the simulation are approximated at uniformily distributed positions throughout the spatial mesh. The plasma is modeled using a number of charged macro particles. The particles and initial conditions are used to update the fields on the problem mesh. These fields are then used to determine particle motion during one full time step. The PIC algorithm uses this two step process to simulate a plasma. A new three dimensional relativistic PIC code is being developed by the Phillips Laboratory, called PICLL (Particle In Cell Linked List). An important part of the project is the preprocessor that generates PICLL's input file. Before the preprocessor is even used, the spatial mesh is created using a grid generation program like CAEDS by IBM. User input along with the output from the mesh generation program are then used by the preprocessor to generate the following information: cell connectivity, two layers of ghost cells, positions of field values on the spatial mesh, and the required relationships among field values. All of the required preprocessor functionality was accomplished in 3500 line of coding. Significant improvement in preprocessor performance is possible by further refining its algorithms.

DEVELOPMENT OF THE PICLL (PARTICLE IN CELL LINKED LIST) PREPROCESSOR

Nicholas Mitchell

Introduction

The advent of massively parallel computers composed of nodes with distributed memory allows significant advances in the size and complexity of certain types of numerical simulations. Particle in cell (PIC) techniques used in modeling non-collisional plasmas show particular promise on these MIMD (multiple instruction multiple data) architecture machines. Phillips laboratory is currently embarked on a multi-year effort sponsored by AFOSR to advance the state of the art in 3D PIC simulations on MIMD machines. Part of this effort involves the development of PICLL (particle in cell linked list), a relativistic 3 dimensional PIC code. The code is composed of three separate codes, a preprocessor, the main parallel code, and an output post-processing module. The main parallel code module contains all the physics and runs on various MIMD platforms to perform the actual plasma simulations. Portability is a key issue with this module, so it is written in strict ANSI C. Computational efficiency of the parallel calculations is maximized by overlapping communications and computations. Extensive documentation is provided in the source code of all the PICLL modules. Complete documentation of all the modules will be provided in a user's manual and physics reference.

The preprocessor code's purpose is fairly simple in theory. It initializes the mesh of cells used by the main PICLL code and creates the field positions for each cell. This seemingly trivial problem becomes enormous when a problem's geometry becomes complex. The preprocessor must be able to handle both simple and complex problems efficiently.

Problem

The preprocessor accomplishes several required tasks. The first is reading the mesh data. IBM's CAEDS program is used to create the actual mesh for the region where the plasma resides. The CAEDS data gives coordinate locations of each cell's corner closest to the origin. The mesh file also contains data

about the bounding surfaces. The bounding surface data defines the corners and type of each surface.

The preprocessor generates connectivity information from this data; that is what are each cell's neighbors to the top, bottom, left, right, front and back. Surface conditions are read for each cell. Next the preprocessor creates two layers of "ghost cells" around all the problem's original cells. These ghost cells are used to minimize the amount of communication between nodes, and therefore optimize the computation to communication ratio.

After the spatial mesh is fully specified by the preprocessor, then the static locations of electric field (E), magnetic field (B), and current (J) components are formulated for the problem. Field and current locations are chosen so that the PIC algorithms are second order accurate. To accomplish this, the individual components of E and J are collocated on the center of cell edges, with only the component of each that is parallel to the cell edge present. The B components are centered on cell faces, with only the component perpendicular to the cell face present.

The preprocessor must uniquely determine all the fields present on a problem's spatial mesh, which is definitely not a trivial task. Linked lists of all the field information are kept separately from the cell information. All the required field structures are first created, and then cell references to the fields are generated. This allows the PICLL code to store a specific field component information in only one unique location in memory, but many other structures may reference this value through the use of pointers.

The last piece of information generated by the preprocessor is required by PICLL's physics algorithm when advancing the values of E and B field components in time. When advancing a specific component of E, the four closest components of B that are not parallel to this component are required. Similarly, for each component of B the four closest nonparallel components of E are necessary. The preprocessor identifies these four required components for each of the field values. When PICLL processes the input file generated by the preprocessor this information is used to create pointers to these four associated components for each field value component. These pointers are stored in the field component's data structure.

Results

The spatial cell connectivity problem was addressed first. All the spatial cells in PICLL are Cartesian and are of a constant size. The output from CAEDS gives the position of each cell in terms of its corner closest to the problem's origin. Also, all the cells from CAEDS are in the first spatial quadrant. Each cell location is incremented in all three spatial directions by a cell width, and the list of cell origins from CAEDS is searched for cells with matching locations. This is a zeroth order approach to solving the cell connectivity problem; clearly a better method of sorting will tremendously improve performance of this task.

Each surface defined within the problem is specified by the location of two of its diagonally opposed corners. The surface of every cell is compared to these specified surfaces, and cell face characteristics recorded. This is a zeroth order approach to this sorting problem, and clearly significant algorithm improvements are possible.

The two layers of ghost cells are created in a two step process. The first layer is created by identifying all the cells with missing neighbors. These ghost cells are created so that none of the original cells are missing a neighbor. The second step of the process is to identify all the spatial cells for the newly expanded mesh with missing neighbors. The missing neighbors are then filled in with a new layer of cells to form the second layer of ghost cells.

To create the fields, the following algorithm is used. The three B fields, and the three collocated E fields and J currents closest to the origin are created for each cell. This causes no overlapping of fields present on the spatial mesh. The neighbor information for each cell is then used to determine which fields still need to be created on the spatial mesh. The end result of this algorithm is that all the problem's fields are uniquely specified.

Attaching the fields to the cells is accomplished next. A function, similar the one used to find cell neighbors, parses the field lists to find a field at each specific spatial location on the cell. The algorithm used to perform this sort is zeroth order; so significant speed ups are possible.

Finally, the problem of identifying the four associated values used to advance each component of E and B is addressed. Since each cell knows all the fields present on it and its associated neighbor cells; the problem is easily solved by correctly correlating this information. The approach used is straight forward and efficient, so no great improvements in performance are possible by revising this algorithm.

Conclusions

The preprocessor code passed an extensive amount of benchmark tests. The performance of the code due to inefficient sorting algorithms was slower than anticipated. For one extreme case, the preprocessor with a 50x50x50 mesh ran for over 48 hours on a Sun SPARC 10 without completing. Many further optimizations of the algorithms used by the preprocessor are possible, especially in the area of sorting. Only with these further algorithm refinements will the preprocessor's performance become practical.

Resources

1. Minor, Bryan M. "Proposed Revisions to PICARD". May 3, 1994. (unpublished)

2. Kernighan, Brian W. and Dennis M. Ritchie. "The C Programming Language Second Edition". AT&T Bell Laboratories, Murray, New Jersey. 1988.

3. Hockney, R.W. and J.W. Eastwood. "Computer Simulation using Particles". Institute of Physics Publishing, Bristol, England. 1988.

4. Birdsall, C.W. and A.B. Langdon. "Plasma Physics via Computer Simulation". Adam Adam Hilger, New York, NY. 1991.

NICKEL-CADMIUM BATTERIES

Julie Ann Niemeyer

Valley High School
1505 Candelaria Rd. NW
Albuquerque NM 87107

Final Report for:
High school Apprentice Program
Phillip's Laboratory

September 1994

11-1

NICKEL-CADMIUM BATTERIES

Julie Ann Niemeyer
Valley High School

Abstract

Nickel-Cadmium battery cells were tested to determine the and condition of the cells and group the cells for satellite use. To test the cells six test stations were established. The testing of the cells was used to condition the cells for use and to also determine the grouping of the cells when used to create batteries. The first station was used to clean and test the cells for any leaks, to take basic measurements, to label the cells, and to apply kapton tape to protect the cells in a space environment. The next were test stations were used to condition the cells in a normal environment. Three stations were necessary to test all batteries in the specified time line and also each station was run and monitored 24 hours a day. The final two test stations were set up on thermal vacuums to test the cells in an environment which the cells will be operating in.

NICKEL-CADMIUM BATTERIES

Julie Ann Niemeyer

Nickel-Cadmium:NiCad batteries are becoming more commonly used in everyday application and also technical application. Many people have started to use Nickel-Cadmium batteries because of their many features. Nickel-Cadmium batteries require little maintenance, have high discharging and charging rate capabilities, constancy of discharge voltage, capability of withstanding extended overcharge, excellent life cycle, and a moderate self-discharge rate.

Nickel-cadmium battery cells require no maintenance under normal conditions. The electrochemical reactions that occur are such that no electrolyte is depleted. When the cells are overcharged at recommended rates the reaction is self-sustaining. There is one problem, when the rates are exceeded the high internal pressure can cause the cell to vent and loose electrolyte. When operating in the space environment venting in cells can cause damage to other cells or objects around them. Also with the venting of cells they will lose some capacity for power.

The high-charge rate of Nickel-Cadmium cells is safe, yet the current must be terminated or reduced before excessive pressures are achieved. The termination or reduction of current is only necessary if the charge will be continued in the overcharge mode. When charging and discharging a cell many times a day this high rate of charge is useful. Nickel-Cadmium cells are normally charged in fourteen to sixteen hours with a charge rate of C/10. If necessary voltage can be monitored and current can be terminated when the voltage reaches a desired level.

11-3

When charging a Nickel-Cadmium cell the direct current must be in the opposite direction of the discharge current. During this part of the cycle the positive electrode in nickel hydroxide and the negative is cadmium hydroxide. While charging the nickel hydroxide is converted to higher valence hydroxides, usually in the trivalent state. If the temperature is high the efficiency of the cell is reduced. To help combat this problem higher minimum current density is required to charge the cell. the temperature at the standard C/10 rate is 32-115*F and for optimum performance the temperature should be between 65-85*F.

If the overcharge mode of Nickel-Cadmium cells is used there is virtually no safety hazards. During this mode of charge most of the charging current generates oxygen on the positive electrode. This limits the overcharge rate of the cells. Other limitations on the overcharge rate is the recombination rate of oxygen-cadmium and the maximum pressure before venting will take place. The recombination rate of oxygen-cadmium is dependent upon the cell temperature, and the ability of the electrode to react with oxygen. The recombination rate is also determined by the crystalline structure which in turn is determined on the surface area, temperature, and pressure. If a cell is partially charged it will and can accept a charge current above the maximum recommended. Even though the cell will accept this charge it must be monitored and charge current must be terminated or reduced to the recommended charge rates before the internal pressure causes the cell to vent. If low temperatures occur the rate of charge should be reduced.

Nickel-Cadmium cells are ideal for high power systems because they can be discharged at pulse rates up to 60C and can withstand continuous discharge rates up to 20C for high voltage operations. The cells can withstand these discharge rates within

the temperature range of 65-85*F. A reduction of both power and capacity will occur when the temperature is low and the discharge current is high. At all discharge rates the average discharge is at its maximum when at room temperature.

Nickel-Cadmium cells can be continuously overcharged at recommended trickle charge rates. The trickle charge rates are used to maintain the cell in ready to use condition for emergency and standby applications. The maximum overcharge is limited not only by the oxygen recombination rate but also by the negative electrode, electrolyte level, and the cell temperature. The continuous overcharging does not affect the cell life except when the recommended rates are exceeded. When these recommended rates are exceeded venting of the cell is highly probable.

The life cycle of Nickel-Cadmium batteries is dependent upon temperature, the depth of discharge, the charge rate, and the extent of overcharge. Cell life will be shortened if Nickel-Cadmium cells are used for long-term operation at high temperatures and deep discharge under routine cycles. Due to the fact that general factors are not additive in their effects it is difficult to predict cell life. Field experience in related and similar applications can provide estimates. With the results of the field experience the minimum life of a cell is 250 cycles.

Storage of Nickel-Cadmium cells is relatively simple. These cells can be stored in either the charged or discharged state. Either of these conditions should not cause significant, irreversible degradation in performance. The cells will loose capacity in the charged state, yet the original performance level can be achieved with conditioning cycles. This feature allows cells to be stored and ready for later applications without the delay of the task to recharge the cells. If cells have been stored for a long period of time

in the discharge state they should only be charged at the recommended C/10 rate for a few cycles to condition the cell.

The most common type of Nickel-Cadmium batteries is the cylindrical cell. The capacity for cylindrical cells between .100 to 7.00 ampere-hours. The reason it is the most common cell is because the design lends itself readily to the use of mass production. It is also the most rugged of the cell types and can operate in a wide range of environmental conditions.

Nickel-Cadmium battery cells were tested to determine the condition of the cells and group the cells for satellite use. To test the cells six test stations were established. The testing of the cells was used to condition the cells for use and to also determine the grouping of the cells when used to create batteries. The first station was used to clean and test the cells for any leaks, to take basic measurements, to label the cells, and to apply kapton tape to protect the cells in a space environment. The next   test stations were used to condition the cells in a normal environment. Three stations were necessary to test all batteries in the specified time line and also each station was run and monitored 24 hours a day. The final two test stations were set up on thermal vacuums to test the cells in an environment which the cells will be operating in. These tests were used to group batteries and also to determine of the cells were operate well in a space environment.

After these tests are concluded the Nickel-Cadmium cells will be qualified and conditioned to become the power source for a satellite to be launched in December of 1994. The charge will come from solar panels that will operate the satellite and charge the batteries during exposure to the sun. When this panel is not exposed the batteries

will become the power source for the satellite. The purpose of conditioning the cells is so they will have maximum capacity and performance levels throughout the mission. The cells will also be grouped together in hopes to create better performance out of all the cells. With the characteristics of Nickel-Cadmium batteries the satellite will have an excellent power source, while the tests that were done will help create a superior power source.

THE CHARACTERIZATION OF
AN ATMOSPHERIC TURBULENCE
GENERATOR

Krista Nuttall

La Cueva High School
7801 Wilshire N.E.
Albuquerque, N.M.   87122

Acknowledgments

This research would have been impossible without the selfless help and patience of Dave Voelz, Dave Holmes, Dennis Dunneman, Joe Ray, Lenore McMackin, Joe Gallegos, Jim Boger, Doug Rider, and Paul Rodriquez.

THE CHARACTERIZATION OF
AN ATMOSPHERIC TURBULENCE
GENERATOR

Krista Nuttall
La Cueva High School

Abstract

A turbulence generator designed for use in optical laboratory experiments needed to be refurbished and characterized. This was accomplished by: 1) rebuilding the electrical parts of the generator; 2) examining the turbulence produced by the generator using an interferometer; 3) altering the air and heat flow using different methods in an attempt to create homogenous turbulence and determine the equipment's best setting; 4) characterizing specific flow regions of the generator using a laser beam probe, lateral effect sensor, and oscilloscope; and 5) recording the tilt spectrum of the laser beam probe using a spectrum analyzer. The setting that created the most homogenous turbulence was 144W on the heating resistors, fans pulling air out of the generator, and the coarse metal screen placed in the bottom of the tube over the resistors.

THE CHARACTERIZATION OF
AN ATMOSPHERIC TURBULENCE
GENERATOR

Krista Nuttall

Introduction:

Turbulence distorts the light generated by a laser beam when the laser beam is propagated through the atmosphere. Changing air densities due to winds and temperature changes create a complicated index of refraction structure that steers and breaks up a laser beam. These distortions are particularly noticeable in laser imaging. When a laser is reflected off of a satellite to create an image, for instance, the recovered picture is degraded.

In the past, turbulence generators have been built in an attempt to simulate atmospheric turbulence. If the turbulence produced accurately replicates the atmosphere, then distortions and image blurring can be studied in the lab and eventually corrected.

Discussion of Problem:

Phillips Lab in Albuquerque, N.M. built a turbulence generator that was not useful because the level of air turbulence and disturbance patterns it created were unknown. The generator produced heat with four four-packs of resistors that are attached to the bottom of a 24 inch long plastic tube with a 4 inch diameter. Air flow is created by two AC fans mounted to the top of the tube. (See figure A) The generator has eight different heat settings including: 9, 12, 18, 36, 72, 108, 144, and zero watts. The fans only operate at one speed; however, they can be turned around to reverse direction of the air flow.

In order to make this piece of equipment functional, a study was needed to determine which settings produce turbulence that most closely represents atmospheric turbulence. We accomplished this by: 1) rebuilding the electrical parts of the generator; 2) examining the

turbulence using an interferometer; 3) altering the air and heat flow using different methods in an attempt to create homogenous turbulence and determine the equipment's best setting; 4) characterizing specific flow regions of the tube using a helium-neon laser beam probe setup and oscilloscope; and 5) recording the tilt spectrum of the probe beam using a spectrum analyzer.

Plastic Tube 24"
Turbulence Generator
Fans
Power Box
Base
Side View

Diameter 4"
Resistors
Front View
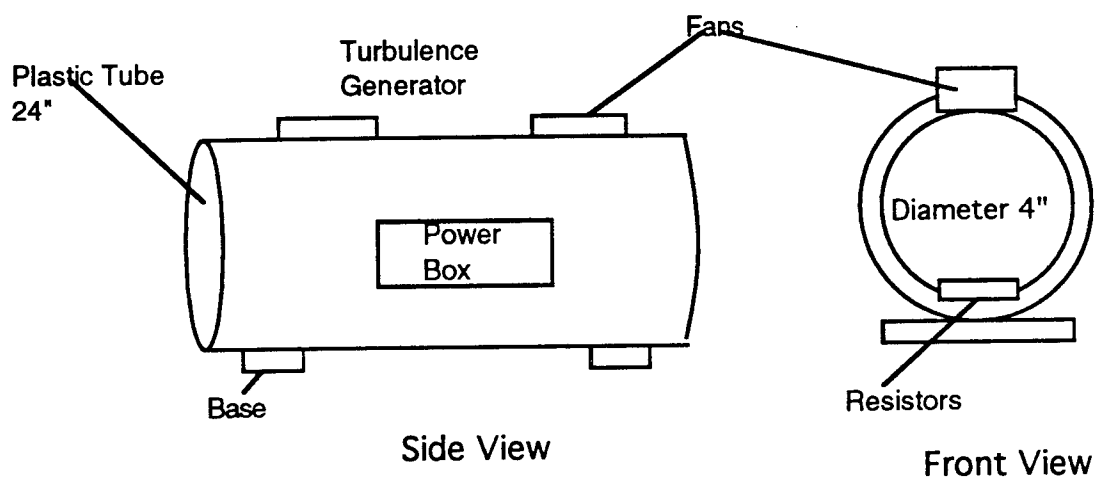
Figure A: Turbulence Generator Diagram

Experiments and Results:

Initially, the generator did not turn on, thus our challenge was to get it in working order. The electrical system had several cold solder joints that were corrected and some of the wiring was replaced. The electrical system worked well after these changes.

We initially examined the generator using an interferometer in order to familiarize ourselves with the turbulence it was creating. The interferometer was equipped with a six inch, ninety percent transmission flat and an optical light screen which dilutes the Helium/Neon laser intensity by fifty percent. The equipment was lined up such that the interferometer laser could be sent through the tubular turbulence generator and reflected back to the interferometer off of a flat mirror. (see figure B)

12-5
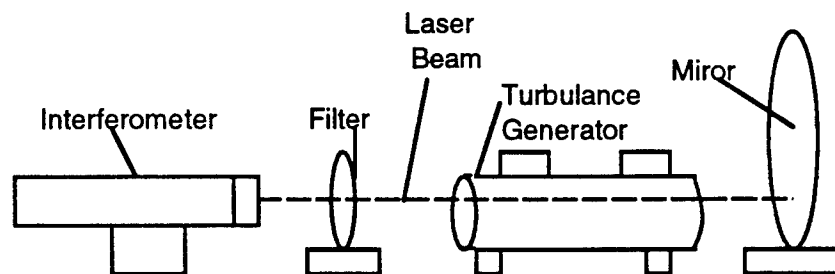
Figure B: Interferometer Set-Up

Pictures with the interferometer were taken every five minutes on each available heat setting of the turbulence generator.   In the first set of pictures, the fans drew air out of the tube.

The interferometer fringe pictures suggested that air was not distributing evenly in the tunnel. Large heat gradients were apparent directly above the resistors; and due to the open-ended tunnel, air exited the apparatus after only passing through the end of the tube and the fan. Interferograms A through E demonstrate these problems.   For example, in interferograms A through C the optical fringes are closer together directly over the resistors suggesting a strong index of refraction gradient, and therefore, a strong heat gradient.   The heat gradients remained strongest near the resistors even when the fans were activated in pictures D and E.   Thus, different methods were executed to alter the air flow.

Interferograms
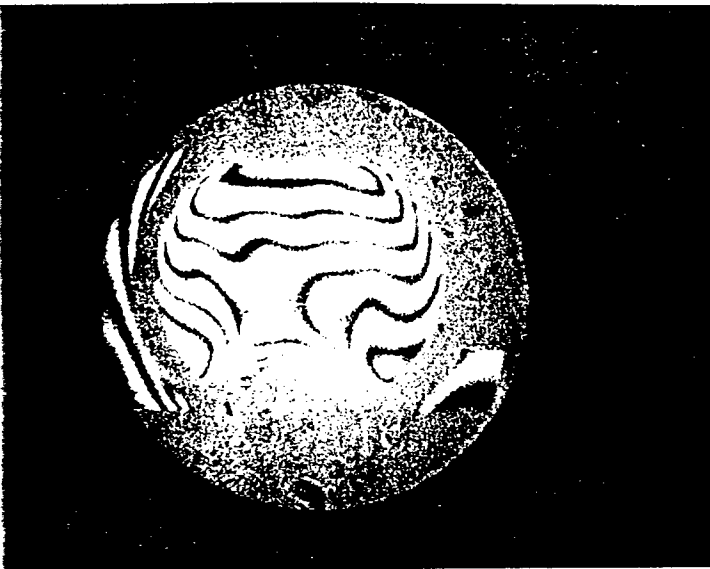
PICTURE A   *12 w next no fans*

2 watts of power, no fans
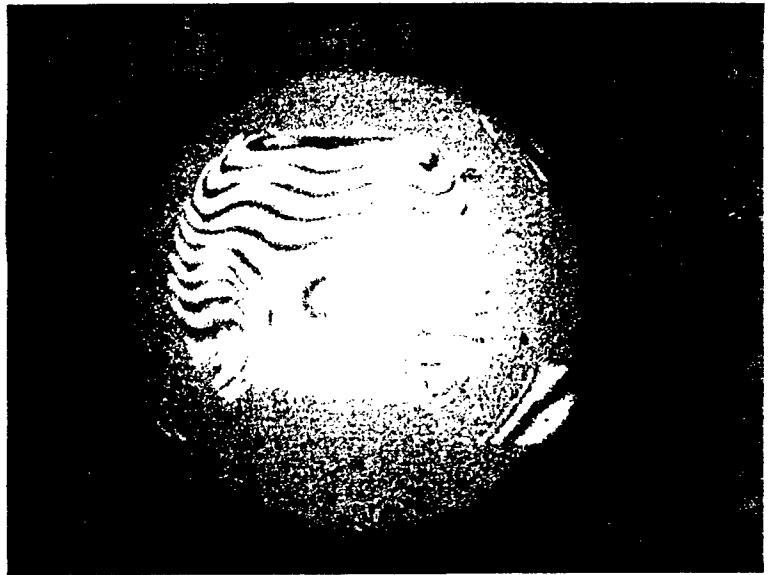
Picture B   *36 w no fans*

36 watts of power, no fans
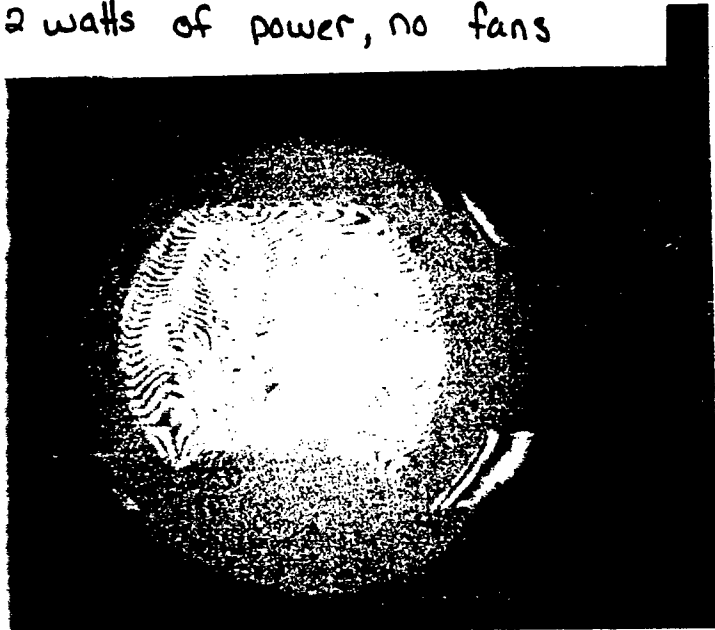
PICTURE C

14 watts of power, no fans
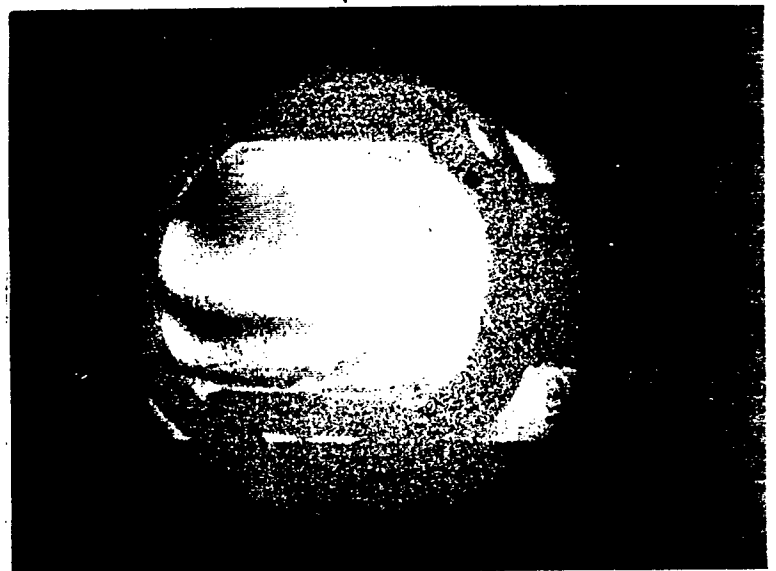
PICTURE D   *fan + 9 w*

9 watts of power with fans
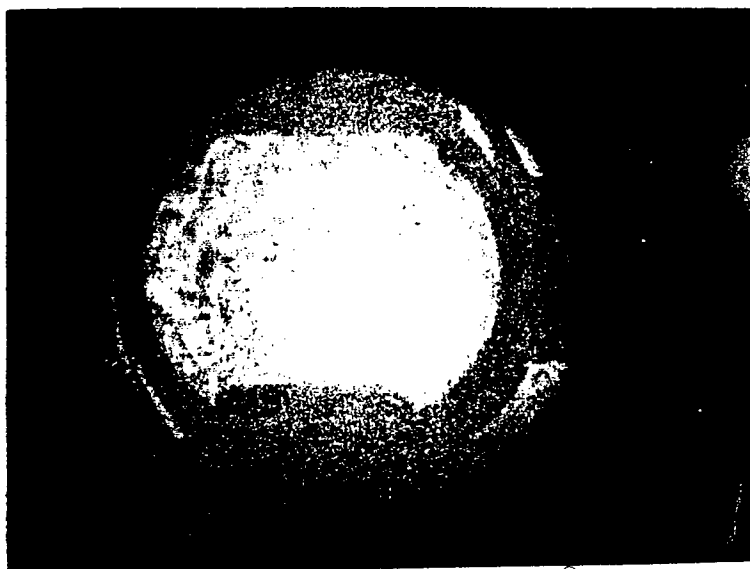
PICTURE E   *fan + 144 w*

Successful Alterations of the Turbulance Generator
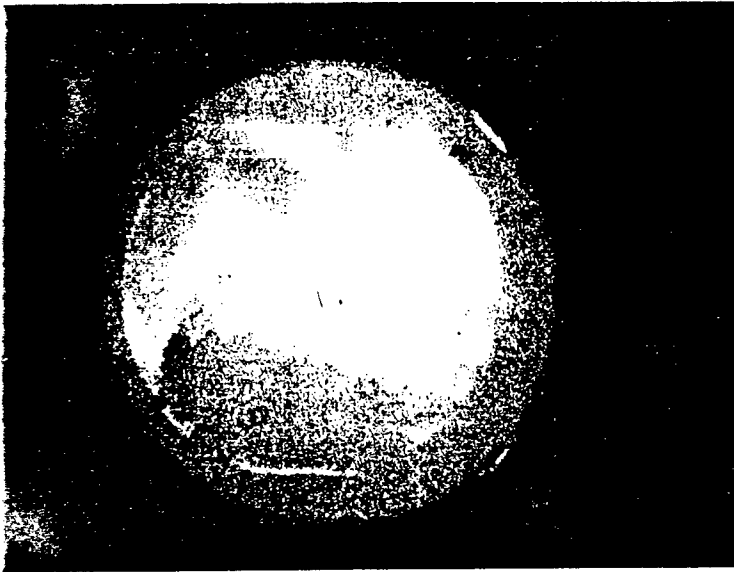
PICTURE F   9w w/f&s

9 watts of Power with fans and
Coarse metal screen
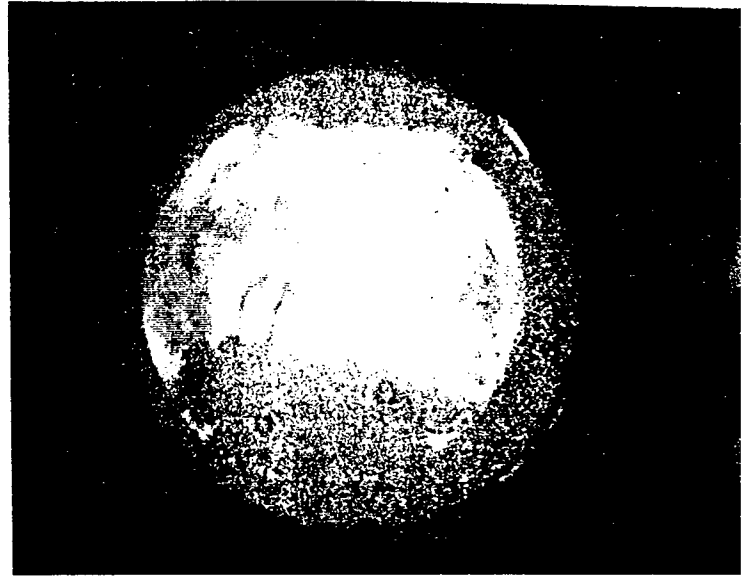
PICTURE G   36 w/f&s

36 watts of power with fans
and coarse metal screen
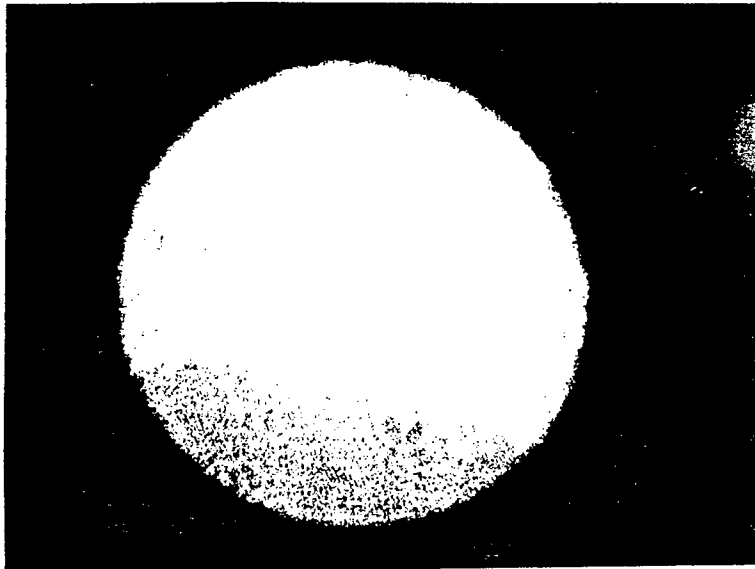
PICTURE H   144 w w/fan, screen
no doughnute

144 watts of power with coarse
metal screen

Alterations of the Turbulance Generator
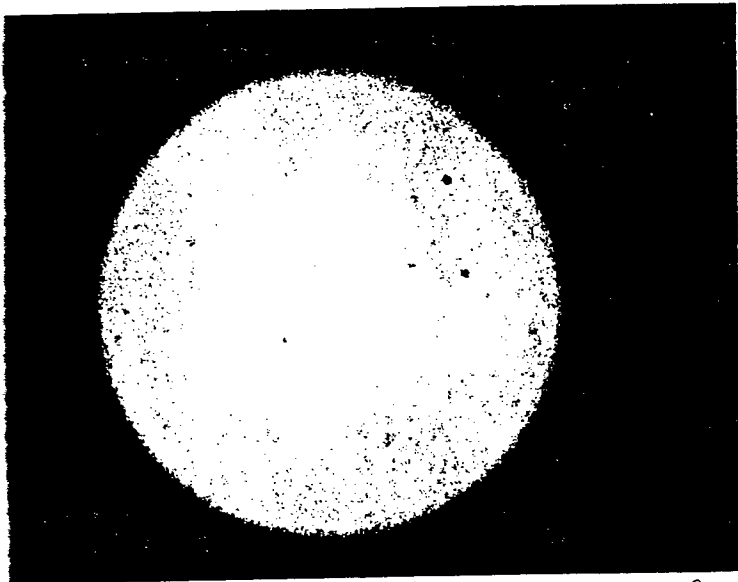
PICTURE I   9 w/ w/screen, fan

Watts of power with coarse screen, cardboard covers and fan
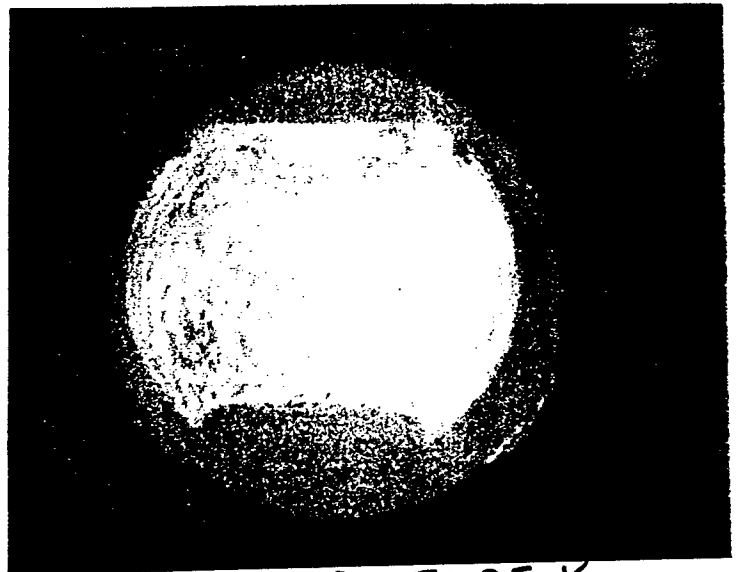
144 watts w/ fan covers   PICTURE K

144 watts of power, fans blowing in, with fan covers
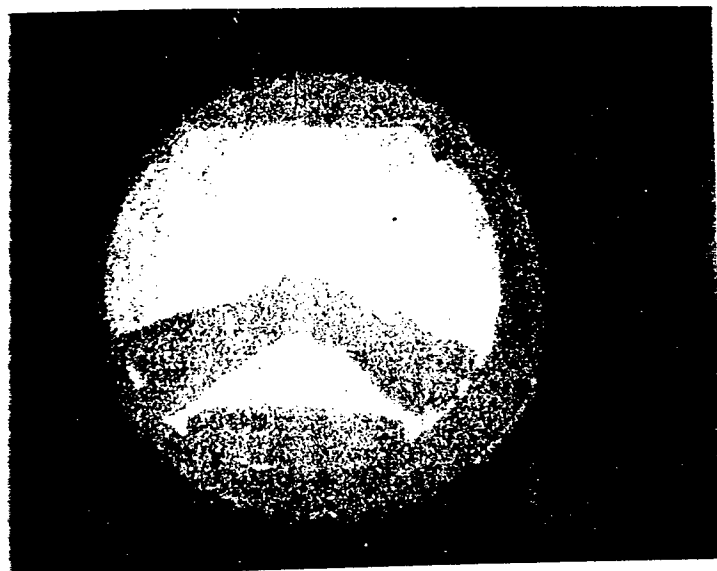
4 watts w/ fine wire mesh   PICTURE J

144 watts of power with fine wire mesh and fans
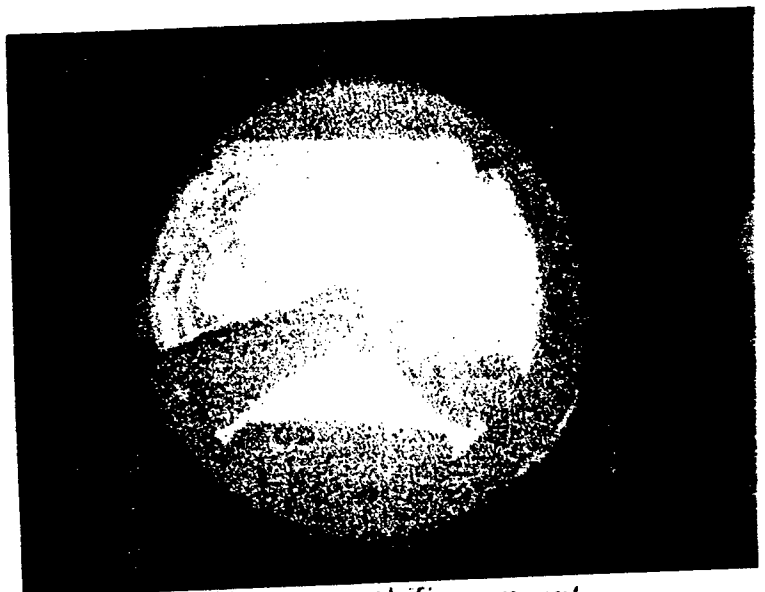
144 watts w/ fan covers and fine wire mesh

PICTURE L

144 watts of power with fan covers and fine wire mesh

First, in an attempt to reduce air flow from the open ends of the tube, cardboard in the shape of a flat toroid was temporarily attached to the ends of the tube. (See figure D) Interferometer pictures were taken at three heat settings (9w, 36w, and 144 w) and with full fans sucking the air out of the tube. After examining the pictures, it did not appear that the mixing of the turbulence over the reduced, clear apperture was much different than the mixing seen in previous pictures without the cardboard. An example of this alteration is represented in interferogram picture I.

Next, a coarse metal screen with holes one half of an inch by one inch was placed into the bottom of the tube over the resistors. The screen was intended to create heat eddies we hoped would help mix make the index of refraction gradients. We took interferograms at the same three wattages as before with the screen, then with the screen and the cardboard. In pictures F, G, and H the coarse metal screen is in place and better mixing is apparent. The strong, layered fringes near the resistor have now been replaced by many more broken fringes. This was eventually deemed the most successful alteration of the unit.

Then, the fans were removed and replaced so they blew air into the tube. Pictures were recorded five minutes apart with the generator on the same three settings. They were taken with the fans and heat alone; then with the fans, heat, and screen; then with the fans, heat, screen, and cardboard. This change caused far too much air flow and completely removed any heat from the tube.

Because it became apparent that the heat was still concentrated in the bottom of the tube, it was necessary to specify the discrepancy between the heat in the top and the bottom of the generator. Therefore, the temperature was taken every five minutes at every setting of the generator with

a temperature probe placed in the top then in the bottom of the tube. Because the most successful addition thus far was the coarse metal screen, the temperature measurements were made with the screen in place. (See Figure C)

Temperature Probe on
the Top of the Tube

Temperature Probe on
the Side of the Tube
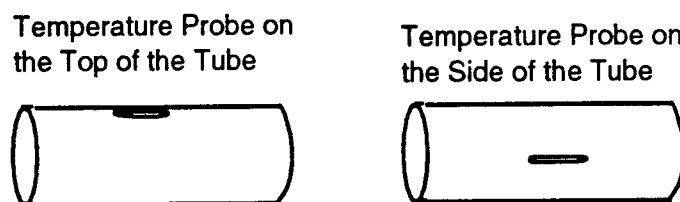
Figure C: Placement of Temperature Probes

The results of gathering the temperature from two different regions of the tube are as follows:

The Top of the Tube (Degrees F):

9w	78.6
12w	78.4
18w	79.2
36w	81.5
72w	87.5
108w	95.6
144w	101.9

The Side of the Tube (Degrees F):

76
76.7
78.1
82.3
83.1
91.7
97.2

The measured temperature values did not turn out as expected. The generator was hotter near the top of the tube rather than on the side. Apparently, the hot air collects at the top of the tube although the interferogram pictures show that the strongest heat gradients occur just above the resistors.

After we recorded the temperature, we tested a metal screen made of fine wire mesh in the turbulence generator. It was placed over the resistors and pictures were taken similar to the method used to test the coarse screen. The generator was put on the three different heat settings and interferograms were recorded. Interferogram picture J shows that the fine metal screen was relatively ineffective in mixing the heat gradients.

12-11

Because the fans blowing in created too much air flow, the last attempt at altering the generator was installing fan covers. Cardboard squares with one centimeter wide holes were fit over the three inch fans. Interferograms were recorded at the three heat settings. We took a set of pictures with only the wire mesh, then we took a set with both the fan covers and the wire mesh. Neither of these methods were successful in creating homogenous turbulence as represented in pictures K and L. When the fine wire mesh was added to the turbulence generator, there was no recognizable difference in the flow patterns, so that material was discarded. Also, the cardboard fan covers did not restrict the blowing fans enough, so they were also eliminated.

24"

Cardboard Cover   Coarse Screen   Fan Cover

Fine Mesh
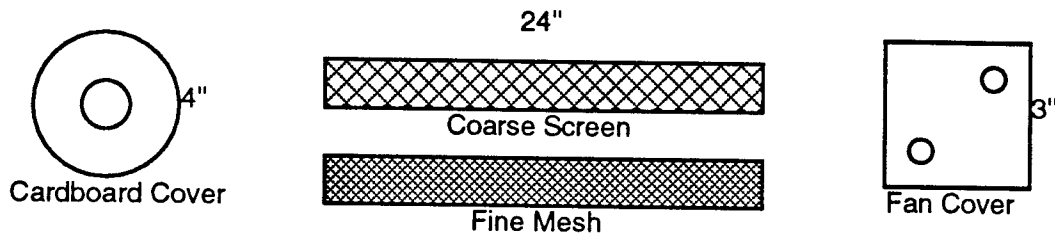
Figure D: Objects Used To Alter Generator

It was determined that the setting which produced the most homogenous turbulence was 144 watts of power with the fans sucking air out of the tube and with the coarse metal screen placed in the bottom of the tube.

The next step was to look at the turbulence in different regions of the tube using a laser beam probe setup. The probe consisted of a small HeNe laser and a lateral effect sensor with outputs connected to an oscilloscope. (See figure E)

12-12
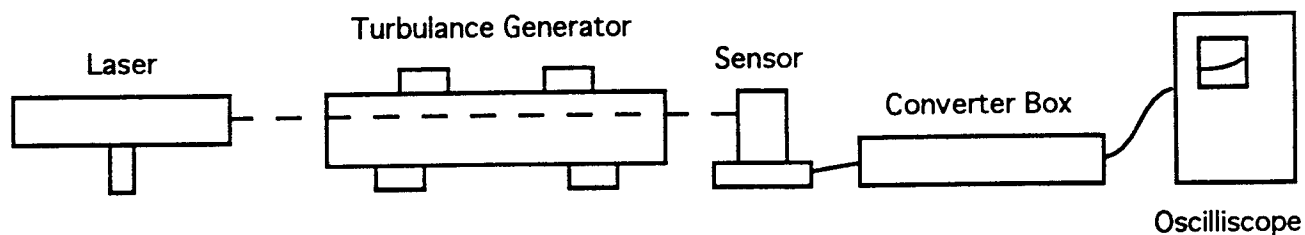
Figure E: Oscilloscope Set-Up

The laser was fired through the turbulence generator near the top, side, bottom, and the center of the tube. (See figure F) The lateral effect sensor detected the vertical and horizontal deflection of the laser beam caused by the turbulence. The sensor output voltages were sent to an oscilloscope. We recorded the maximum peak-to-peak voltage for the x and y axis of each position of the laser in order to identify significant differences in various areas of the tube.

	X Position	Y Position
	50mV	70mV
	70mV	50mV
	170mV	100mV
	70mV	60mV

Figure F: Different laser beam positions for tilt measurements and peak-to-peak voltages recorded for the x and y axes. The lateral effect sensor was measured to be 40 V/m.

Then the lateral effect sensor was connected to a spectral analyzer. Records of the vertical (Y) and horizontal (X) spectrum were recorded for the probe positions shown above. The spectrum shown on the analyzer screen was photographed with an oscilloscope Polaroid. (see photograph pages 12-15, 12-16, 12-17) For the graphs in the photographs, the x axis units are Hz and the Y axis is Volts in a dB scale. The general trend of the spectra appeared similar to that of the atmosphere with the energy dying out beyond 100 Hz. However more work needs to be done on comparing these graphs with atmospheric theory.

SPECTRUM ANALYZER PICTURES OF SIGNAL GENERATED BY TURBULENCE GENERATOR AT VARIOUS SETTINGS

Noise:

Volts plotted on a dB scale
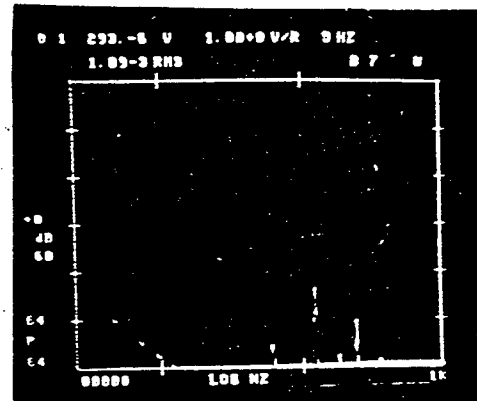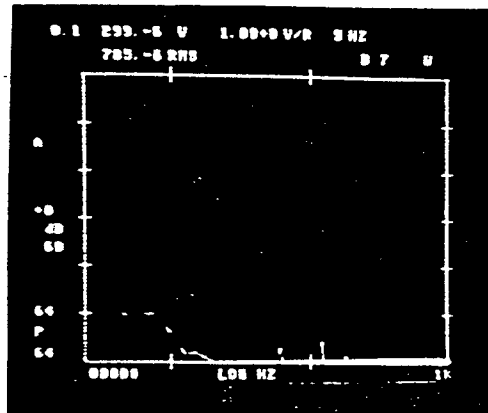
H_z (cyc/sec)

X Axis:
Max. Voltage: 299×10^{-6} volt
Min. Voltage: 27.3×10^{-6} volt

Y Axis:
293×10^{-6} volts
27.2×10^{-6} volts

Laser fired through top of tube:
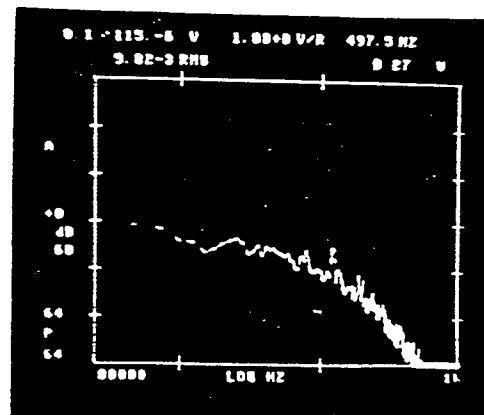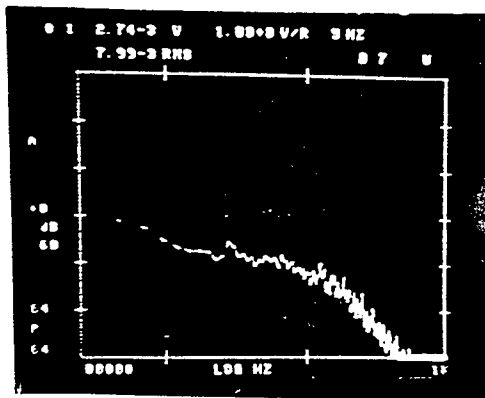
X Axis:
Max Voltage: 2.74×10^{-3} Volts
Min Voltage: 104×10^{-6} volts

Y Axis:
2.77×10^{-3} volt
115×10^{-6} Vol

Laser fired through side of tube:

Volts plotted on a dB scale
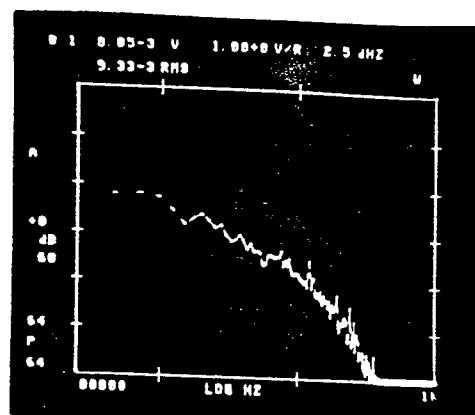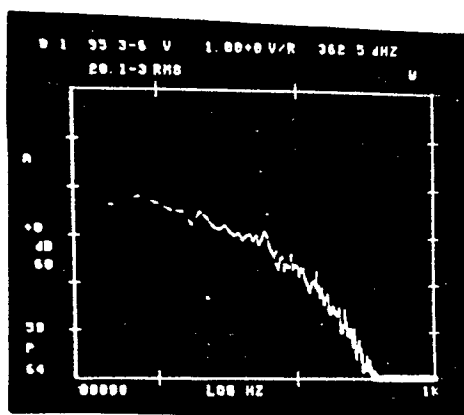
Hz (cyc/sec)

X axis:
Max. Voltage: 6.71×10^{-3} volts
Min. Voltage: 95.3×10^{-6} volts

Y axis:
8.05×10^{-3} volts
78.2×10^{-6} volts

Laser fired through bottom of tube:
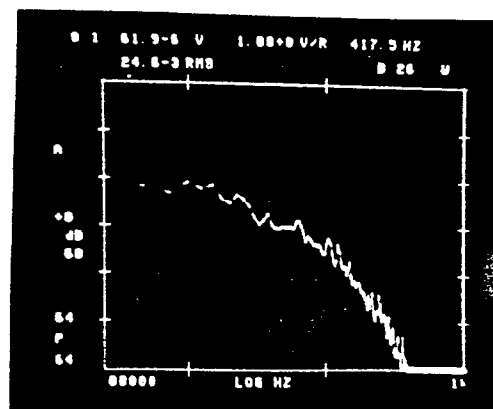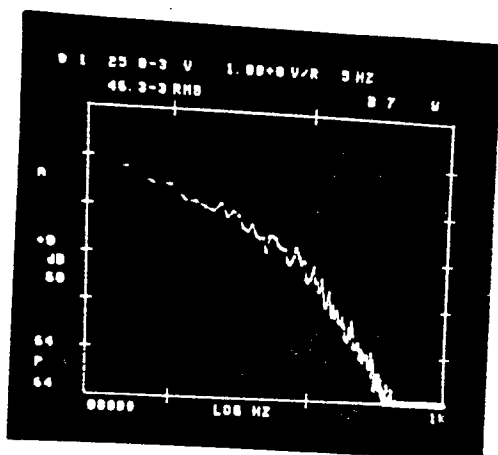
X axis:
Max. Voltage: 25.0×10^{-3} Volts
Min. Voltage: 98.2×10^{-6} volts

Y axis:
8.42×10^{-3} volts
104×10^{-6} volts

Laser fired through center of tube:
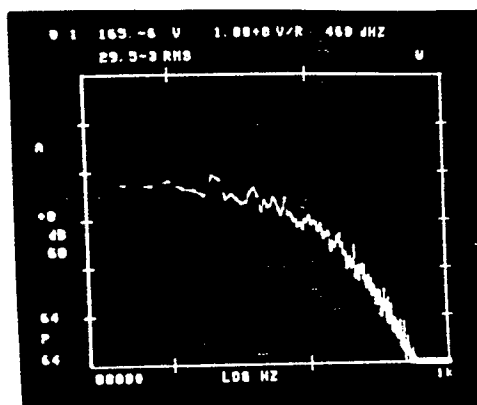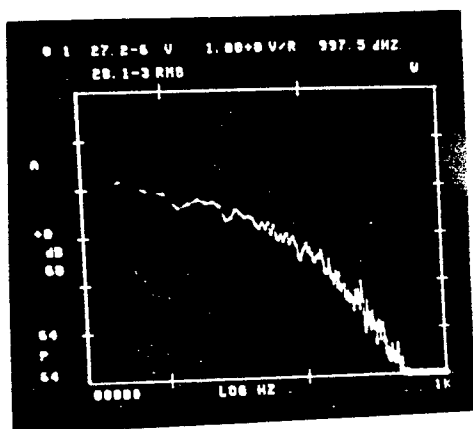
Volts plotted on a dB scale:

Hz (cyc/sec)

X axis:
Max. Voltage: 12.3 × 10⁻³ volts
Min. Voltage: 122 × 10⁻⁶ volts

Y axis:
7.32 × 10⁻³ Volts
109 × 10⁻⁶ volts

Laser fired through center of tube:

12-17

Laser fired through center of tube:

Volts plotted on a dB scale:

Hz (cyc/sec)

X axis:
Max. Voltage: 12.3×10^{-3} volts
Min. Voltage: 122×10^{-6} volts

Y axis:
7.32×10^{-3} Volts
109×10^{-6} volts

Laser fired through center of tube:

Conclusion:

The setting that created the most homogenous turbulence was 144W, fans pulling air out of the tube, and the coarse metal screen placed in the bottom of the tube over the resistors. The maximum heat setting produced stronger heat gradients which seemed to break into more homogenous turbulence cells as opposed to the cells produced at lower heat settings. When the fans extracted air from the generator, the interferograms showed that the heat mixed with the air rather than exiting the tube as it did when the fans blew inward. The coarse metal screen broke up the close fringes and distributed heat; thus it encouraged more even turbulence. However, the generator does not produce perfectly homogenous turbulence even when it is on the optimal setting. The spectra that was measured with the laser beam appeared appropriate. Unfortunately, though, we did not have time to sort out the differences between the scales on our spectrum analyzer and those typically used to measure the atmosphere, so we could not compare the results directly with atmospheric spectra. This work should be done in the future.

References:

Brown, James H., *A Nighttime Structure Model of atmospheric Optical Turbulence*, PL-TR-93-2016, Environmental Research Papers, No. 1119, January 1993.

Magee, Eric P., and Welsh, Byron M., *Characterization of Laboratory Generated Turbulence by Optical Phase Measurements*, Phillips Laboratory, Kirtland AFB, NM 87117, 1993.

Pries, Thomas H., Lt. Col., USAFR, *Atmospheric Sensitivities of High Energy Lasers*, Air Weather Service (Mac), Scott AFB, Illinois 62225, September 1980.

Vaucher, G. Tirrell, Vaucher, C.A. , and Walters, D.L., *Atmospheric Optical Turbulence Measurements Taken at Anderson Mesa, Flagstaff, Arizona Between 10-19 July 1990*, Naval Research Laboratory Washington, D.C. 20375, July 1990.

Wroblewski, Michael Raymond, *Development of a Data Analysis System for the Detection of Lower Level Atmospheric Turbulence With an Acoustic Sounder*, Naval Postgraduate School, Monterey, California, June 1987.

A STUDY OF THE CRITICAL IONIZATION VELOCITY PHENOMENON
AND SECONDARY AND BACKSCATTER ELECTRON EMISSION MEASUREMENTS

Matthew J. Pepper

St. Pius X High School
5301 St. Josephs Dr. NW
Albuquerque, NM 87120

Final Report for:
High School Apprentice Program
Phillips Laboratory

A STUDY OF THE CIV PHENOMENON AND THE
SECONDARY AND BACKSCATTER ELECTRON EMISSION MEASUREMENTS

Matthew J. Pepper
St. Pius X High School

Abstract

CIV

My summer apprentiship supported two experiments. The first is the critical ionization velocity (CIV) phenomenon that was first proposed by H. Alfven in 1954 in his book *On the Origin of the Solar System.* In this process released neutral gas is ionized and then emits ultraviolet and visible light. I calculated how much light at wavelengths of 2.7 and 4.6 microns would reach earth from an orbit at 850 kilometers.

Secondary Electrons

There have been problems with spacecraft that buildup an electrical charge caused by high energy electrons. This charge interferes with the sensitive electronics on board a spacecraft. The builders of the spacecraft can try to counteract this charge, but there are no accurate measurements of charge production by high energy electrons on spacecraft materials.. The resulting high energy electrons can be measured by irradiating spacecraft materials in a vacuum chamber at certain angles and measuring the number of electrons emitted. This was the second experiment.

A STUDY OF THE CIV PHENOMENON AND THE

SECONDARY AND BACKSCATTER ELECTRON EMISSION MEASUREMENTS

Matthew J. Pepper

Introduction

CIV

The CIV phenomenon was first proposed by H. Alfven {1}in 1954 in his book *On the Origin of the Solar System.* He theorized that a strong increase of the ionization rate should occur if a plasma and a neutral gas component are in relative motion across a magnetic field with a velocity exceeding the critical ionization velocity V_c, which is given by

$$V_c = SQRT\ (2eU_i/M_n)$$

where U_i is the ionization potential and M_n is the mass of the neutral atom or molecule (see appendix A). Phillips laboratory is sending up an experiment in early 1996 on ARGOS (Advanced Research and Global Observation Satellite). ARGOS will do 20 ten second releases of xenon gas {2}. This will be observed from the Air Force Maui Optical Site (AMOS).

Secondary Electrons

Space is a harsh environment. It is very difficult to design hardware that will survive in the space environment. High energy electrons that bombard satellites cause secondary electrons to be emitted{4}. It is these secondary electrons that were measured. An aluminum vacuum chamber, 5 feet by 3 feet was built for this purpose. It is surrounded by a magnetic field that cancels the magnetic field of the Earth.

Methodology

CIV

Software called Lowtran7 was used to calculate how much light AMOS could see and at what wavelengths. I worked mainly with CO transmittance and the Total transmittance. I tested the sensitivity of these two transmittance, by, for example, changing the program to include clouds. I also tried changing the angle of the satellite to the horizon to find where in the sky would be best to release the gas.

Secondary Electrons

The experiment consisted of an electron gun irradiating a spacecraft material. An electron detector measures the number of electrons emitting off the spacecraft material. Changing the angle would change the output. The material or the beam was changed and the different readings recorded. I did several things for the experiment. I installed a Data Acquisition and Control Systems computer board. Then I wrote two codes for its use (see appendix B). The first read the data from three channels, computed voltages, and printed the voltages to the screen and a separate file. This data then formed the graph of the magnetic field along the chamber axis versus position. The second program provided a beam profile by measuring the beam width.

Results

CIV

A sample plot showing transmittance as a function of wavelength is shown in appendix C. The light source is 15 degrees from directly overhead. The solid line is the total transmittance and the dashed the contribution from CO.

Secondary Electrons

For a beam profile, see appendix D.

Conclusion

CIV

From the results above, we found that above 60 degrees (as measured from the horizon) no light was lost. So, 60-90 degrees is the best place to measure the light.

Secondary Electrons

There is really not a conclusion because the purpose of the experiment was to gather data. This data will be used by many people to decrease the chance of losing a satellite to high energy electrons. This can be accomplished by surrounding the satellite with its own plasma or building a satellite with carefully chosen materials.

References

{1} H. Alfven. *On the Origin of the Solar System*. Oxford University Press, 1954

{2} N. Brenning. *Review of the CIV Phenomenon.* Kluwer Academic Publishers, 1992

{3} D. Cooke, R. Biasca, and L. Wright. *Simulation of Ion Production in the Argos Critical Ionization Velocity Experiment.* 1993

{4} W. Wilson. *Secondary and Backscatter Electron Emission Measurement.* April 1994
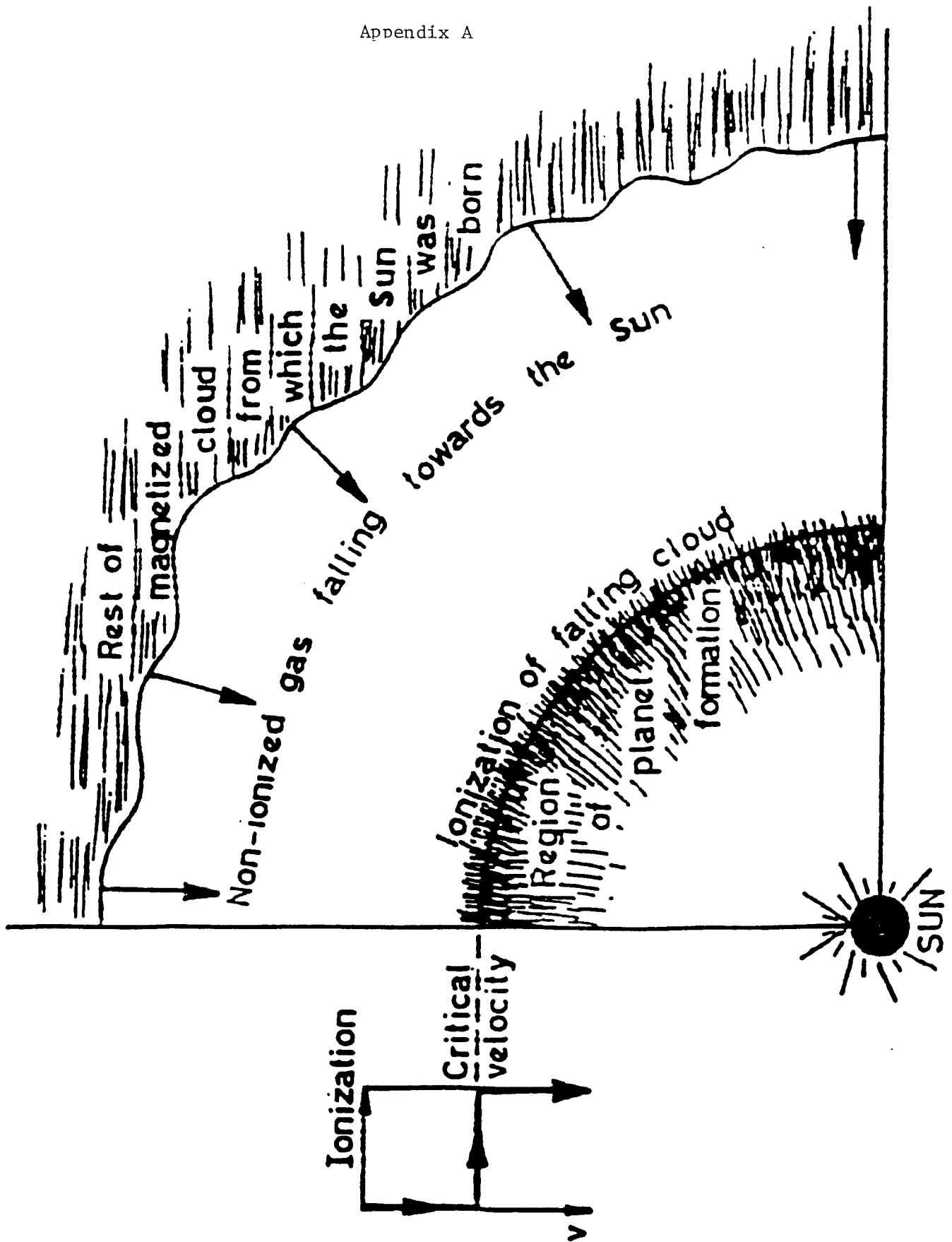
```
10  ''
10      CLS : PRINT
20  PRINT "        MAGNETIC FIELD TEST"
30  PRINT "       PROGRAM WRITTEN BY THE GREAT COMPUTER WIZARD, MATTHEW PEPPER"
35  PRINT "ADSCHANNEL=0; ADMCHANNEL=1; ADECHANNEL=2"
36  PRINT "CHANNEL 0 = Vx, CHANNEL 1 = Vy, CHANNEL 2 = Vz"
37  PRINT "Enter 999 as position to quit program!"
40      PRINT : PRINT
000 ''
010     DEFINT A-Z
020     BASE.ADDRESS         = &H2EC
030     COMMAND.REGISTER     = BASE.ADDRESS + 1
040     STATUS.REGISTER      = BASE.ADDRESS + 1
050     DATA.REGISTER        = BASE.ADDRESS
060     COMMAND.WAIT         = &H4
070     WRITE.WAIT           = &H2
100     READ.WAIT            = &H5
110 ''
120     CSTOP                = &HF
130     CCLEAR               = &H1
140     CERROR               = &H2
150     CADIN                = &HC
200 ''
230     PGH(0) = 1 : PGH(1) = 2  : PGH(2) = 4   : PGH(3) = 8
240     PGL(0) = 1 : PGL(1) = 10 : PGL(2) = 100 : PGL(3) = 500
250     PGX(0) = 1 : PGX(1) = 1  : PGX(2) = 1   : PGX(3) = 1
260 ''
270     SE.CHANNELS = 16           : DI.CHANNELS = 8
300 ''
310     FACTOR.10# = 1024          : FACTOR.12# = 4096
320     FACTOR.16# = 32768!
330 ''
340     UNI.RANGE = 10             : UNI.OFFSET = 0
350     BIP.RANGE = 20             : BIP.OFFSET = 10
360     BIP16.RANGE = 10           : BIP16.OFFSET = 0
370     UNI8.RANGE = 5             : UNI8.OFFSET = 0
020 ''
030     STATUS = INP(STATUS.REGISTER)
040     IF NOT((STATUS AND &H70) = 0) THEN GOTO 9800
120 ''
130     OUT  COMMAND.REGISTER, CSTOP
140     TEMP = INP(DATA.REGISTER)
150     WAIT STATUS.REGISTER,  COMMAND.WAIT
160     OUT  COMMAND.REGISTER, CCLEAR
310     FACTOR# = FACTOR.12#
320     GAIN(0) = PGH(0) : GAIN(1) = PGH(1)
330     GAIN(2) = PGH(2) : GAIN(3) = PGH(3)
340  GOSUB 7000:GOSUB 7500
395 PRINT "ENTER THE NAME OF THE OUTPUT FILE (DISK A: IS ASSUMED!)"
400 INPUT DF$:DF$="A:"+DF$
405 OPEN DF$ FOR OUTPUT AS #2
410 PRINT "          SET GAIN AND CHANNEL TO BE USED FOR A/D CONVERSIONS"
420 PRINT : PRINT "          ";
430 PRINT "LEGAL VALUES FOR GAIN ARE ";GAIN(0);", ";GAIN (1);
440 PRINT ", ";GAIN(2);", AND ";GAIN(3);"."
450 INPUT "          GAIN VALUE = ";Y
460 FOR GAIN.CODE = 0 TO 3 : IF GAIN(GAIN.CODE) = Y THEN GOTO 2473
470 NEXT GAIN.CODE
473 PRINT "ENTER OFFSET VOLTAGES (IN VOLTS): "
475 INPUT "Vx OFFSET = ";A#
480 INPUT "Vy OFFSET = ";B#
490 INPUT "Vz OFFSET = ";C#
500 ''
950 CLS
955 R = 0
965 PRINT " Vx          Vy          Vz        Hx        Hy        Hz        Ht"
000 INPUT "ENTER POSITION";Z
010 IF Z = 999 THEN CLOSE 2:GOTO 10180
370 CHANNEL = 0
390 GOSUB 4580
400 CHANNEL = 1
410 DATA.VALUES# = DATA.VALUE#
420 GOSUB 4580
430 CHANNEL = 2
440 DATA.VALUEM# = DATA.VALUE#
450 GOSUB 4580
455 DATA.VALUEE# = DATA.VALUE#
460 GOTO 6100
580 WAIT STATUS.REGISTER,  COMMAND.WAIT
000 ''
```

```
040    OUT  COMMAND.REGISTER, CADIN
100 ''
130    WAIT STATUS.REGISTER,   WRITE.WAIT, WRITE.WAIT
140    OUT  DATA.REGISTER,     GAIN.CODE
200 ''
230    WAIT STATUS.REGISTER,   WRITE.WAIT, WRITE.WAIT
240    OUT  DATA.REGISTER,   CHANNEL
300 ''
340    WAIT STATUS.REGISTER,   READ.WAIT
350    LOW = INP(DATA.REGISTER)
360    WAIT STATUS.REGISTER,   READ.WAIT
370    HIGH = INP(DATA.REGISTER)
380    DATA.VALUE#  = HIGH * 256 + LOW
400 ''
410    IF DATA.VALUE# > 32767 THEN DATA.VALUE# = DATA.VALUE# -65536!
000 ''
030    WAIT STATUS.REGISTER,   COMMAND.WAIT
040    STATUS = INP(STATUS.REGISTER)
050 IF (STATUS AND &H80) THEN GOTO 9400
060 RETURN
100 ''
130    VOLTS# = ((RANGE * DATA.VALUES#/FACTOR#) - OFFSET)/GAIN(GAIN.CODE)
160 PRINT USING "###.###### ";VOLTS#;
172 VOLTM#=((RANGE * DATA.VALUEM#/FACTOR#)-OFFSET)/GAIN(GAIN.CODE)
185 PRINT USING "###.###### ";VOLTM#;
195 VOLTE#=((RANGE * DATA.VALUEE#/FACTOR#)-OFFSET)/GAIN(GAIN.CODE)
220 PRINT USING "###.###### ";VOLTE#;
240 PRINT#2,USING"##.##  ##.####  ##.####  ##.####";Z,VOLTS#,VOLTM#,VOLTE#
280 J# = -(VOLTS#-A#) * 100
290 K# = -(VOLTE#-C#) * 100
300 L# = -(VOLTM#-B#) * 100
305 H# = (J#^2+K#^2+L#^2) ^ .5
310 PRINT USING "####.# ";J#;
320 PRINT USING "####.# ";K#;
330 PRINT USING "####.# ";L#;
340 PRINT USING "####.# ";H#
355 R = R + 1
360 IF R = 10 THEN GOTO 3950
500 GOTO 4000
540    GOTO 9998
000 ''
200 ''
220 ''
230    RANGE = BIP.RANGE : OFFSET = BIP.OFFSET : RETURN
300 ''
500 ''
830    NUMBER.CHANNELS = DI.CHANNELS : RETURN
000 ''
030    PRINT : PRINT "            Please respond with 'Y' or 'N' only."
040    RETURN
400 ''
430 PRINT
440 PRINT "FATAL BOARD ERROR"
450 PRINT "STATUS REGISTER VALUE IS ";HEX$(STATUS);" HEXIDECIMAL"
460 PRINT :BEEP:BEEP:GOSUB 9600
500 PRINT "ERROR REGISTER VALUES ARE:"
510 PRINT "        BYTE 1 -   ";HEX$(ERROR1);"   HEXIDECIMAL"
520 PRINT "        BYTE 2 -   ";HEX$(ERROR2);"   HEXIDECIMAL"
530 PRINT : GOTO 9998
600 ''
630    OUT  COMMAND.REGISTER, CSTOP : TEMP = INP(DATA.REGISTER)
640 ''
650    WAIT STATUS.REGISTER, COMMAND.WAIT
660    OUT COMMAND.REGISTER, CERROR
670 ''
680    WAIT STATUS.REGISTER, READ.WAIT
700    ERROR1 = INP(DATA.REGISTER)
710    WAIT STATUS.REGISTER, READ.WAIT
720    ERROR2 = INP(DATA.REGISTER)
730 RETURN
800 ''
998    PRINT : PRINT
10000 ''
10010    INPUT "        Run program again (Y/N)";Y$
10020    IF Y$ = "Y" OR Y$ = "y" THEN GOTO 110
10030    IF Y$ = "N" OR Y$ = "n" THEN GOTO 10170
10040 ''
10150    PRINT : PRINT "            Please respond with 'Y' or 'N'."
10160    GOTO 10100
10170 CLOSE 2
```

.0180 END
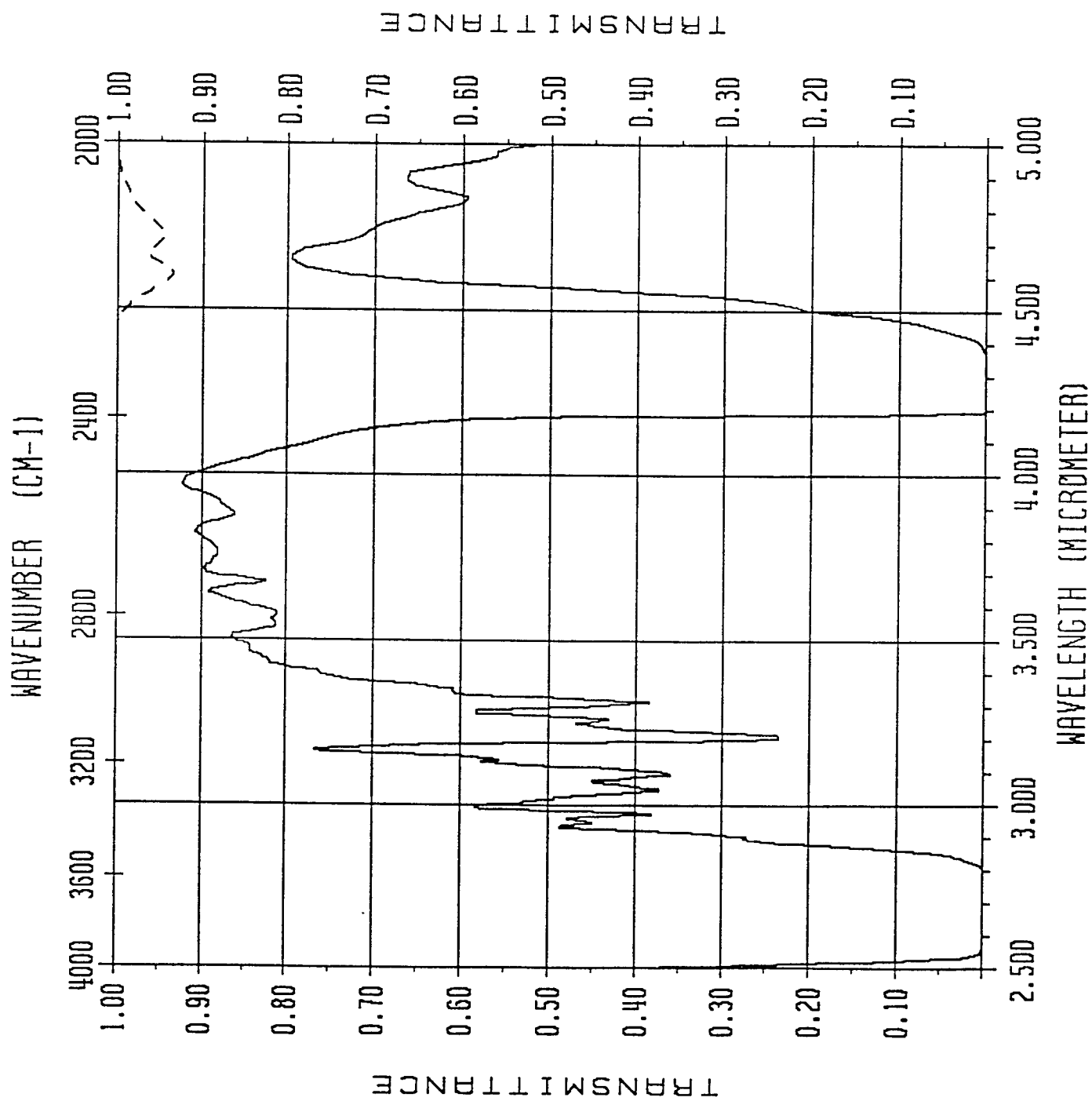
WAVENUMBER (CM-1)

TRANSMITTANCE

WAVELENGTH (MICROMETER)

ARGAS CO2 2.7 & 4.6 UM. 15 DEGREES

1KEVC
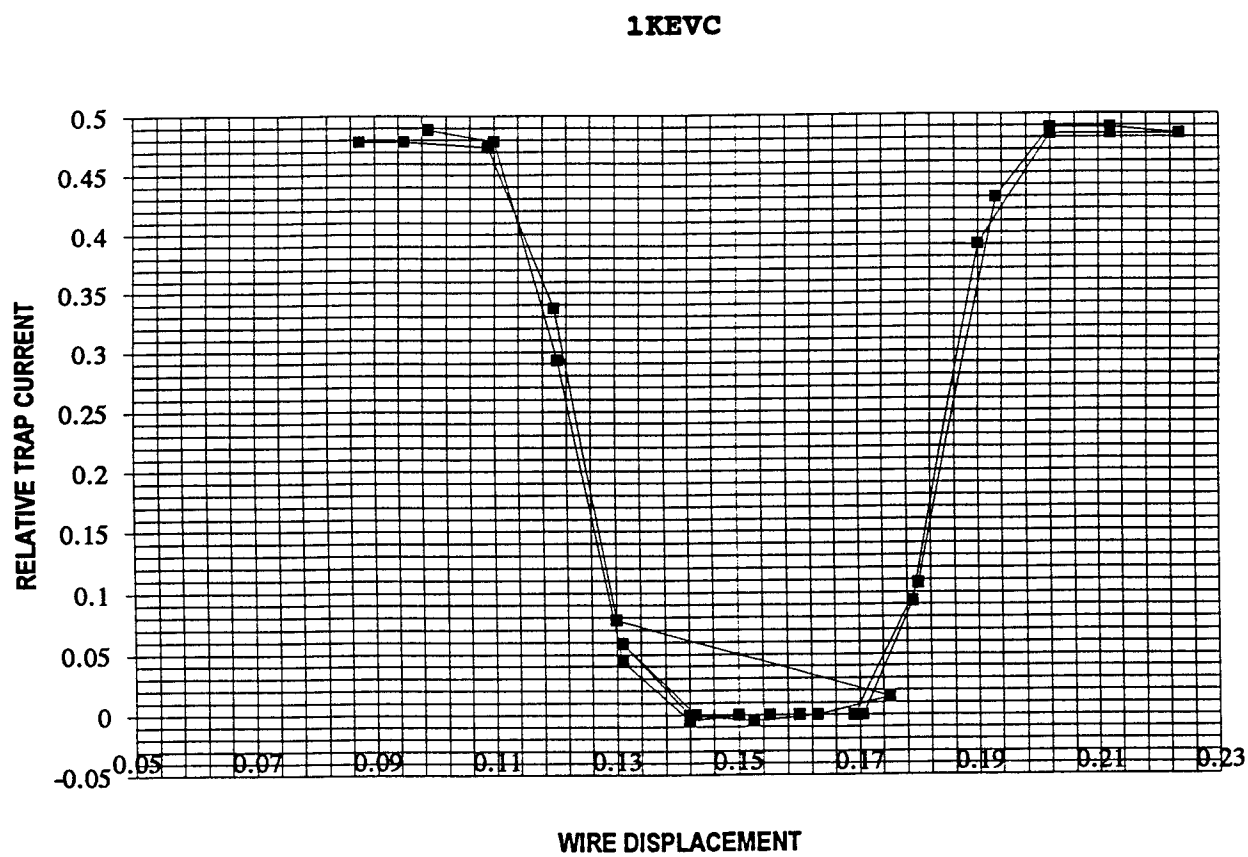
THE PSPH COMPUTER CODE
AND THE WSCD REFERENCE DATABASE

Jeremy G. Pepper

St. Pius High School
5301 St. Joseph's Dr. N. W.
Albuq. N. M. 87102

Final Report for:
High School Apprentice Program
Phillips Laboratory

August 1994

THE PSPH COMPUTER CODE
AND THE WSCD REFERENCE DATABASE

Jeremy G. Pepper
St. Pius High School

Abstract

During my eight weeks working at PL/WSCD, I worked on two main projects. The first was creating a database of all of the reference materials that have been collected by the Space Kinetic Impact and Debris staff over their years of research. The second was familiarizing myself with the Parallel Smooth Particle Hydrocode which was developed at Phillips Laboratory in the Space Kinetic Impact and Debris Branch. The PSPH code is used to model hypervelocity impacts. The advantage that PSPH has over the SPH code designed by J. J. Monaghan{1} is that the PSPH code can be run over a multiple number of computers. This addition makes the program run much faster.

THE PSPH COMPUTER CODE

AND THE WSCD REFERENCE DATABASE

Jeremy G. Pepper

<u>Introduction</u>

The PSPH code is a variation of the SPH code. SPH stands for Smooth Particle Dynamics. The code computes

numerical simulations of problems involving hydrodynamics. Numerical simulations of hydrodynamics can be either

Eulerian or Lagrangian{2}. Eulerian Simulations place cells in the problem volume and the fluid being modeled flows

through these cells. A Lagrangian follows material elements in the fluid. It is usually done by placing a grid over the

fluid. The grid is distorted as it is carried along with the fluid. Smooth Particle Dynamics is a Free Lagrangian method

for simulating hydrodynamics. SPH follows certain particles in the fluid. These particles sample the physical qualities

in their neighborhood and carry the averaged information with them. Eulerian and typical Lagrangian problems require

a mesh generator to create the grid over the fluid. SPH does not need a grid, and therefore does not need a mesh

generator. The absence of a mesh prevents many problems{3}. When the mesh of a problem is severely distorted, the

grid can become tangled, called "mesh tangling" or "keystoning." The user has to periodically rezone the mesh to

prevent this tangling. The SPH cuts down on the time the user has to spend on a program because of the absence of a

grid. The absence of a grid does cause a few problems{4}. In the SPH code, each particle represents the sum all of the

particles close enough to contribute to that value. There are many more interactions in an SPH problem than there are in

a typical Lagrangian or Eulerian problem{5}. For example, in a three dimensional Eulerian or Lagrangian problem

using a cubic mesh, a Eulerian or Lagrangian cell would communicate with about twenty-six neighbors. In the same

problem done with SPH, a particle would communicate with about ninety neighboring cells{6}. Overall, the Eulerian

and typical Lagrangian methods give better results if the problem is only one dimension. Mesh tangling is very rare in

one dimensional problems so the user would not have to periodically rezone the mesh. In two dimensions, SPH is

roughly equal to the other two methods, particularly in impact simulations and when the problem involves complex

geometry. The SPH code is superior in three dimensional problems, particularly because the time and effort needed to

set up and execute the problem is greatly lessened{7}.

The SPH code was designed to model the time evolution of a flow{8}. It does this by applying the laws of motion to

each of the particles. For example, SPH moves a particle by first reviewing the physical quantities that the particle has collected. For movement, the pressure gradient would be computed to determine all of the forces pushing against that particle. Newton's first law of motion is then applied and the particle is moved.

The PSPH code

As stated before, the PSPH code is an advanced version the SPH code. The advantage that the PSPH code has is that it can be run on any number of machines. This cuts down on the time it takes for a problem to finish because the user can take advantage of more processing power. PSPH stands for Parallel Smooth Particle Hydrocode, the word parallel meaning that the problem can be split up and run on different machines at the same time. The way PSPH splits up the problem is shown in figure 1. The PSPH code can be run on any UNIX compatible computer, parallel supercomputer,

Figure 1
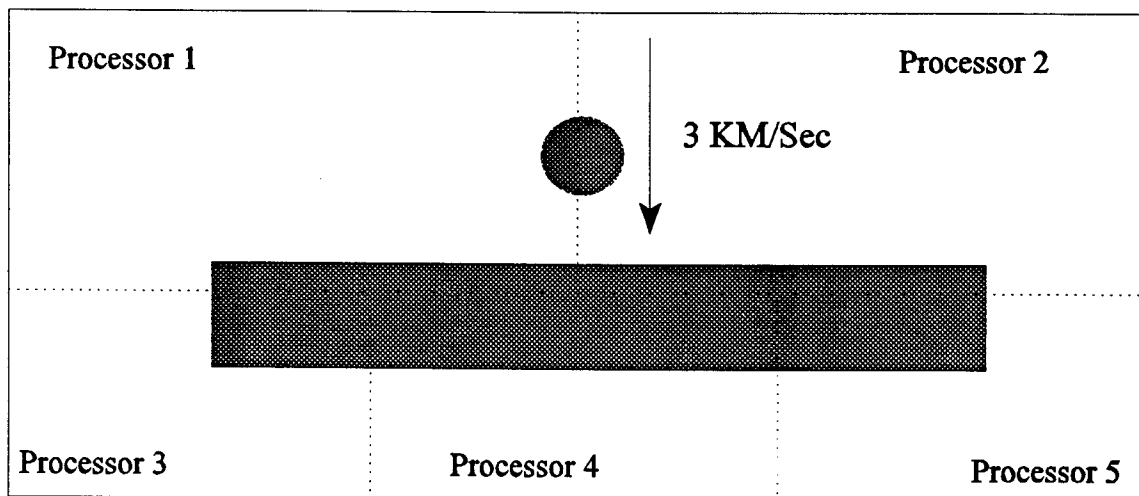
or standalone serial machine.

PVM

The most common and efficient configuration for connecting all of the computers that are running the code is a package called Parallel Virtual Machine (PVM){9}. PVM, developed at Oakridge National Laboratories, creates a single parallel machine out of a number of totally different machines. PVM is very easy to set up. The user only has to start the PVM console on one machine and then add machines to make a parallel network. When the user starts the PSPH problem, PVM automatically splits up the work between all of the machines the user has chosen. The problem gets done much faster because the user can exploit more computing power. While the problem is running, the user can

return to any of the computers at any time to check the status of the problem, add or remove machines, or terminate the

problem.

The Problem

While I was working at WSCD, I duplicated a

problem done by Andrew J. Piekutowski{10}. I became

familiar with PSPH and PVM as I worked on the

problem. The problem involved a copper ball hitting a

copper plate. The ball is one gram of pure copper. It

was fired into a 1.52 mm thick copper plate at the

velocity of 6.46 km/s{11}.

When PSPH computes a problem, it shows the

results through dump files. The dump files are arranged

according to time. The information about how the file is

Figure 2

1 gram

6.46 km/s

1.52 mm thick

setup is dump.00000.0000. After one microsecond of the problem has passed, PSPH writes dump.00001.0000. PSPH

will write dumps until the problem ends. This allows the user to easily access information about any time period. The

user can change the dump interval if they want to have more detailed information. The information can be viewed very

easily. Using the viewdump command, the user can look at the information in 22 different ways. A few examples of the

ways the information can be looked at is material, density, temperature, and energy.

In order to run the A. J. Piekutowski problem, I had to first learn about PSPH and PVM. Before I started working on

the problem, I read the PSPH users manual and the SPH review article by J. J. Monaghan, "Smoothed Particle

Hydrodynamics," in *Annual Review of Astronomy and Astrophysics*, 1992, vol. **30**, pp. 543-74. Both of these reports

should be read if the user is new to PSPH. To enter the parameters of my problem, I had to copy the psph.dat file from a

local user library. The editing program vi was used to enter in the parameters of the problem into the new psph.dat file.

Vi is a program editor and was very useful throughout the development of the project. The psph.dat had the parameters

of a sample problem in it so I entered in the new parameters. PSPH is designed so that the problem is entered as a two

dimensional graph. I first designed the problem on graph paper, using an x- and y-axis. The units used in the graph are

centimeters. The problem was confined to a rectangle with its bottom left corner at (0,0) and top right corner at (20,12).
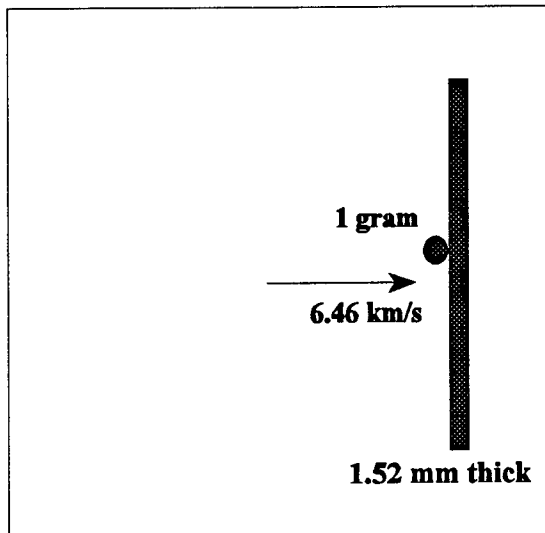
The copper plate's bottom left corner is at (5,3). The plate is six centimeters high and 0.152 centimeters thick. The copper ball is to the left of the plate and is right next to it. The ball's center is at (4.7,6) and it has a radius of 0.3. I changed the color of the ball so I could distinguish between particles from the ball and particles from the plate. During this time, I also entered the velocity of the ball.

Figure 3
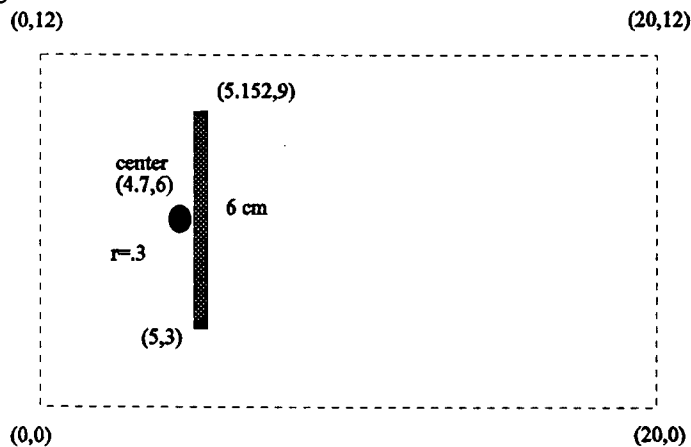
This was the last piece of information that the psph.dat file needed. The final psph file is shown as Appendix One. PSPH needed one more thing before it could be executed. It needed the materials.dat file. This file contains the specific density, speed of sound, specific heat, and other physical properties about certain materials. In this problem, the physical properties of copper were needed. Fortunately, the materials.dat file already had these properties. The PSPH file was ready to be executed. The computer took two hours and fifty minutes to finish computing the problem.

The Results

The results were interesting but hard to analyze. I had modelled a problem done by Andrew J. Piekutowski hoping to compare my results to his results and learn about PSPH while I worked on the problem. Piekutowski did not include the time frame of the photographs that were printed in his article{12}. I could not properly compare his photographs to my pictures because I did not know which ones were taken at the same time. Appendix Two shows two photographs included in Piekutowski's article. One of the photographs is actually four photographs laid on top of each other. One photograph is the copper ball and impact plate before the collision. The other three photographs are debris clouds at different time periods. Using the known radius of the ball, a ruler, and the results of my test, I estimated that the first debris cloud is approximately five microseconds after impact and the second debris cloud is approximately fifteen seconds after impact. The third debris cloud is off the scale of my problem so it could not be computed.

As explained before, information about the problem is put into dump files at an interval set by the user. These dump files can be translated into pictures using the viewdump command. In this problem, the dump interval was once every

14-6

microsecond. A picture of the problem can be viewed for every microsecond that the problem ran. Appendix Three is a picture of the problem at 0 microseconds. Appendix Four is a picture of the problem at five microseconds. This is the picture that most closely resembled the first debris cloud in the photographs included in Piekutowski's article. It is important to remember that the problem that I ran was two-dimensional while the problem that Piekutowski ran was three-dimensional{13}. This accounts for some of the differences between the PSPH picture and Piekutowski's photographs. A picture of the problem at ten microseconds was included as Appendix Five so the reader could see how the problem developed. Appendix Six is a picture of the problem at fifteen microseconds. This is the picture that most closely resembled the second debris cloud in Piekutowski's article.

Conclusions

I believe that I have completed both of my goals that I set when I started this project. The first, which was to model Piekutowski's problem, was completed even though there was no time given with the photographs. The PSPH code succeeded in computing the problem successfully. The second goal, which was to familiarize myself with the PSPH code, was also attained. I learned enough to run a basic problem and analyze the output. I needed a little help along the way but overcame most of the obstacles myself. I do not consider myself an expert in PSPH or even close to it, but I do now know enough to run a problem independently with no outside help. I received an added bonus while learning the PSPH code. I learned the basics of a UNIX based system and the program editor vi. I can now properly execute commands in the UNIX system and edit a program in vi.

The WSCD Reference Database

The other project that I worked on while at WSCD is the WSCD Reference Database. This database was created so the staff of WSCD could easily access reports and books that have been collected over the years. What was needed was a database where any article, author, or key word could be easily called up and examined. The entries were first written down in shorthand. The title, author(s), and publisher were recorded. After all of the entries had been written down, they were entered into the computer. The program used was Word Perfect 6.0. This program was chosen because it was very advanced and had the very useful Find and Sort commands. A table was made and the entries were entered in the categories of title, author(s), and publisher. After all of the entries were entered, they were sorted alphabetically according to title. Copies of the file were copied onto some disks and made easily accessible to the staff. A help document was made to explain how to use the database. This was also put on the disk. Articles and books are now

found very easily. The staff can look for all articles written by a specific author by using the Find command. Key words can also be easily found using this command. The Sort command can be used to put all of the entries into a different order. This can be done to put all of the books together or to put all of the entries written by an author together. The file has a total of nine-hundred and seven entries and has already proven its usefulness. The database can be updated easily by entering new files.

NOTES

{1} Monaghan, J. J. 1992. "Smooth Particle Hydrodynamics." Annu. Rev. Astron. Astrophys. (1:543)

{2} Smith, Bradley and Baker, Lou. 1994. PSPH User's Manual. (4:5)

{3} Smith, Bradley and Baker, Lou. 1994. PSPH User's Manual. (4:5)

{4} Smith, Bradley and Baker, Lou. 1994. PSPH User's Manual. (4:5)

{5} Smith, Bradley and Baker, Lou. 1994. PSPH User's Manual. (4:5)

{6} Smith, Bradley and Baker, Lou. 1994. PSPH User's Manual. (4:5)

{7} Smith, Bradley and Baker, Lou. 1994. PSPH User's Manual. (4:6)

{8} Smith, Bradley and Baker, Lou. 1994. PSPH User's Manual. (4:6)

{9} Smith, Bradley and Baker, Lou. 1994. PSPH User's Manual. (4:10)

{10} Piekutowski, Andrew J. "A Simple Dynamic Model for the Formation of Debris Clouds." Int. J. Impact Engineering. Vol. 10. (2:466)

{11} Piekutowski, Andrew J. "A Simple Dynamic Model for the Formation of Debris Clouds." Int. J. Impact Engineering. Vol. 10. (2:466)

{12} Piekutowski, Andrew J. "A Simple Dynamic Model for the Formation of Debris Clouds." Int. J. Impact Engineering. Vol. 10. (2:466)

{13} Piekutowski, Andrew J. "A Simple Dynamic Model for the Formation of Debris Clouds." Int. J. Impact Engineering. Vol. 10. (2:466)

BIBLIOGRAPHY

1. Monaghan, J. J. "Smooth Particle Hydrodynamics." Annu. Rev. Astron. Astrophys., 1992, pp 543-573

2. Piekutowski, Andrew J. "A Simple Dynamic Model for the Formation of Debris Clouds." Int. J. Impact Engng., Vol. 10, p 466

3. Smith, Bradley and Baker, Lou. PSPH User's Manual. 1994

4. Sobell, Mark G. *A Practical Guide to UNIX System V.* The Benjamin/Cummings Publishing Company, Inc., 1991

ACKNOWLEDGEMENTS

I would like to thank the staff of PL/WSCD for making my eight weeks at Phillips Laboratory exciting, challenging, and fun. Special thanks to James Winter for all of his help with my PSPH problem. I would also like to thank the Research and Development Laboratory for supporting and financing my project. Last, I would like to thank all of the people at Phillips Laboratory for being so open and kind to me.

```
; Parallel SPH Sample Configuration File
; Capt Brad Smith, PL/WSSD
;
; Comments - may be denoted by a ; in the first column.
;
[Problem]
title=Copper Ball Test
; Number of dimensions in problem
dimensions=2
; Load balancing options
; Percent deviation in loads tolerated before load rebalance (1-100)
bal_thresh=15
; Minimum and max number of steps between load rebalances
min_bal_step_thresh=10
max_bal_step_thresh=100


;
; Section defining problem boundaries - absolute
[Bounds]
minx=0.0
maxx=20.0
miny=0.0
maxy=12.0
; Cell multiple - used to generate initial cell size
;   a multiple of H - generally 2.0 is pretty good
HCellMult=2.0
; Reflect may be XMIN, XMAX, YMIN, YMAX, ZMIN, ZMAX
reflect=XMIN YMIN XMAX YMAX

; Section defining graphing boundaries - absolute
[GraphBounds]
minx=0.0
maxx=20.0
miny=0.0
maxy=12.0

; Time specifications
[Time]
sigma=0.3
; Maximum time and number of time steps
max_time=17.5
max_step=5000.0
; Dump interval and format
dump_interval=2.5
; Format may be: 0=SPHC dump (1=Magi when implemented )
dump_format=0
; Restart dump interval - in steps
restart_interval=100


; Problem constants
[Consts]
; Constants for artificial viscosity
alpha=2.5
beta=2.5
```
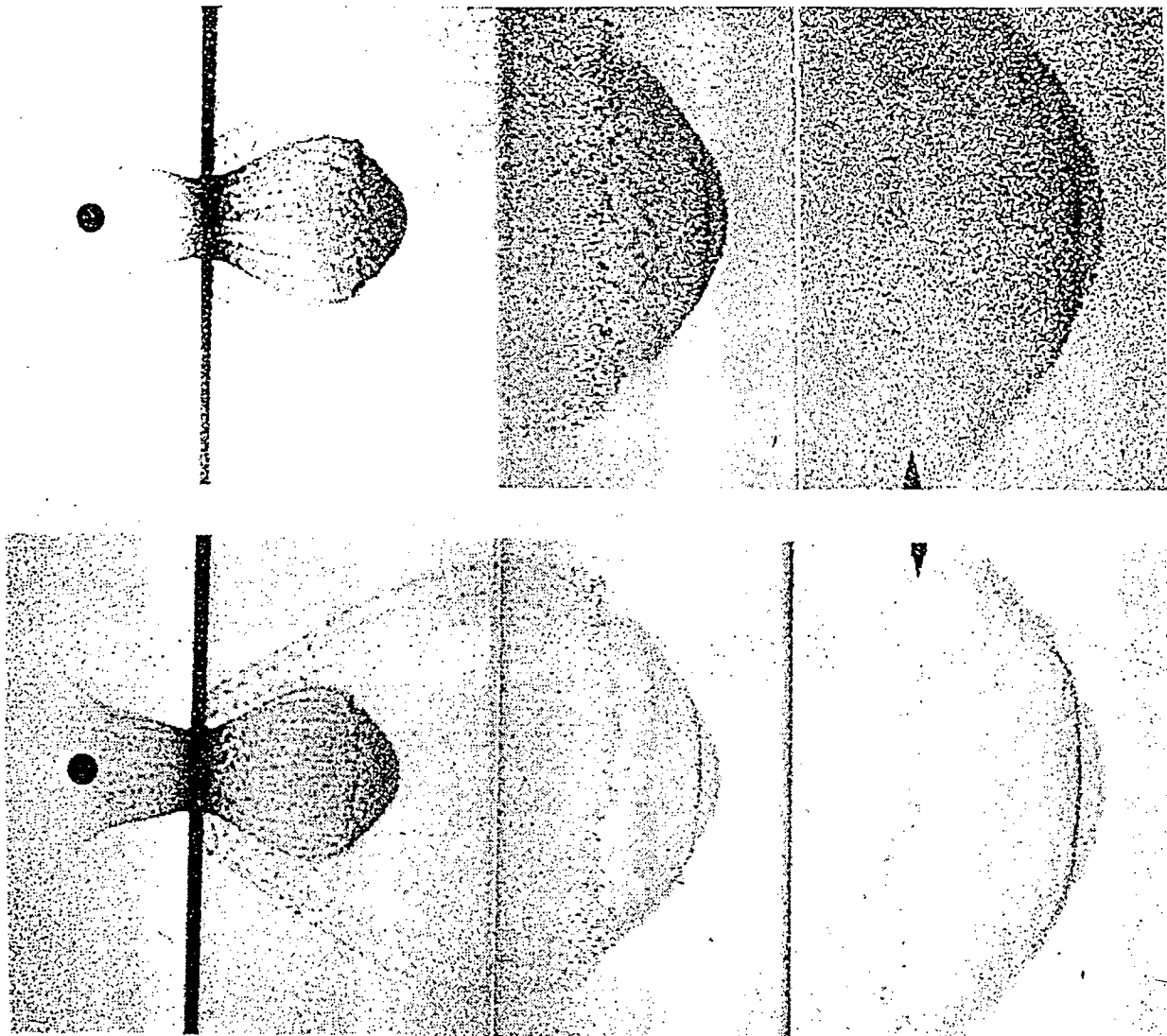
```
epsilon=0.1
; Constants for wall heating
g1=0.5
g2=1.0
; Density is 0=Summation, 1=Continuity
density=0
; Activity flag - calculates active particles only - 0=off 1=on
activity=1
; Fracture models - 1=PMIN 0=NONE 2=Johnson-cook
fracture=1
; Strength model 1=ELASTIC_CPP 2=Johnson-cook
strength=1
; Temperature - Fixed=0 Variable=1 (Only with MieGruneisen)
temperature=0
; Baker's H-Diffusion coefficient 0.0=off 0.1-0.2 are reasonable on values
hdiffcoef=0.1

;Shapes section - format is [shapeX] where X is an integer count
; followed by the actual shapes and modifiers.
;Valid shapes include:
;    shape=box(material, x0, y0, {z0}, x1, y1, {z1} , {thickness})
;    shape=triangle(material, x0, y0, x1, y1, x2, y2)
;    shape=circle(material, x0, y0, {z0}, radius)
;    shape=circle(material, x0, y0, {z0}, radius)
;    shape=cylinder(material, x0, y0, z0, height, radius, {inner_rad})
;Valid modifiers include:
;    nph=1.5         ; Number of particles per h
;    h=0.01          ; Smoothing length
;    e=2.5           ; Initial particle energy
;    uvel=0.0        ; X component of shape velocity
;    vvel=0.0        ; Y component of shape velocity
;    wvel=0.0        ; Z component of shape velocity
;    eos=1           ; Equation of state 0=MIE_GRUNEISEN, 1=IDEAL_GAS, 2=JWL_EXPLOSIV
E 3=SESAME
;    index=0  ; Sesame index for use with sesame equation of state tables
;    rotate=0.0    ; Angle in degrees to rotate shape counterclockwise (2-D)
;    rotate_point=(0.0,0.0,0.0)   ; Point to rotate this shape about
;    rotate_phi=0.0       ; Angle in degrees to rotate shape (3-D)
;    rotate_psi=0.0       ; Angle in degrees to rotate shape (3-D)
;    rotate_theta=0.0       ; Angle in degrees to rotate shape (3-D)
;    sitecount=0   ; Number of ignition points for explosives
;    igntimeX=0.0 ; Ignition time for site X (sites are numbered [1..sitecount])
;    ignsitexX=0.0         ; Ignition site x coordinate for site X
;    ignsiteyX=0.0         ; Ignition site x coordinate for site X
;    ignsitezX=0.0         ; Ignition site x coordinate for site X
;
[shape1]
shape=circle(copper1,4.68,6.0,0.3)
nph=1.5
h=0.02
e=.000001
eos=0
uvel=0.646
[shape2]
shape=box(copper2,5.0,3.0,5.152,9.0)
nph=1.5
h=0.02
e=.000001
eos=0
```

1g Copper Ball

1.52-mm-thick Copper Bumper

$V_o = 6.46$ km/s
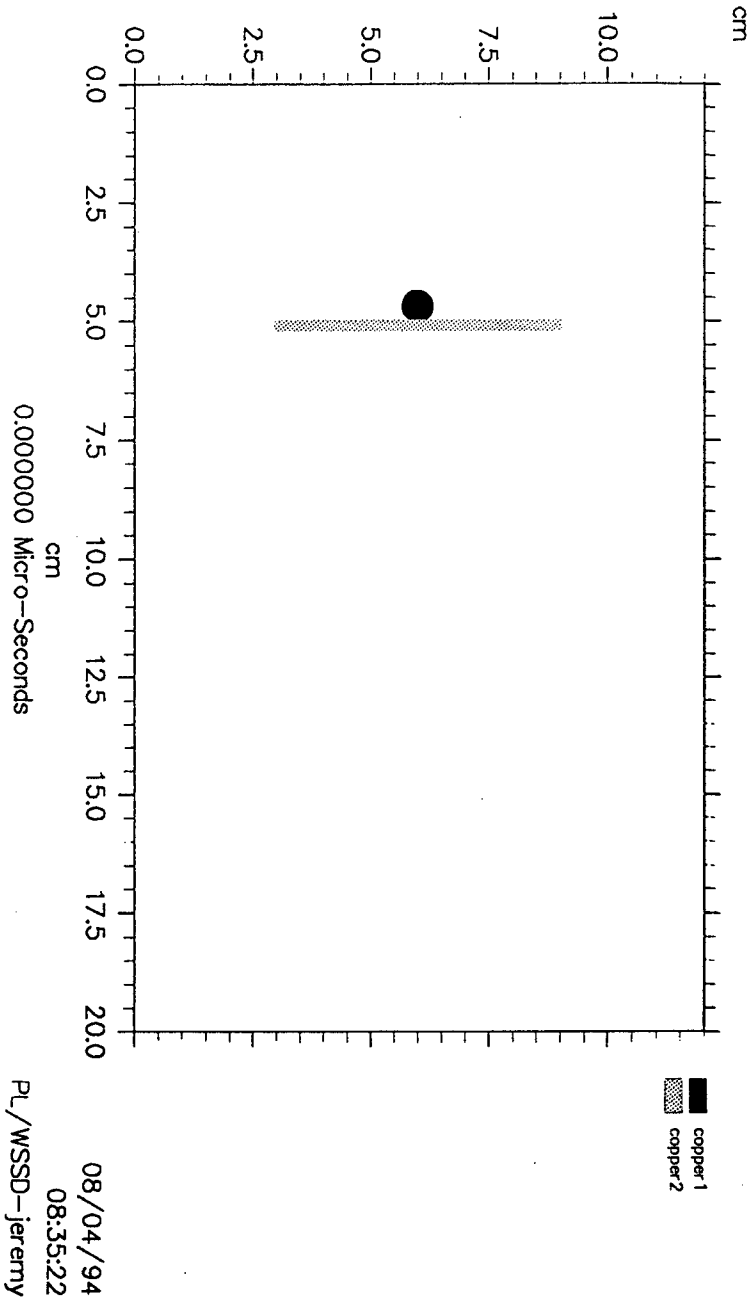
Material Plot
Copper Ball Test

cm

0.000000 Micro-Seconds
cm

copper 1
copper 2

08/04/94
08:35:22
PL/WSSD—jeremy

Material Plot
Copper Ball Test

cm

5.000000 Micro-Seconds

cm

copper 1
copper 2

08/03/94
10:13:40
PL/WSSD-jeremy

Material Plot
Copper Ball Test

cm

cm
10.000000 Micro−Seconds

copper 1
copper 2

08/04/94
08:31:04
PL/WSSD−jeremy

Material Plot
Copper Ball Test

cm

copper 1
copper 2

15.000000 Micro-Seconds
cm

08/04/94
08:27:45
PL/WSSD-jeremy
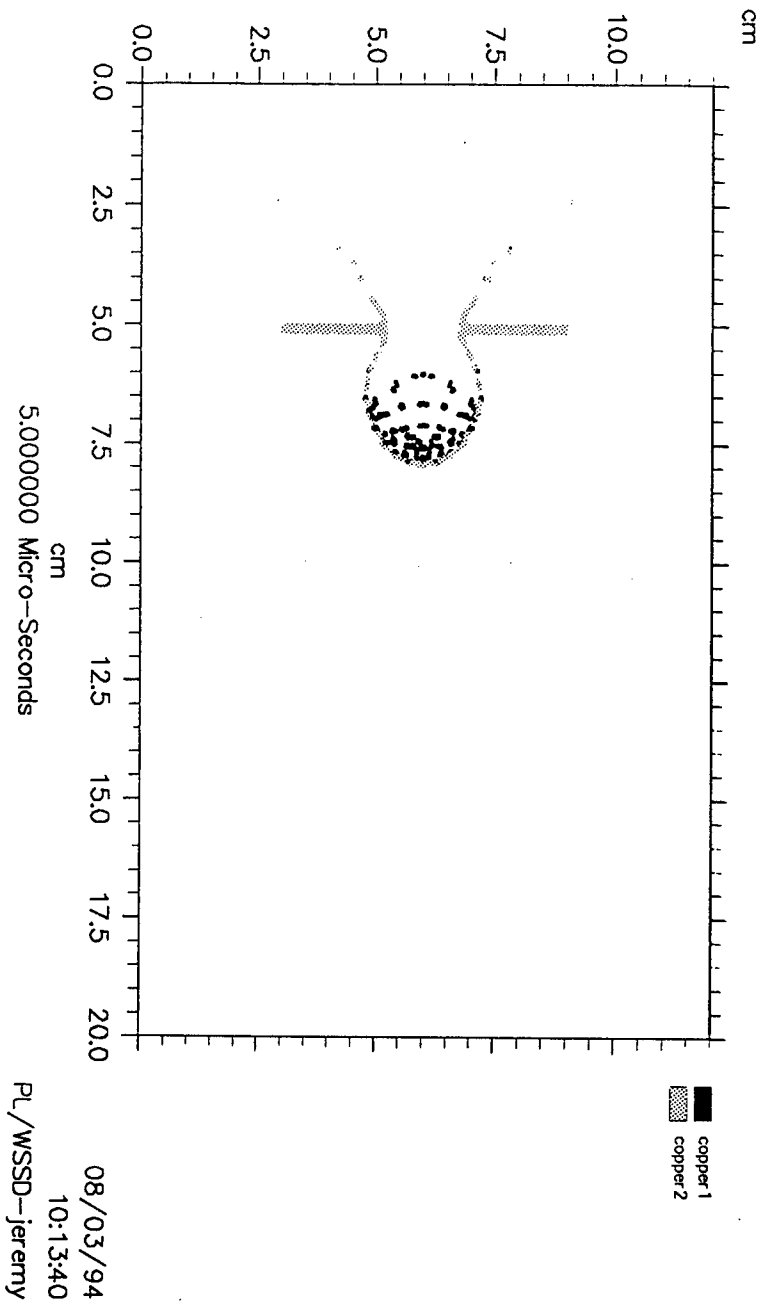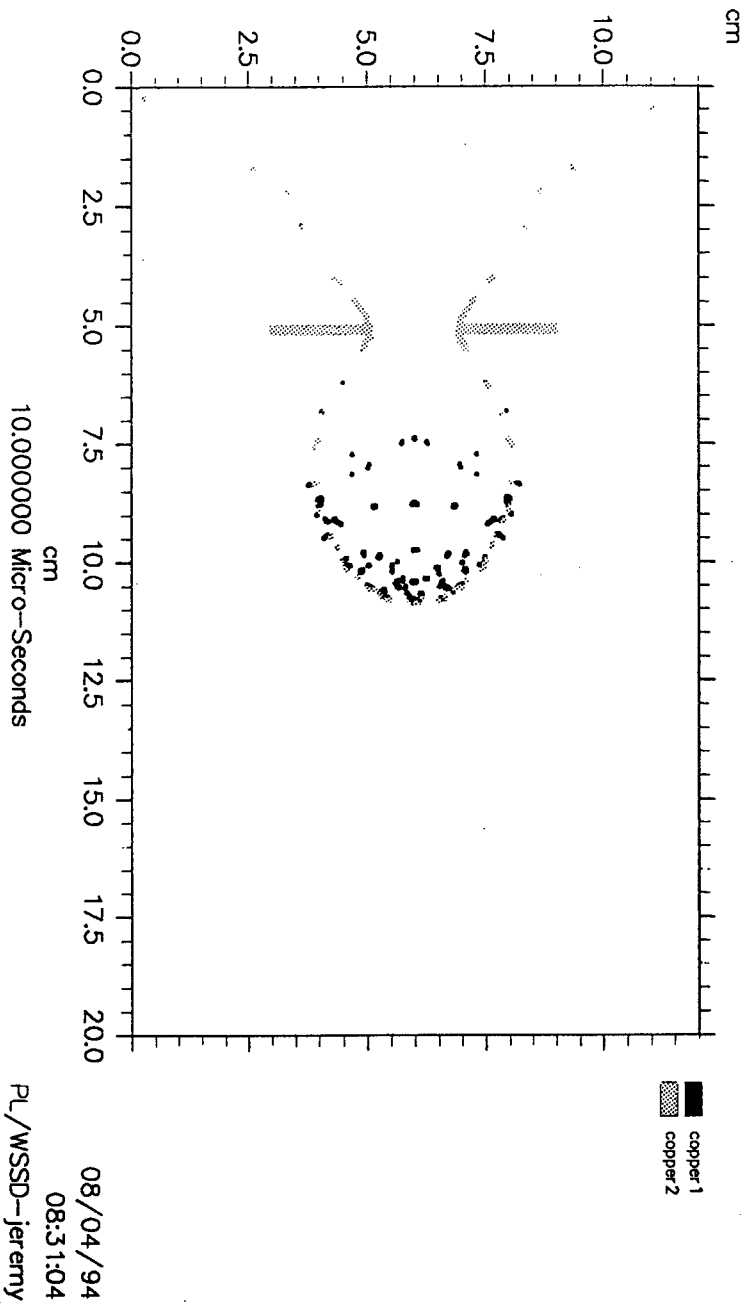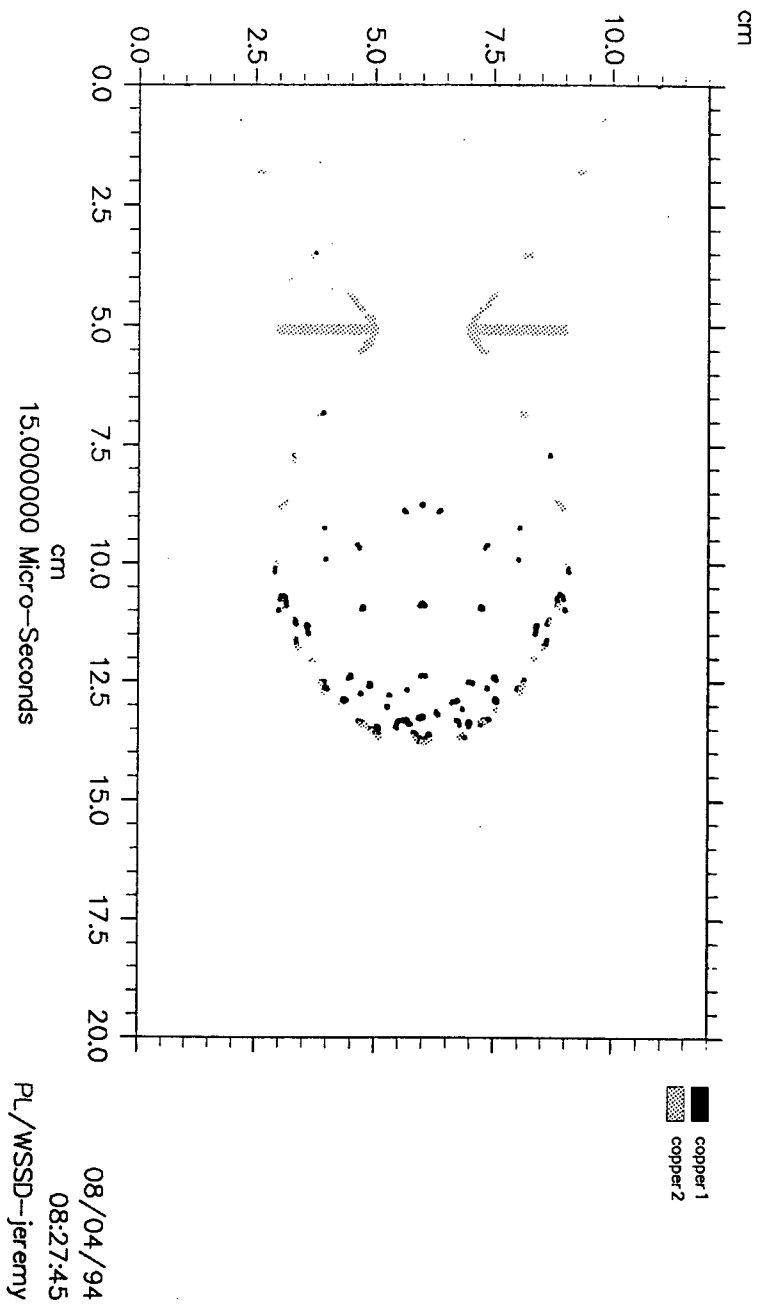
USING IMAGE PROCESSING PROGRAMS
TO AID SPACE TO GROUND SATELLITES

Paul A. Rodriguez

Santa Fe High School
5874   Siringo Dr.
Santa Fe, N.M. 87505

Final Report For:
High School Apprentice Program
Phillips Laboratory

August 1994

USING IMAGE PROCESSING PROGRAMS
TO AID SPACE TO GROUND SATELLITES

Paul A. Rodriguez
Santa Fe High School

Abstract

The use of image processing to prepare the data for space to ground satellite neural networks was studied. Image processing requires computers, so the computer language C was studied. Image processing programs were created using the knowledge of C. Possible applications for these programs were developed concurrently with creation of these programs. These applications include sharpening of unfocused images, extracting the edges of objects in the images, and reducing the amount of noise an image may contain.

USING IMAGE PROCESSING PROGRAMS
TO AID SPACE TO GROUND SATELLITES

Paul A. Rodriguez

Introduction:

Lansat and SPOT are two examples of space to ground satellites. Their basic mission is to survey the Earth's surface on a systematic, repetitive, and continual basis. The satellite is in a constant state of receiving information, eventually it contains enormous amounts of data. Not all of the collected data is useful to scientists, and the data is also very expensive to send from the satellite to the Earth. Thus if one could devise a computer program that will allow the computer on board the satellite to choose what information should be sent to the Earth, the satellite would become faster. In turn, this would also be more cost effective. The method that allows the satellite to choose what information is usable or unusable would be combination of image processing and neural networks.

Image processing is the method used for changing an image. The image processing that is to be used along side of some neural networks on the space to ground satellites changes the images coming into the satellite to an image which a neural network can use.

The satellite cannot physically change the image so a computer is required. Programs must be written for the computer to allow it to change the image in a specific way. These programs must be written by a computer programmer who is able to communicate with the computer when it is in use. The communication between programmer and computer requires the programmer to comprehend the language in which the program was written.

Discussion of Problem:

The space to ground satellites need a collection of image processing programs to use with a collection of neural networks. This is because transferring information is expensive and time consuming. Image processing programs must overcome two obstacles before they can be used to process the image. The first obstacle is the ability for the computer to compile the program. Compiling is the way the computer decides if a program is error free. The second obstacle is if the program will change the image to the desired result. This project is designed for that problem.

<u>Methodology:</u>

Learning to use the computer language C was the first step in this project, because communication between the computer and the user is essential. Writing programs in C was the method for learning C. The programs progressively increased in difficulty. Once a program was successfully written, a new more challenging program was attempted. As the programs increased in difficulty, my knowledge of C increased. Each program was a step that lead to a long term goal. The programs that were written are:

1. **Hello World Program**-This program was the most basic program. It used a command which wrote a collection of characters, words for example, on the screen.

2. **1 and 10 Program**-This program was designed to be a guessing game. It allowed the user to guess a number between one and ten. When the user chose the incorrect answer, the computer said whether the number was too high or too low. This program uses a write command to write characters on the screen just as in program 1. It also used "if" statements which allow the computer to run a set of commands until the user enters the correct number. The last command used in this program was the "scan" command. This command is designed to obtain a value entered by the user to use in the program.

3. **Circle Program**-This program is designed to create a circle inside a graphics window at a certain position on the screen. This program uses the command "color". The use of this command taught me how to manipulate color. The next command, "window," created a graphic window fin which to display the output. This program taught me much about graphics, which are a large part of image processing .

4. **Spectrum Program**-This program was designed to change the color spectrum in the color map of the computer. This program created a color spectrum from white to black with 256 color values. This program uses many commands that involve the color map.

5. **Black to White Program**-This program was devised to create a diagonal array of pixels in a graphic window that gradually change from white to black. This program uses commands that manipulate the color values of single pixels using the color spectrum created by program 4.

6. **Image Program** -This program was designed to create a window that displays an image. This program began the process of image processing because one must see the original image before it can be changed. The specific image that was used came from the landsat satellite. (see Figure 1)

Figure 1: Landsat Satellite Image

The basics of the language C were understood by the completion of program 6.

Using C to produce basic image processing programs was the second step to this project. Basic programs were chosen due to their simplistic nature. The programs increase in difficulty as time progresses. The type of programs that were created in this project include thresholding and edge extraction.

The first program to be written for image processing was a thresholding program. This program changes the color of an image. Pixels are used to explain how this color change works. Every pixel has a value which represents its color. For example, a black pixel has the value of zero. A thresholding program changes all these values to either zero or 256. This change will make the pixels either pure white or pure black. (see Figure 2 and 3)

Figure 2: image before thresholding

Figure 3: image after thresholding

The second basic image processing program created during this project was an edge extraction program. This program extracted the edges from the objects in the image. (see Figure 4 and 5)
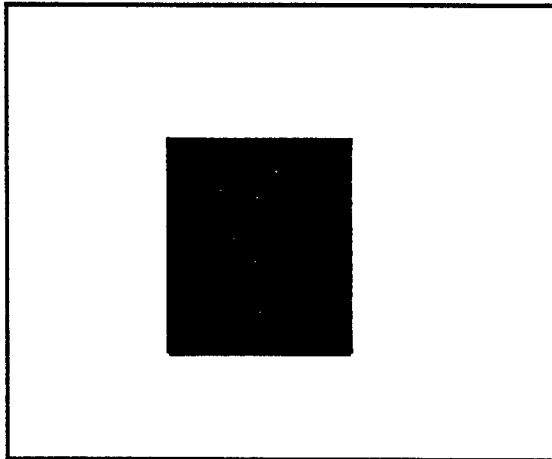
Figure 4: the image before edge extraction   Figure 5: the image after edge extraction
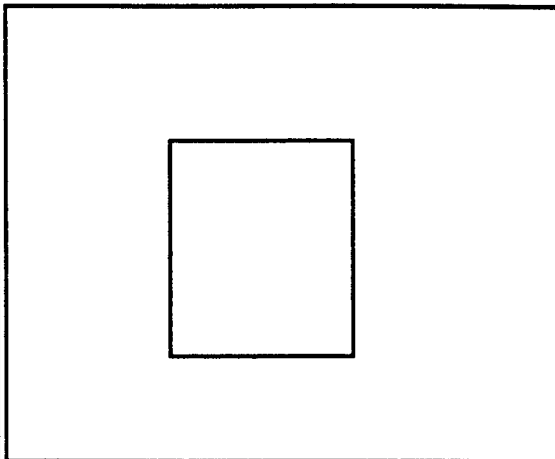
A mask was created to scan the entire image. This mask was three squares wide and three squares high (squares represent pixels). (see Figure 6)
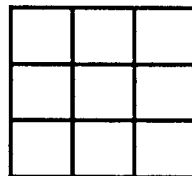
Figure 6: visual representation of the mask
used in edge extraction

This mask moves from left to right pixel by pixel until it reaches the end of the image. On the next sweep the mask starts on the left side one pixel lower. The constant moving of the mask continues in this fashion until the entire image has been scanned. Every square of the mask had a numeric value. The numeric values of the mask gave it edge extraction ability.   (see Figure 7)

-1	-1	-1
-1	8	-1
-1	-1	-1

Figure 7: mask used in edge extraction
with numerical values included

As the mask scans the image, the values in the mask are multiplied by the corresponding values of the image. (see Figure 8)

-1	-1	-1	
-1	8	-1	
-1	-1	-1	
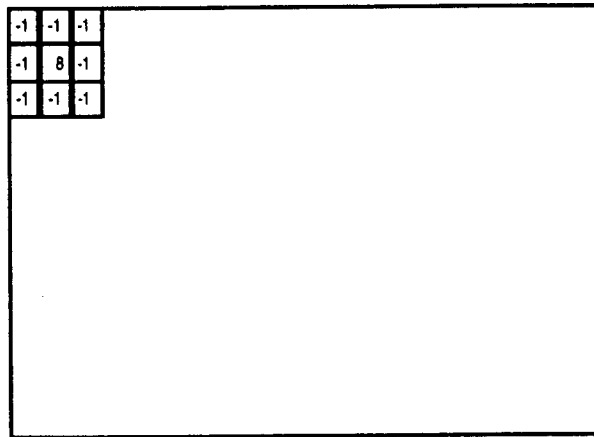
Figure 8: The nine pixel values in the top right
corner are multiplied by the
corresponding values.

The final step to the project was to use image processing to sharpen an unfocused image. There was two ways to do this. First, a mask was used to sharpen an image. The mask had the same as the edge extraction mask with one main difference. This mask has separate numerical values to it. (see Figure 9)

-1	-1	-1
-1	M	-1
-1	-1	-1

Figure 9: the mask used in edge extraction where
M=9-A*1 and 1<=A=<2

15-7

The method behind the mask is simple. It scans a three by three section of the image. The numeric values are than multiplied with the corresponding pixels. These new values are than averaged. The center square is than substituted with this average. This process sharpens the image. (see fig. 10)
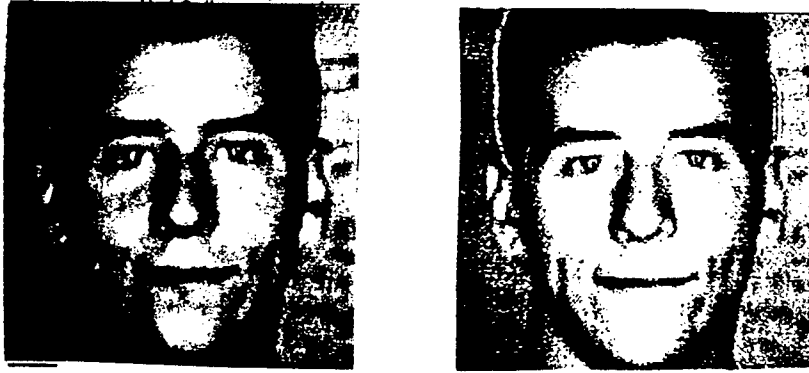
Figure 10: an image sharpened using a mask

Second, a Fourier transform will sharpen an image also. A Fourier transform changes the image from a two dimensional collection of points to a collection of sine waves. All images are made up of a collection of sin waves. The Fourier transform allows a programmer to exclude some low frequency sin waves. The low frequency sine waves act like noise and are the reason why the image is out of focus to begin with.

This second method is better than the mask method to sharpen the image because it solves the problem. The first method treats the symptoms but does not solve the problem.

<u>Results and Conclusions:</u>

Starting with the basic image processing programs possible applications were produced for each of the image processing programs.

1. **Thresholding** - One application for thresholding is on an image which has a desired color to be taken out, such as some noise in a satellite image.

2. **Edge Extraction** - One application for this program deals with pattern recognition, and neural networks. Programs exist that scan an image and will identify the objects in the image. This program seems to work faster if only the edges are being scanned. This could be implemented on a satellite.

3. **Sharpening of an Image** - One application for sharpening images, by either method, is if the satellite image was out of focus when it was obtained. If one of these programs were used, than the image sharpens and the image is more recognizable.

These applications show that image processing can be used to prepare an image for neural networks. A neural network will be used on the satellite to select which data will be transferred. So image processing will help in the future when the images to be sent from the satellites are chosen by the satellites. This help will make the satellites more productive and more cost efficient.

References:

Warren, Steven D. and Bagley, Calvin F., 1992, *SPOT Imagery and GIS in Support of Military Land Management*, Champaign, IL 61826-9005

National Aeronautics and Space Administration, January 1980, *The Landsat Story*, Earth Resources Satellite Data Applications Series , Washington D.C.

Plum, Thomas, 1980, Learning to program in C, Prentice-Hall, Inc., Englewood Cliffs, New Jersey 07632

PROJECTS IN THE NONLINEAR OPTICS BRANCH
OF THE PHILLIPS LABORATORY

David M. Schindler

Los Lunas High School
Drawer 1300
Los Lunas, NM 87031

PROJECTS IN THE NONLINEAR OPTICS BRANCH OF THE PHILLIPS LABORATORY
David M. Schindler

This summer during my second tour at Phillips Laboratories I worked on a couple of interesting projects. Phillips Labs has an equipment account called the PMEL (Precision Measurement Equipment Laboratory) account. The people from PMEL have a list of all the equipment that the lab owns and when each piece needs to be re-calibrated. The equipment needs to be re-calibrated so no major miscalculations are made that could ruin an experiment totally. Some one from PMEL comes every Tuesday and picks up the equipment that is due for re-calibration. They also leave a list for us to see which pieces are to be picked up next. The section of this job that I worked on was to make it easier to find the equipment to send away. I used an image scanner to take pictures of equipment to put in a book to be able to see what the different equipment looks like. Many people do not know what a function generator, digital-multimeter, or a programmable amplifier looks like; so by having a book of images, it is easier to locate equipment that has to be picked up. The image scanner was interesting because it took a picture from paper and put it on a computer screen. Once on the screen, I can change the contrast, brightness, and put as much of the picture on the screen as I want.

I was also involved in an experiment in one of the labs. I mostly observed what the engineers were doing because I have not gone through all of the schooling that they have but I still helped. Most of what I did with this experiment was work with the laser and learn more about how it works and what can be done with a laser. The work that I did on the experiment was not anything remarkable but for what I know about lasers I contributed as much as I could.

The work in my first tour through the AFOSR program was more experimental than my second tour. This time I did more hands-on work. Not only did I learn about different kinds of equipment by making that picture book, I made something that the labs could use if needed. By being in the

laboratory, I learned a lot more about the uses for lasers and how they worked. I enjoyed my second tour more than the first because I was kept busy most of the time and because I did more hands-on work.

A STUDY OF IONOSPHERE

Min Shao
High School Student

Arlington High School
869 Massachusetts Avenue
Arlington, MA 02174

Final Report For:
AFOSR Summer Research Program
Phillips Laboratory
Geophysics Directorate
Hanscom Air Force Base
Bedford, MA 01731

July 1994

A STUDY OF THE IONOSPHERE

Min Shao
High School Student
Arlington High School

Abstract

The ionosphere is a partly ionized region of the upper atmosphere. It is important to the Air Force because anything that is (radio) signal passing through the ionosphere will be effected by it. The Air Force has both communications and radars that are effected by the ionosphere. At Phillips Laboratory, GPS (Global Positioning System) satellite signals are used to study the ionosphere. Phillips Laboratory has operated stations to receive the signals from the GPS satellites in Shetland ,United Kingdom, Shemya, Alaska, Hanscom Air Force Base, Massachusetts, and Thule, Greenland. The stations at Shemya are being run currently.

A STUDY OF THE IONOSPHERE

Min Shao

Introduction

We have known that the ionosphere can effect the electromagnetic material, like radio signal. Obviously the ionosphere can produce significant effects on RF propagation for Space Surveillance, such as range error due to ionospheric Total Electron Content (TEC) and variations in RF signal strength and phase. In order to avoid having errors in scientific, military, and civic electromagnetic applications, it is important to understand and anticipate the ionosphere will. In this paper, it talks about the ionosphere itself, like where is it; what does it look like; what's in there' why can it exist, and so on. Also, it talks about how the systems work to calculate the TEC which is a standard to determine the ionosphere and the GPS satellites.

Ionosphere

The ionosphere is partly ionized region of the upper atmosphere. Typical ionization levels are on the order of five percent. The majority of the ionospheric effects are due to contributions from the region near the altitude where the density of ions is at a peak. This altitude varies but is generally at 300-350 km. Above this altitude (see figure 1), the density of atmosphere is so low that there are fewer ions and charged particles. Below 300 km altitude, the atmospheric density is so high that the recombination of ions with electrons is fast. There is not much ions and electrons, either. The peak density of the ions is about $5 * 10^{11} /M^3$. Actually, electrons are the contributors to the RF effects. The ions are too heavy to interact substantially. That is why we use total electron content (TEC) to determine the ionosphere. The majority of the electron content of the ionosphere comes from the region within about 50 km of the peak ionization density.

The origin of the ionosphere in general is ionizing solar ultraviolet radiation, but other factors can contribute to the local ionosphere that can be observed from a particular location. Charged particles precipitation, like solar rain (usually in auroral regions), effects the ionosphere. Sometimes, part of ionization can be transported from one place to another place, which causes the ionosphere.

The ionosphere keeps changing all the time. Many factors can influence the ionosphere greatly. Magnetic storms, different geographic regions, sunspot, different time in a year, in a month, even in a day, all of these are major factors. It

is easy to understand why the ionosphere changes daily. The reason is that the ionization is generated by solar radiation. At night, there is not enough solar radiation. The ionization goes up in the morning. It reaches the peak in the early afternoon. At that time, the Total Electron Content (TEC) reaches the maximum also. As we can the figure 2, the maximum point usually appears at 2pm-3pm. The altitude of the ionization peak changes daily, too. At night, it rises higher because of the recombination in the lower altitude. The ionosphere changes a lot even in one day. Obviously, the change of the ionosphere depends on the sun greatly. The unusually behaviors of the ionosphere occurs at the same time when the sun is unusually active. Difference in latitude can cause the difference in the ionosphere markedly. The reason is the same. For instance, the solar radiation in the auroral region is very active so that the ionosphere is also active.

Systems and Operation

Global Positioning System (GPS) is used to determine the ionosphere. There are more than 20 this kind of satellites running around the earth. Each satellite sends two different signals to the ground. The signals were effected by the ionosphere. Many factors of the signals can be changed by the it, such as the time of the signal needs to reach the ground, which can be delayed. The receivers receive the signals and determine how much the signals are changed by the ionosphere. The data can be translated to the TEC. Computers are used to calculate and plot. See figure 3 and figure 4.

The receiver we use has four channels. The receiver can track four satellites simultaneously throughout the day. When we make the plots of the TEC vs. Time, we need the location of the satellites. Each location file contains 7 days' information of the satellites as a period. So, the plots overplotted contains 7 days. The behavior of the ionosphere is different in different latitude regions. In order to show this, the data are separated into three latitude regions. They are the north, overhead, and the south, with respect to the receiving station. Each directional plot contains all four channels' information. As the plots shown, the station used in the plots is at Shemya, Alaska.

Channel's plots are shown as "tracker". There four tracers' plot with respect to the four channels. The trackers' time is universal time (Greenwich time). Greenwich time is 12 hours ahead of the local time at Shemya. On the plots, the peak of TEC is seen around midnight universal time which is noon at Shemya. This is the time that the ionosphere is the most active. The directional plots' time is the universal time directly below the ionospheric penetration point (local time at IPP). The IPP the point where the line of site from the receiver to the satellite is at altitude of 350 km.

Summer Accomplishments

In addition to learning about the ionospheric research being done, an increase in knowledge of computers was gained. Fortran programs are used to process the data. They are run in the DOS environment. The DOS version is 5.0. Batch files are set up so that the processing of data can be automatic.

Six months of data from Shemya, Alaska have been processed. In the figures 3 and 4, several days of data are overplotted. The data are collected by the receivers on four channels, or trackers. The same data are also sorted according to latitude and plotted as north, overhead, and south relative to the receiver location.

The plots are studied to determine the behavior of the ionosphere, These plots sometimes contain traces that are uncharacteristic of ionospheric data. These are usually processing artifacts. Each unusual trace is marked, and a list of them is made so that they can be carefully reviewed and their origins determined.
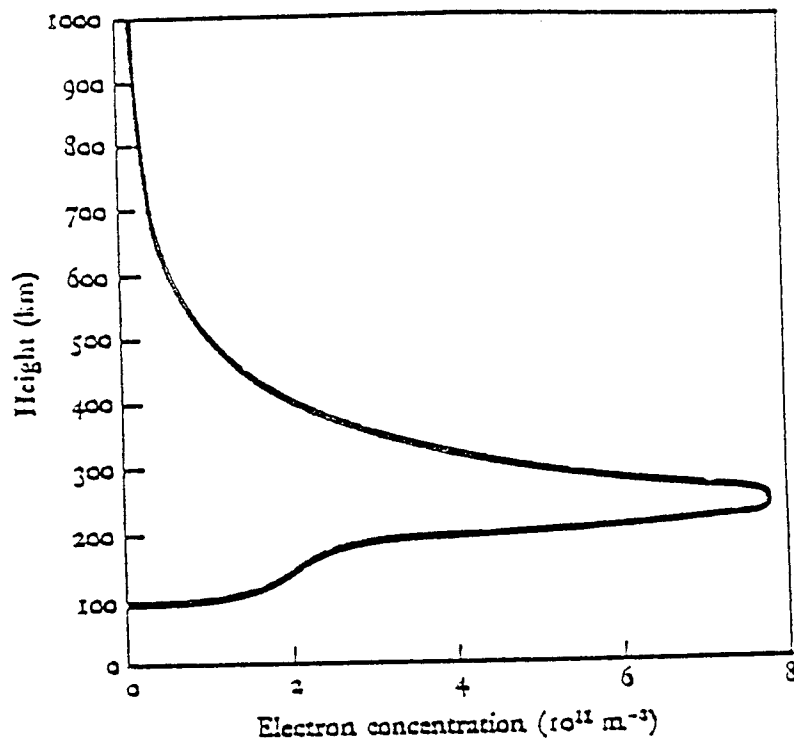
FIGURE 1

Typical Electron Density Profile of the Ionosphere
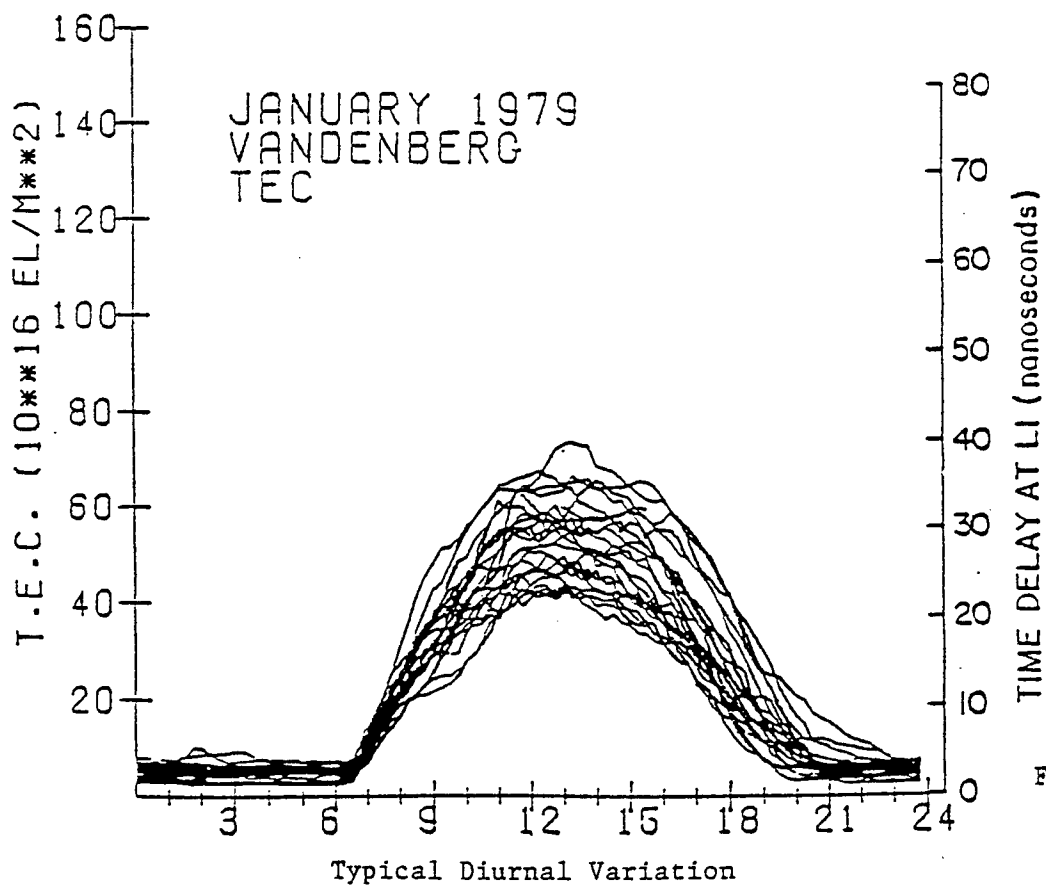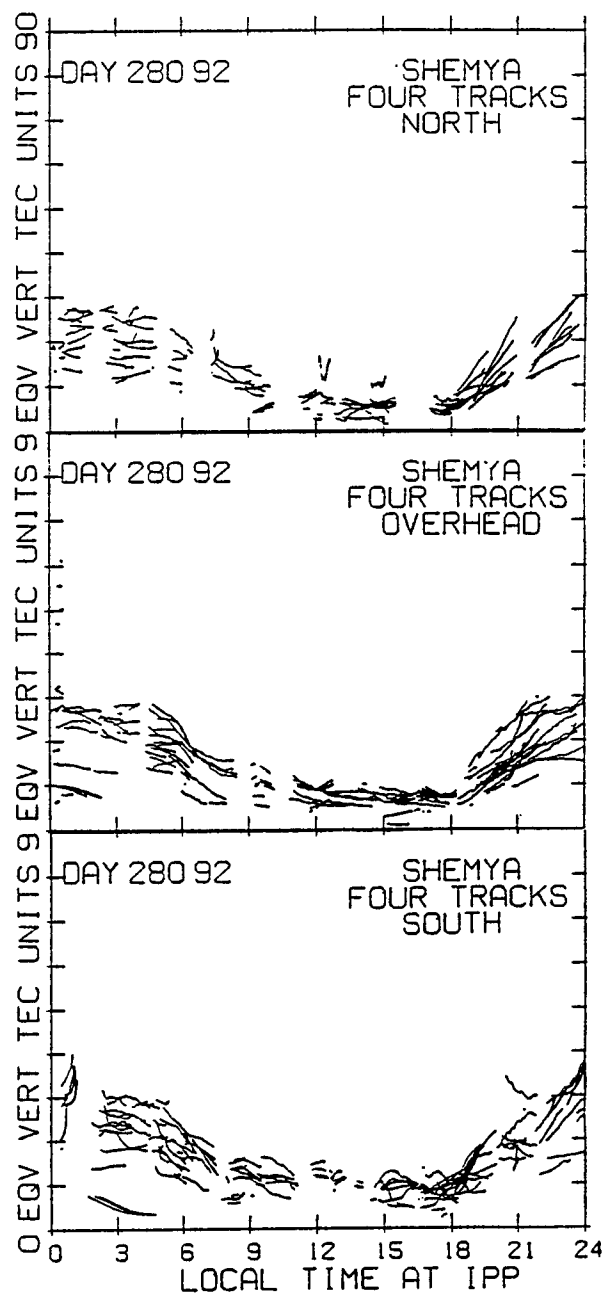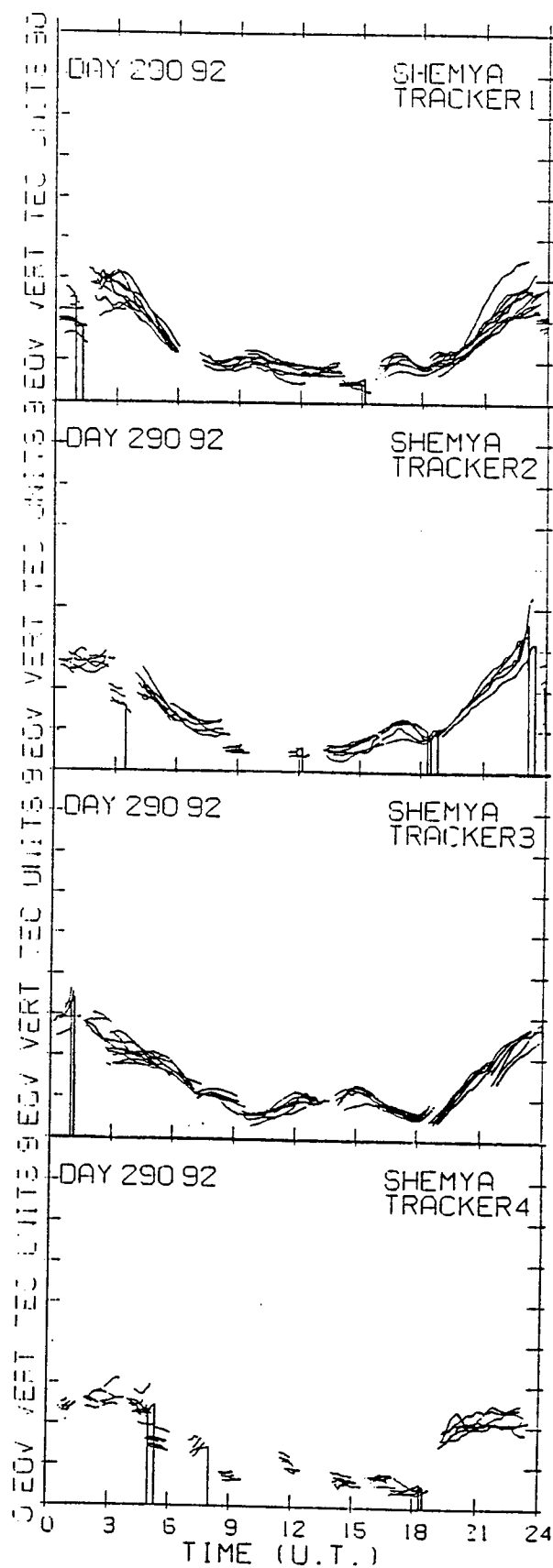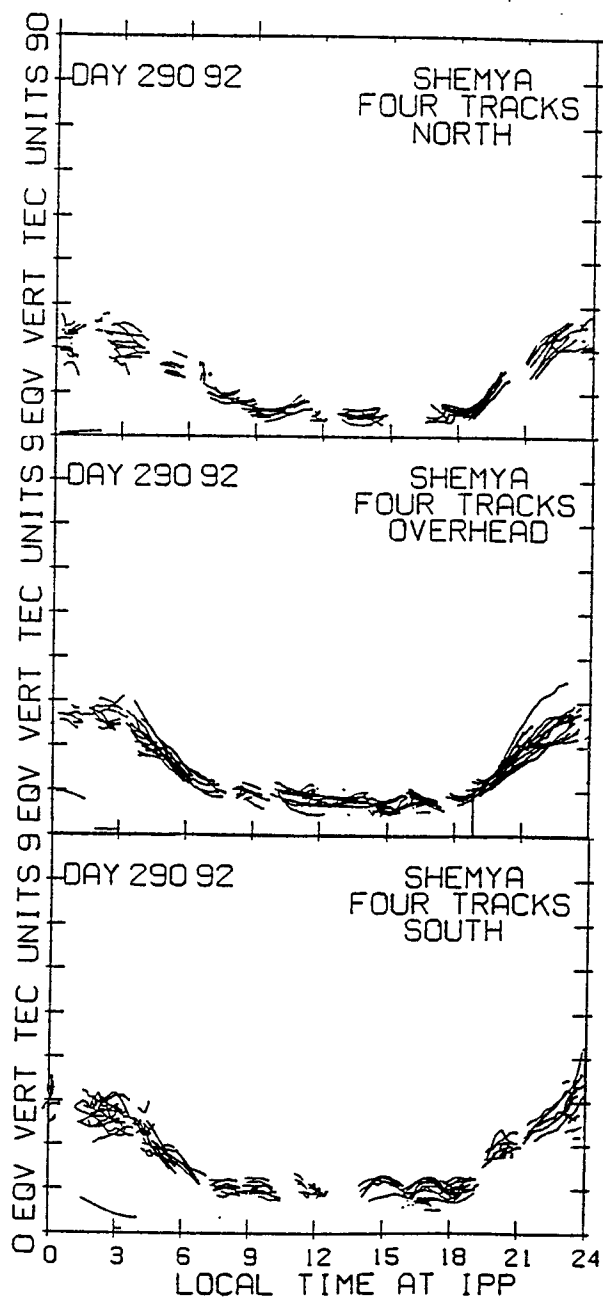
JANUARY 1979
VANDENBERG
TEC

FIGURE 2

Typical Diurnal Variation

FIGURE 3

FIGURE 4

Left column (TIME (U.T.)):
DAY 290 92 — SHEMYA TRACKER1
DAY 290 92 — SHEMYA TRACKER2
DAY 290 92 — SHEMYA TRACKER3
DAY 290 92 — SHEMYA TRACKER4

Right column (LOCAL TIME AT IPP):
DAY 290 92 — SHEMYA FOUR TRACKS NORTH
DAY 290 92 — SHEMYA FOUR TRACKS OVERHEAD
DAY 290 92 — SHEMYA FOUR TRACKS SOUTH

A STUDY OF INFRARED DEVICES AND RADIOMETRIC MEASUREMENT TECHNIQUES

RAUL TORREZ

SANDIA PREPARATORY SCHOOL
ALBUQUERQUE NEW MEXICO

FINAL REPORT FOR:
HIGH SCHOOL APPRENTICE PROGRAM
PHILLIPS LABORATORY

SPONSORED BY:
AIR FORCE OFFICE OF SCIENTIFIC RESEARCH
BOLLING AIR FORCE BASE, DC

AND

PHILLIPS LABORATORY

AUGUST 1994

A STUDY OF INFRARED DEVICES AND RADIOMETRIC MEASUREMENT TECHNIQUES

RAUL TORREZ
SANDIA PREPARATORY SCHOOL

ABSTRACT

This summer's research was centered primarily upon the recent technology developed in the field of infrared detection, as well as the different means of testing the overall performance of that technology. The work was carried out at the Infrared Device Laboratory, a branch of the Passive Sensors department of Phillips Laboratory, on Kirtland Air Force Base.

The work done this summer involved the extensive testing of Quantum Well Infrared Photodetectors or QWIPs. Unlike Photovoltaic devices, QWIPs are a more recent development in the field of thermal detection and are as yet still experiencing some of the quirks expected in newer technology. The two main testing procedures involved in the screening of this type of device are spectral analysis and optical or noise analysis. Both methods of testing provide critical information regarding the efficiency of the device and reveal information about its overall performance. Spectral and optical tests are the radiometric measurement techniques which enable one to discern the elements of a detector that optimize performance and ultimately lead to further advances in the field of thermal detection.
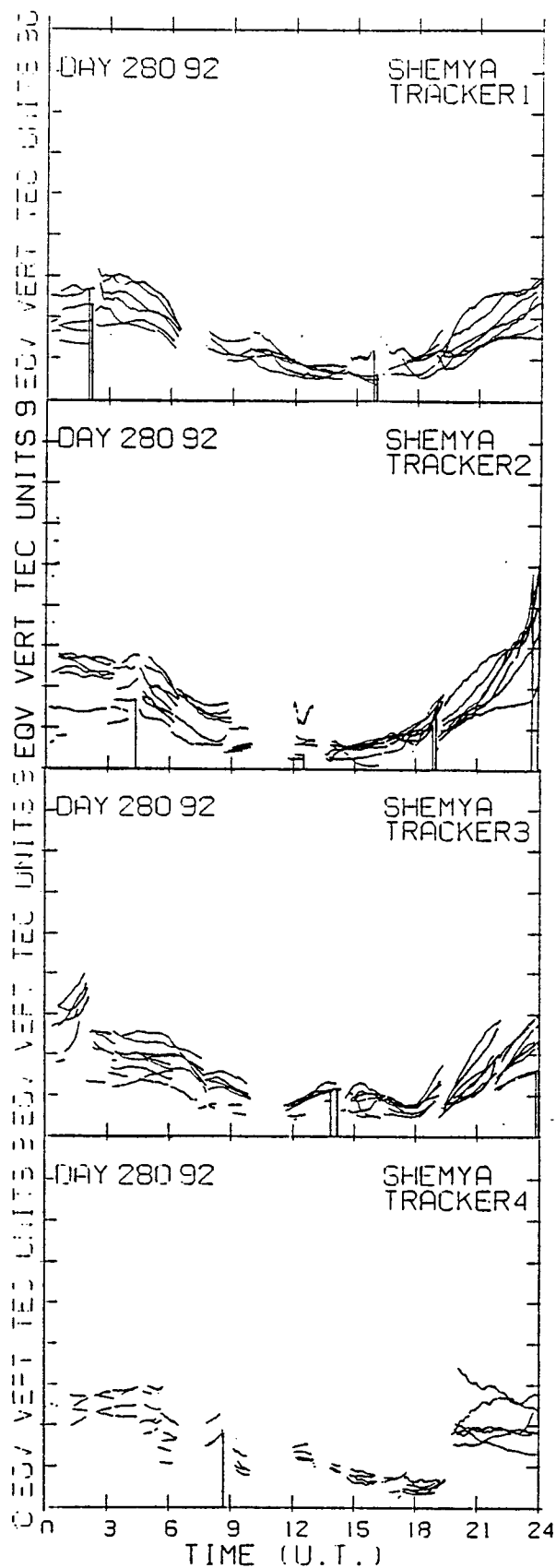
A STUDY OF INFRARED DEVICES AND
RADIOMETRIC MEASUREMENT TECHNIQUES

RAUL TORREZ

INTRODUCTION:

In order to understand the test work done in the IR laboratory one must first be familiar with some of the basics in the science of thermal detection. An infrared detector or device is simply a type of transducer designed to detect either part or all emissions within a specific segment of the electromagnetic spectrum known as infrared. The infrared portion of the spectrum can be anywhere from 1 to 1000 microns in wavelength, however most IR detectors are only tuned to a "primary region" of 3 to 12 microns.(OB) Infrared does lie beyond the visible spectrum, yet while one cannot see infrared it can certainly be felt or sensed because of the heat transfer associated with infrared or thermal radiation. While the detection of thermal radiation could be applicable in a variety of fields, the devices tested this summer were designed specificly for space based applications.

Quantum Well Devices: The crystalline layout of the Quantum Well Infrared Photoconductor is extremely precise, after all it is the QWIP's unique structural characteristics which make it a viable infrared detector. In this and any type of quantum device it is important to understand that to carry out functions on a quantum level, the device must be setup literally on an atomic scale.

The QWIPs tested this summer were composed of a GaAs layer 40 angstroms in depth and an AlGaAs layer 500 angstroms in depth, grown in an alternating layer structure upon a semi-insulating GaAs substrate. Within the structure, the highly n-doped GaAs layer is referred to as the "well," because of its relatively narrow energy band gap in comparison with the AlGaAs or "barrier" layer which has a much wider energy band gap. The well layer possesses an excess amount of loosely bound valence electrons because of its silicon n-doping, however because the layer is so extremely narrow and lies between the much wider barrier layers those electrons are trapped within the well. The only method by which the electron can be "freed" from the well is through an external energy source, however, due to the incredibly small dimensions involved, the energy required is not continuous but discrete, in quantified packets. It is at this point that thermal radiation comes into play, it serves as the source when it radiates the device, provides the discrete energy required, and compensates for the difference in band gap energy between the layers. It is the specific photon energy provided in the infrared spectrum which "lifts" the loosely bound electrons in the well layer either par or above the energy gap of the barrier layer. At this point the electrons move into a biased conduit or continuum and into an external circuit that reads a change in current. It is this change in current which indicates infrared radiation incident upon the device, with a signature maximum current output for a pre-designated, specific wavelength input. In its processing each device can be programmed or tuned to yield a maximum output when radiated by a select wavelength in the spectrum, by varying either layer thickness, band gap difference, or the amount of doping. It is this feature which makes QWIPs

19-4

most appealing because unlike most other devices it can, in theory, be tuned to any desired wavelength or small range of wavelengths in the infrared spectrum and hopefully filter out the majority of the undesired wavelengths.

The following is a description of the types of tests conducted this summer upon the QWIPs that the Infrared Laboratory received from various sources and manufacturers. The primary object of the tests conducted was to obtain raw data which indicates the overall level of performance of each device. The following are the parameters, used to characterize the devices, that one must first be familiar with in order to understand the purpose behind each test:(OB)

Noise. The "clutter" that tends to hide the true signal.

Responsivity. Electrical output for a given IR photon input

Signal-to-Noise Ratio. A measure of the fidelity of a signal pattern

Spectral Response. How the responsivity varies with the wavelength of infrared power

Dynamic Range. The range of IR signal levels for which the detector is useful.

Testing Procedure: All of the devices tested this summer were mounted in a high vacuum dewar and cooled anywhere from 20 to 80 Kelvin before testing began, this was done to minimize thermal noise. It is also often necessary to shield or isolate the device from noise due to vibrations and or electrical fields. One should note that all such infrared devices require these conditions in order to operate and therefore the support equipment that this technology demands must be an important consideration in the viability of this technology.

Spectral Analysis: The first testing done upon a device in the Infrared Laboratory is spectral analysis, a test that determines both responsivity and spectral response. The test is run on a Fourier Transfer Infrared spectroscopy system which basically exposes the device to a range of infrared radiation from 2 to 20 microns while a voltage bias anywhere from -5 to +5 is applied. It is through varying the applied voltage bias that one can manipulate the rate of the electrical signal as it is put forth by the QWIP's current continuum and in turn predict the expected electrical output, for that device, at a given bias and temperature. The system and device are monitored by a customized, Nicolet computer which both determines the specific wavelength which produces the maximum electrical yield and calculates the intensity of that yield relative to a known value set by an internal detector within the FTIR system. This method of testing proves quite useful in determining a QWIP's overall level of performance based upon its relative photoconductivity.

Optical Analysis: This method of testing is used primarily to determine a device's basic photoconductivity, its signal-to-noise ratio and its dynamic range. Like spectral analysis the device is once again exposed to an infrared source however this source is a blackbody with an emmisivity of 1, a smooth and uniform source of infrared radiation. The blackbody emits the entire spectrum of infrared wavelengths and the power emitted at each specific wavelength can be represented by a blackbody radiation curve. The area under this blackbody curve represents the total exitance of the infrared spectrum, this area always remains the same however the slope and placement of the peak, in reference to the wavelength, can vary with

19-6

temperature. A typical optical test can range from 300 to 900 Kelvin. Since the QWIP devices detect only a narrow band of wavelengths only a small section of the blackbody emission is detected. The test is monitored by an HP Dynamic Signal Analyzer which measures the amount of signal actually detected by the device, thus revealing its dynamic range. One knows the exact amount of exitance for that specific band of wavelengths based upon Planck's Law and his study of blackbodies; in turn one knows what range of power should be detected by the device. Finally based on the data gathered in the test one can calculate the quantum efficiency of the device by dividing the amount of exitance detected by the actual amount of exitance emitted. Further by running a check on the background noise received by the device at various temperatures and isolating that noise from true signal, the detector's signal-to-noise ratio can be calculated. This method of testing proves very effective in not only revealing how much of the signal is not detected, but it also shows, that of the signal that is detected, what percentage of that signal might be accounted for as noise.

CONCLUSION:

QWIP devices as well as similar photoconductive devices do show considerable potential in the science of infrared detection. While the older Photovoltaic technology does not require a voltage bias and the equipment needed to sustain it, as does Quantum Well technology, the advantage in the QWIP's ability to be tuned to specific wavelengths might be sufficient to justify further developments in this type of technology. Certainly as the quality of devices is furthered so shall the radiometric test procedures be enhanced, producing superior results in the technology's final application.

REFERENCES:

1)The Fundamentals of Infrared Detector Operation and Testing,
John David Vincent, Santa Barbara Research Center 1990

2)Electronic Properties of Materials, Rolf E. Hummel, Springer-Verlag Berlin
Heidelberg 1993

3)Optical Radiation Detectors, Eustace L. Dereniak and Devon G. Crowe,
John Wiley &Sons Inc. 1984

Introduction to the Arcjet

Christian G. Warden

Rosamond High School
2925 Rosamond Blvd.
Rosamond, CA 93560

Final Report for:
High School Apprentice Program
Phillips Laboratory

August 1994

Christian G. Warden

1.1 Introduction to Electric Propulsion

Electric propulsion has been present since the first orbital flights. The first arcjets were low power and run on hydrazine. They were mainly used in commercial applications aboard communication satellites.

Electric propulsion can be summarized as "the acceleration of gases for propulsion by electrical heating and/or by electric and magnetic body forces" [1]. Three categories of electric propulsion have been defined. The categories are *electrothermal, electrostatic, and electromagnetic*. First, electrothermal propulsion uses propellant gases that are electrically heated and expanded through a nozzle to obtain thrust. Electrostatic propulsion uses electricity to ionize propellant gases. The ions are accelerated by direct application of electric body forces. Electromagnetic propulsion systems ionize the propellant gases, which are accelerated by internal and external magnetic fields with electric currents driven through the ionized propellant stream.

The principal advantage of electric propulsion over chemical propulsion systems is that the thrust produced by electric propulsion systems is not limited by chemical properties of the propellant [1], as is the case with chemical systems. The specific impulse (I_{sp}), the measure of the thrust produced per unit mass flow of propellant, of chemical systems is limited by the chemical reactions involved. Electrically powered thrusters can produce specific impulses between 1.5 and 25 times that available from comparable chemical thrusters since the heating of propellant in electric systems in not limited by chemical reactions. Electric propulsion systems can produce specific impulses greater than 1,000 seconds. Because of the much higher specific impulses, electric propulsion devices use less propellant mass to produce the same impulse as chemical thrusters, thereby enhancing spacecraft capabilities and reducing life cycle costs [2,3].

Unfortunately, the increased specific impulse of electric propulsion systems has its penalties. Electric propelled spacecraft have fixed power, which is proportional to the produce of specific impulse

and thrust. Therefore, high specific impulses result in low thrust levels [4]. There are applications for low thrust, high I_{sp} in space propulsion. These applications include satellite stationkeeping, repositioning, and attitude control. Because of electric propulsion's very high specific impulses, it may also be used in orbit raising, plane changes, and orbital repositioning. Low thrust levels allow for more precise positioning and attitude control than higher thrust chemical devices [2].

1.2 Introduction to Arcjets

Electrothermal electric propulsion, thus far, has been the most developed category of electric propulsion. The resistojet is the simplest form of electrothermal electric propulsion. It consists of a resistive heating mechanism through which a propellant gas passes. As the gas passes through the resistojet, the heating element increases the enthalpy of the gas, which is then expanded out of a nozzle to produce thrust [1]. Currently, resistojets in the US can achieve specific impulses of approximately 300 seconds using hydrazine, running at 0.3 to 0.8 kW. Arcjets use an electric arc to transfer energy to the propellant gas, and can produce higher specific impulses than resistojets. At this time, arcjets represent the most mature electric propulsion concept [5].

There are three basic parts to an arcjet. These are the plenum chamber, the constrictor region, and the expansion nozzle. The propellant is initially injected tangentially into the rear portion of the plenum chamber, which creates a swirl in the propellant. This swirl serves two purposes. First, the swirl is used to promote heat conduction between the cathode and the propellant stream to help cool the cathode so that it may withstand the intense heat generated by the arc. Second, the swirl is believed to stabilize the arc within the arcjet. The propellant gas subsequently flows to the front portion of the plenum chamber where the propellant stream comes under the influence of the electric arc coming from the tip of the cathode. Some gas is directly heated by the arc. Most of the heating is due to radiation and conduction from the arc as well as the hot walls of the constrictor. In addition to being an important region for heat transfer to the propellant gas, the constrictor also serves to stabilize the arc. As the gas

exits the constrictor region, it enters the expansion nozzle portion. In this region, the arc attaches to the nozzle, which also serves as the anode. The propellant undergoes expansion before it is discharged from the arcjet nozzle. The arcjet must be made of materials able to withstand very high temperatures (>2000K). Therefore, refractory metals such as tungsten are generally used for the cathode and anode portions of the arcjet. Cooler portions of the arcjet, found in the rear portions, are often made of molybdenum [1]. Some water-cooled laboratory models are constructed using a copper anode, but these experience many difficulties since copper is only able to withstand the temperatures produced by the internal arc with active water cooling [6.7].

Two types and three classes of arcjets have been recognized. The arcjet type is determined by the method of cooling used. The two types are radiatively cooled and regeneratively cooled. The nozzle of the former is cooled by radiation into space, while the latter have small channels around the nozzle, through which the propellant gas flows prior to being injected into the plenum chamber. The aim of this added complexity is to capture some of the energy that would otherwise be lost if it was allowed to radiate from the nozzle. Arcjets are also classified by the power levels for which they were designed: low, medium, and high. Low power arcjets are below 3 kW, most commonly 2 kW. Medium power arcjets range in power levels between 3 and 10 kW. High power arcjets are designed to run at between 10 and 30 kW. To run an arcjet above approximately 30 kW would require very large solar arrays or nuclear power sources to provide sufficient power for the arcjet [3].

Arcjets can operate on a variety of propellants. There are certain qualities desired in an arcjet propellant. The ideal propellant should have a low molecular weight. In addition, high stagnation temperatures and pressures are also seen to be desirable [9]. Tungsten anodes and electrodes are thus favorable for flight models since tungsten has the highest melting point of any metal in use. Hydrogen and helium are the lightest gases available. Although also used, nitrogen and other gaseous compounds such as ammonia (NH_3) and hydrazine (N_2H_4) have the drawback of having higher molecular weights [10]. Oxygen and oxygen compounds cannot be used in tungsten arcjets due the reactive nature of oxygen and tungsten at high temperatures and pressures. An oxygenated propellant would rapidly result

in large amounts of yellow tungsten oxide forming on and damaging the inner surfaces of the arcjet [11].

The main technical concerns of using arcjets in spacecraft have been thruster performance, lifetime, power availability, and integration into current satellite configurations. Non-technical concerns have included development costs and a lack of knowledge by project managers with regard to the strengths and limitations of arcjets in particular and electric propulsion in general.

Currently, there is an array of satellites in space that are used for surveillance and communications. Unfortunately, these satellites are not always positioned in the necessary orbits. The repositioning of these satellites consumes fuel originally set aside for orbit maintenance. Electric propulsion performs much better than chemical propulsion in such tasks as stationkeeping and orbit repositioning because of its much higher I_{sp}. In fact, the low thrust trajectories used for orbit repositioning would result in quicker repositioning maneuvers when compared to chemical systems [4]. In addition, the lower thrust levels are capable of much more accurate orbital positioning than higher thrust chemical systems [12].

Overall, there are three major applications of electric propulsion. The first is attitude control. Attitude control requires extremely small levels of thrust, and is therefore in the capability of all electric propulsion systems. The second of these regimes is geosynchronous stationkeeping. This requires many corrections in positioning and the expenditure of substantial amounts of propellant. The third application is electric orbit adjustment. With current low power arcjets and other similar electric propulsion devices, this refers to orbital repositioning of satellites at the expense of stationkeeping fuel. However, it may come to signify orbit raising from low earth orbit (LEO) to higher altitude orbits such as geosynchronous orbit (GEO) [3].

Geosynchronous stationkeeping is the current focus of arcjet application. Without accurate orbit positioning, communication satellites cannot achieve high rates of data transfer and have problems with radio interference from other satellite networks. Stationkeeping requires velocity increment of approximately 52 m/s per year. Communication satellites currently mass approximately 25% propellant

for stationkeeping at the beginning of GEO life using monopropellant hydrazine thrusters [2,3]. Due to the greater I_{sp} of an arcjet over a monopropellant system, the maneuverability of the satellite would be increased. This increase in maneuverability could result in improved mission flexibility, extended mission life, or lower launch costs by reducing the stationkeeping propellant mass launched with the spacecraft.

1.3 History of Arcjets

The development of arcjets began in the late 1950's and was sponsored by the USAF and NASA. Initially, arcjets were used in wind tunnels as plasma sources in the study of ablative heat shields for projected reentry vehicles. After research found that arcjets could provide high I_{sp}, and relatively good thrust efficiency, arcjets became an appealing propulsion system for spacecraft with power levels in the 10's of kilowatts [13].

There was a problem with using arcjets in spacecraft, though. The only power supplies able to produce the 10's of kilowatts needed to power the proposed arcjets were space based nuclear reactors. When the space nuclear power program was canceled, it was clear that the arcjet programs lacked suitable space-based power supplies, and arcjet development programs were discontinued.

Until the early 1980's, arcjet technology remained dormant. Then, the use for arcjet technology was recognized. Satellite power levels had risen to new highs. Larger solar arrays were placed on satellites to provide the necessary power making solar electric propulsion feasible again [2,3].

1.4 Current Research Programs

Electric propulsion research programs have been organized worldwide. European research into electric propulsion has been extensive. In Europe, the University of Stuttgart, BPD, and Centrospazio in Italy, research into a variety of arcjets has been performed. These range from 2 kW radiatively cooed arcjets to 100 kW radiatively and water cooled laboratory models. Arc attachment and arc behavior inside the constrictor have been studied using segmented intermediate power water cooled arcjets with quartz windows. A series of tests was conducted at Centrospazio to examine stabilization of the arc utilizing externally applied magnetic

fields. This added stability would result in an increased I_{sp} by allowing lower mass flow operation and would also result in longer thruster lifetimes.

Russian research in electric propulsion has been focused on plasma thruster, or Stationary Plasma Thruster (SPT) as they are commonly known. They can be best described as gridless ion engines with very high thrust densities. Electrons emitted from the anode are slowed in their motion toward the anode by a transverse magnetic field. This interaction creates an electric field that accelerates the ions out of the discharge portion of the thruster thus generating thrust [3].

Japan's experimental work has mainly been conducted on laboratory models which are water cooled and unfortunately exhibit large variation form radiatively or regeneratively cooled flight models. Japanese researchers have used propellants such as nitrogen and helium in their work. These propellants are not likely to be used aboard spacecraft due to either storage problems or the fact that better, lighter molecular weight propellants are available. They have, however, repeatedly examined the interior characteristics of arc behavior in the constrictor region and have even recently begun studies of the nozzle expansion process using quartz windows in their water cooled arcjets [14].

Research in the US is conducted by several government agencies, private industry, and several universities. NASA Lewis, along with industry and the USAF, is researching high power arcjets due to the widespread interest in electric orbit transfer. NASA was also part of the effort that resulted in the first generation of low power hydrazine arcjets recently space qualified by Odin Aerospace. In addition, NASA and JPL have performed numerous studies of nuclear electric propulsion. The conceivable power supplies would be able to provide sufficient power for missions with electric thrusters beyond Earth orbit using several different types of electric propulsion. However, the NASA nuclear power studies were recently halted due to budgetary constraints [8].

The USAF through Phillips Laboratory at Edward's Air Force Base has been working to advance 30 kW arcjet technology. The primary portion of this effort has been the Electric Propulsion Space Experiment (ESEX). In this program, a 30 kW class arcjet running on ammonia will be tested in orbit to check thruster effects on the spacecraft. In addition, the USAF will gain experience in space with integrated arcjet flight hardware. The Phillips Laboratory is also participating in the Electric Insertion Transfer Experiment (ELITE).

ELITE will perform significant orbit raising using two derated 30 kW class arcjets running at 10 kW each [4]. The electric propulsion group of the Phillips Laboratory is engaged in an extensive effort to examine arcjet interior behavior using a variety of plasma diagnostics including triple Langmuir probes, laser induced fluorescence, electron beam fluorescence, emission spectroscopy, laser imaging, as well as current modulation velocimetry, a diagnostic which was developed at Phillips Laboratory in conjunction with the University of Southern California (USC).

1.5 Overview of Experimental Objectives

The high power arcjet is recognized as the most likely candidate to be used for orbit raising and maneuvering. The fraction of the input energy exiting in each energy mode of the propellant must be better understood, though, if advances are to be made in producing more efficient arcjets [5].

The aim of these experiments is to determine the fraction of the input energy in each energy mode inside the expansion nozzle of a 30 kW class arcjet. Computational models have predicted the flow characteristics inside arcjets, but little experimental verification of these internal models has been performed. Several studies have examined the interior propellant flow in an arcjet by emission spectroscopy, either axially, angled into the arcjet, or by small optical access ports into the side of the arcjet nozzle [15,16,17]. These studies have been performed on low power radiatively cooled arcjets, and thus apply to the current generation of low power space qualified arcjets. Emission spectroscopy was chosen to study the interior propellant characteristics of the arcjet since this technique is nonintrusive and is capable of providing detailed information on a variety of flow parameters [12]. This program utilized emission spectroscopy through small holes in the side of the arcjet nozzle to examine the propellant energy modes inside the nozzle and investigate scaling issues of a 30 kW class radiatively cooled arcjet. A series of 0.5 mm diameter holes was drilled into the diverging portion of the tungsten arcjet nozzle to provide optical access to the propellant expansion process occurring inside the arcjet. These ports consisted of a series of three holes placed along the centerline of the arcjet nozzle. The holes were used to examine the propellant expansion process through the arcjet nozzle. The arcjet propellant examined was ammonia at a power level of 17.7 kW and a massflow rate of 250 mg/s. Atomic

excitation and electron temperatures were determined using a relative line intensity technique utilizing the hydrogen Balmer series and ionized atomic nitrogen. Molecular vibrational temperatures were determined from relative line intensity measurements of NH vibrational bands. Molecular NH rotational temperatures were obtained from comparisons between the observed molecular rotational bands and theoretical distributions. Electron densities were determined from hydrogen Balmer beta line Stark broadening.

References

1. Jahn, R.G., Physics of Electric Propulsion, McGraw-Hill Book Co., New York, 1968.

2. Janson, S.W., "The On-Orbit Role of Electric Propulsion," Paper AIAA 93-2220, 29th Joint Propulsion Conference, 28-30 June 1993, Monterey, CA.

3. Pollard, J.E., D.E. Jackson, D.C. Marvin, A.B. Jenkin, and S.W. Janson, "Electric Propulsion Flight Experience and Technology Readiness," Paper AIAA 93-2221, 29th Joint Propulsion Conference, 28-30 June 1993, Monterey, CA.

4. Perkins, D.R., "An Overview of the Air Force's Electric Propulsion Program," Paper IEPC 93-004, 23rd International Electric Propulsion Conference, 13-16 Sept. 1993, Seattle, WA.

5. Sutton, A.M., "Overview of the Air Force ESEX Flight Experiment," Paper IEPC 93-057, 23rd International Electric Propulsion Conference, 13-16 Sept. 1993, Seattle, WA.

6. Tahara, H., T. Sakakibara, K. Onoe, and T. Yoshikawa, "Experimental and Numerical Studies of a 10 kW Water-Cooled Arcjet Thruster," Paper IEPC 91-015, 22nd International Electric Propulsion Conference, 14-17 Oct. 1991, Viareggio, Italy.

7. Tahara, H., N. Uda, K. Onoe, Y. Tsubakishita, and T. Yoshikawa, "Optical Measurement an Numerical Analysis of Medium-Power Arcjet Non-Equilibrium Flowfields," Paper IEPC 93-133, 23rd International Electric Propulsion Conference, 13-16 Sept. 1993, Seattle, WA.

8. Bennet, G.L., F.M. Curran, D.C. Byers, J.R. Brophy, and J.F. Stocky, "An Overview of NASA's Electric Propulsion Program," Paper IEPC 93-006, 23rd International Electric Propulsion Conference, 13-16, Sept. 1993, Seattle, WA.

9. Hill, P.G. and C.R. Peterson, *Mechanics and Thermodynamics of Propulsion*, Addison-Wesly Publishing Co., Reading, MA, 1965.

10. Brown, T.L. and H.E. Lemay, Jr., *Chemistry: The Central Science*, Prentice Hall, Englewood Cliffs, NJ, 1988.

11. Hoskins, W.A., Personal Communication, 15 Sept. 1993, Redmond, WA.

12. Bartoli, C. and G. Saccoccia, "European Electric Propulsion Activities in the Era of Application," Paper IEPC 93-003, 23rd International Electric Propulsion Conference, 13-16 Sept. 1993, Seattle, WA.

13. Pivirotto, T.J., D.Q. King, J.R. Brophy, and W.D. Deiniger, "Performance and Long Duration Test of a 30 kW Thermal Arcjet Engine," Report AFAL-TR-87-010, Air Force Astronautics Laboratory, Nov. 1987, Edwards AFB, CA.

14. Arakawa, Y., "Review of Electric Propulsion Activities in Japan," Paper IEPC 93-005, 23rd International Electric Propulsion Conference, 13-16 Sept. 1993, Seattle, WA.

15. Storm, P.V. and M.A. Cappelli, "Axial Emission Diagnostics of a Low Power Hydrogen Arcjet Thruster," Paper IEPC 93-219, 23rd International Electric Propulsion Conference, 13-16 Sept. 1993, Seattle, WA.

16. Ruyten, W.M., D. Burtner, and D. Keefer, "Spectroscopy Investigation of a Low-Power Arcjet Plume," Paper AIAA 93-1790, 29th Joint Propulsion Conference, 28-30 June 1993, Monterey, CA.

17. Zube, D.M. and R.M. Myers, "Nonequilibrium in a Low Power Arcjet Nozzle," Paper AIAA 91-2113, 27th Joint Propulsion Conference, 24-27 June 1991, Sacramento, CA.